POLITECNICO DI TORINO

MASTER's Degree in Environmental and Land Engineering

Atmospheric moisture dynamics: a precipitationshed and evaporationshed analysis across Italy

Supervisors

Eng. ELENA DE PETRILLO

Prof. FRANCESCO LAIO

Prof. LUCA RIDOLFI

Prof. MARTA TUNINETTI

Candidate

GIANMARIA PAOLO ZANZI

March 2025
A.Y. 2024-2025

Abstract

Human activities have determined deep changes in the global water cycle, with significant effects on the availability and quality of hydrological resources. This study investigates the dynamics of atmospheric moisture and hydrological connectivity in Italy and in three regions (Piemonte, Lazio, Sicily) through the analysis of two main concepts: evaporationsheds – that is, the downwind areas where the precipitations supplied by the evaporation in the region of interest occur – and precipitationsheds – that is, the upwind areas from which the evaporation contributing to precipitations in the region of interest originates.

The study has been implemented through the use of two different datasets: UTrack – a Lagrangian atmospheric moisture tracking model developed by Tuinenburg et al. (2020) – and RECON, a post-processed version of UTrack. Both datasets allowed for the reconstruction of the annual atmospheric moisture forward and backward flows relative to the regions of interest. While UTrack provided a detailed analysis on both an annual and seasonal scale, RECON focused only on annual flows. The comparative analysis between the outputs of the two datasets highlights a better consistency of RECON, which shows greater uniformity with ERA5 data and better adherence to the principle of mass conservation.

Italy emerges as an evident 'atmospheric bridge,' receiving most of its precipitations from moisture coming from the west, particularly from the North Atlantic Ocean, and redistributing this water mainly towards the east, reaching far areas such as Russia. The quantitative analysis, based on RECON data, highlights that 92.59% of Italian precipitations come from external sources to the country, while 87.72% of the water evaporating from the national territory is transported beyond the Italian territory. This trend points out a clear condition of hydrological interdependency, challenging any possible claims of water autarchy.

This study, the first one realized in Italy, provides an innovative perspective regarding water management policies and adaptation to climate change, highlighting the strong interconnection bewteen different areas of the world and the importance of a global approach in water conservation.

Contents

Introduction

Human activity has entered a new geological epoch—the Anthropocene—defined by humanity's role as the primary force driving planetary environmental change (Crutzen, 2002; Steffen et al., 2015). Among the most critical aspects of this change is the impact on the global water cycle. Human pressures on water resources now operate across all scales, from local watersheds and aquifers to large river basins and even regional climate systems. Evidence indicates a significant, human-induced decline in both the quality and availability of water, accelerated since the mid-20th century's "Great Acceleration" in industrial activity (Kummu et al., 2016; Wada et al., 2011). Today, four billion people experience severe water scarcity for at least one month each year (Mekonnen and Hoekstra, 2016), and for the past seven years, water-related risks have ranked among the World Economic Forum's top five global risks (World Economic Forum, 2018).

The Earth's water fluxes and storage systems are essential to climate regulation, ecosystem health, and food, water, and energy security. However, human activities are reshaping the water cycle at an unprecedented scale. These modifications include the extraction of surface and groundwater, deforestation, land use change, and accelerated glacial melt due to climate warming. The consequences of these disruptions are profound.

With each degree of global warming, mean precipitation increases by 1–3%, and by the end of the century, this could rise by up to 12% compared to 1995–2014 levels. However, these increases in precipitation will not likely be uniform; both floods and droughts are expected to become more extreme. In addition, human activities that modify the land cover—for example, from fields to urban areas, or cutting down forests—can have impacts on every part of the water cycle. These land-use changes can, indeed, alter precipitation patterns, affect the infiltration of water into the soil, change runoff of water into streams and rivers, contribute to surface flooding, and disrupt the evaporation of moisture back into the atmosphere.

Recent advances in atmospheric science have led researchers to view water sources and destinations as linked precipitationsheds" and "evaporationsheds"—concepts

analogous to watersheds on land. Precipitationsheds track the origins of rainfall, while evaporationsheds denote the destinations of evaporated water. The use of meteorological data coupled with advanced climate models help scientists to better investigate how atmospheric water flows link different regions. Notably, no country obtains more than half of its precipitation from its own territory showing a global dependency on atmospheric moisture derived from other states and seas.

To guide policy and resource management, researchers must continue assessing the distribution and movement of "blue" and "green" water (surface and soil water) on both local and global scales. The advent of satellite monitoring, big data, and Earth-system models is crucial for tracking shifts in water availability, extreme weather patterns, and disruptions in the freshwater cycle. Particularly, understanding the costs and impacts of extreme events—like droughts and floods—within the context of precipitationsheds and evaporationsheds will be important to foster water resilience in a changing world.

This thesis will analyze the complex dynamics of atmospheric moisture flows, focusing on the case of Italy and three of its regions: Piedmont, Lazio, and Sicily. Because of its peculiar position in the Mediterranean basin, Italy represents a critical node for moisture transport, acting as a bridge between the western Mediterranean and the Atlantic and eastern regions like the Balkans and Russia.

The investigation is structured to provide a comprehensive analysis of atmospheric patterns. It begins with a theoretical overview of key hydrological parameters. This is followed by the main part of the study, which applies two advanced modeling approaches—UTrack and RECON—to map and quantify the forward and backward moisture footprints for Italy and selected regions.

Regarding Utrack, which is a Lagrangian (trajectory-based) moisture tracking model developed by Tuinenburg and Staal (2020) based on the ERA5 dataset, the analysis of the precipitationsheds and evaporationsheds will be carried on seasonally and annually.

On the other hand, the RECON dataset is a post-processed version of the UTrack dataset and provides only yearly averaged moisture flows.

Both dataset deliver moisture flow in cubic meters from evaporation sources to precipitation targets and vice versa and offer global coverage at a resolution of 0.5° for an average year based on the period 2008–2017.

The outcomes of these models will be then compared to evaluate which of them provides the most consistent and reliable results.

These results will provide an overview of the linkages between regional and global water cycles, putting the focus in the necessity of a holistic approach to water resource

management. They will highlight the interconnectedness of different and distant areas of the word, contributing to a comprehensive understanding of atmospheric moisture dynamics with a view to develop more effective water management policies and strategies in a rapidly changing climate.

Chapter 1

Foundations and Concepts

1.1 The hydrological cycle

Water is indispensable for life. To quote the Swedish hydrologist Malin Falkenmark, 'It is the bloodstream of the biosphere', connecting people and places while playing a key role in human livelihoods and ecosystem functions across terrestrial and aquatic environments. In its three phases (solid, liquid, and gas), water bonds together the main components of Earth's climate system — air, clouds, oceans, lakes, vegetation, snowpack, and glaciers - creating a complex and sophisticated web of interactions that sustains life on our planet.

The total volume of water on or near Earth's surface is estimated at approximately 1.4×10^{18} m^3, which corresponds to a mass of 1.4×10^{21} kg. Although water covers 71% of Earth's surface, its distribution is highly uneven: saline ocean water accounts for about 96.6% of the total, while terrestrial freshwater represents only 1.8%, with the remaining 1.6% primarily composed of saline groundwater and lakes (Durack, 2015; Abbott et al., 2019). Of the precious freshwater resources, approximately 97% is locked in ice sheets, glaciers, and snow packs, leaving less than 3% easily accessible for essential ecosystem functioning and human needs. This accessible portion amounts to about 835 thousand km^3, with the majority contained in groundwater (630 thousand km^3) and the remaining 205 thousand km^3 stored in lakes, rivers, wetlands, and soils (Abbott et al., 2019).

This accessible freshwater plays a central role in sustaining human civilization, supporting activities ranging from irrigation to industrial processes, including hydroelectric power generation and cooling of thermoelectric power plants (Bates et al., 2008; Schewe et al., 2014). These activities extract water from various sources such as rivers, lakes, groundwater stores, and increasingly, desalinated seawater. The scale

of human impact on these water resources is significant — recent estimates suggest that half of global river discharge is redistributed each year by human water use (Abbott et al., 2019), highlighting the profound anthropogenic influence on this pivotal resource.

While water management traditionally focuses on visible water bodies and their use and pollution by humans, the majority of global freshwater flows occur through largely invisible pathways. In this context, the ocean plays the most important role. Its evaporation, of about 420 thousand km^3 per year, exceeds its precipitation of about 40 thousand km^3 every year. This net moisture transfer from oceans to the atmosphere ultimately reaches land masses, where land precipitation (110 thousand km^3 per year) significantly surpasses land evapotranspiration (69 thousand km^3 per year), creating the conditions necessary for the terrestrial life as we know it. Refer to Fig.1.1, for the visualization of the annual fluxes.

This ongoing movement of water, known as the hydrologic cycle, represents an intricate circulation system through Earth's climate elements. Water moves among the ocean, atmosphere, cryosphere, and land in its various forms — liquid, solid, and gas. The cycle is primarily driven by solar energy, causing evaporation and precipitation at Earth's surface, including transpiration from vegetation. Water that falls as precipitation over land, nourishing soil moisture, replenishing groundwater, and feeding river flows, typically originates from ocean evaporation or ice sublimation before its atmospheric transport as water vapor. In some regions, local evapotranspiration contributes significantly to this process (Gimeno et al., 2010; van der Ent and Savenije, 2013).

When air becomes saturated with water vapor, it condenses into clouds at various atmospheric altitudes, with local conditions determining their distinct types and characteristics. Though water vapor comprises only a small fraction of the atmosphere—roughly 0.3% by mass and 0.5% by volume—its impact on Earth's climate system is profound. Indeed, clouds covers approximately 60% of Earth's surface, serving as visible evidence of the importance of water vapor in the atmosphere. This process of cloud formation and precipitation does more than just produce rain; it also regulates a complex energy exchange. As water vapor condenses, it releases latent heat into the atmosphere, providing vital energy that powers atmospheric circulation and weather patterns. These phase transitions—from vapor to liquid to ice and back again—form a critical heat distribution network. The latent heat carried by water vapor acts as a global thermal conveyor belt, helping regulate temperatures worldwide and shaping our planet's diverse climate regions.

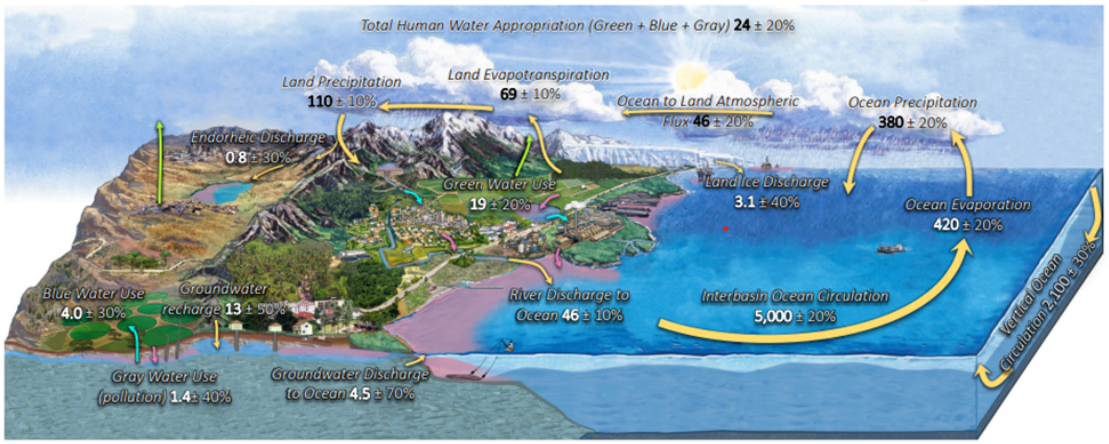

Figure 1.1: Main fluxes in the global hydrological cycle in 10^3 km^3 yr. Human water appropriation is separated into green (green arrows), blue (blue arrows) and grey (purple arrows), water use. Source: W. Abbott et al. 2020

1.1.1 Anthropogenic water cycle modifications

Water, a defining element of our planet, cycles on a vast scale, often measured in thousands of cubic kilometers or trillions of metric tons. Although the enormity of the water cycle might suggest that it is beyond our influence, human activities have disrupted it in many different ways. Anthropogenic actions are, indeed, exerting unprecedented pressure on essential planetary processes, pushing Earth beyond the stability of the Holocene epoch—the only known period in Earth's history capable of sustaining sedentary, complex human civilization. In this emerging Anthropocene, human influence is at a scale and intensity that risks triggering critical shifts, potentially compromising Earth's habitability for many ecosystems and human society (Barnosky et al., 2012; Steffen et al., 2018). Central to this challenge is the transformation of the water cycle, a core planetary system essential to countless Earth processes, interactions, and feedback mechanisms, yet increasingly disrupted by human actions on a global scale.

Such extensive human-driven change has made natural dynamics-based models inadequate for predicting groundwater levels, droughts, floods, and precipitation patterns. These impacts manifest both indirectly, through climate change resulting from greenhouse gas and aerosol emissions, and directly, through land surface alterations and extensive extraction of water resources for agriculture, industry, and domestic use.

First, nearly all agricultural, industrial, and domestic activities depend on water,

whether directly or indirectly. This usage, categorized as green (soil moisture used by crops and livestock), blue (direct consumption and transport of water), and gray (dilution of pollutants), has escalated to levels exceeding the global groundwater recharge rate (Döll and Fiedler, 2008; Gleeson et al., 2016) and now amounts to nearly half of the total water flow from land to sea—approximately 24,400 km^3 per year (Abbott et al., 2019).

Second, humans have transformed approximately 77% of Earth's land surface (excluding Antarctica) through agriculture, deforestation, and wetland destruction (Watson et al., 2018). These land-use changes alter essential hydrological processes such as evapotranspiration, groundwater recharge, and runoff, influencing water distribution both within and beyond local catchments in significant and often unexpected ways.

Third, climate change is fundamentally altering nearly every component of the water cycle, including ocean circulation, land ice melt, precipitation patterns, and drought and flood intensities (Famiglietti, 2014; Huang et al., 2016; Abbott et al., 2019; Falkenmark et al., 2019). A warming climate, for example, increases atmospheric moisture, which amplifies precipitation intensity during wet events and heightens flood risks. Specifically, for every 1°C of warming, near-surface atmospheric moisture increases by approximately 7%, intensifying extreme precipitation events from sub-daily to seasonal scales. Both extremely wet and extremely dry events have become more severe as a result of warming, although changes in atmospheric circulation create substantial regional and seasonal variability in the occurrence of these extremes. Furthermore, rising temperatures over land elevate atmospheric evaporative demand, intensifying drought conditions.

Pollution further exacerbates these alterations, particularly through aerosols that influence atmospheric physics, affecting cloud formation and, consequently, precipitation. Collectively, these human-driven changes underscore the urgent need to understand and address our impact on the global water cycle as we navigate the Anthropocene.

It follows, therefore, that the global hydrological cycle, generally renewable through its cyclical nature, is increasingly subject to significant spatial and temporal variability due to enhanced human interventions and recent rapid changes in climate and land use. Variability has given rise to a set of water challenges where climate fluctuations and land surface changes engender disparities in water resources in more than one dimension. These changes in turn have a huge influence on the timing, intensity, and duration of vaporization of water into the atmosphere, as well as on the subsequent distribution and impacts of precipitation in many areas.

1.1.2 Four core Earth system functions

The role of water in the Earth's natural system is expressed in four basic functions: hydroclimatic regulation, hydroecological regulation, storage, and transportation. Of these, every function underscores one or more aspects of water's critical role in promoting environmental stability and fostering biodiversity, making it of utmost importance to the resilience of ecosystems and the sustainability of human communities.

The first function considered is the hydroclimatic regulation, whereby water in its cycles of evaporation, condensation, and precipitation acts to moderate the climate of Earth. Indeed, water vapour operates as a greenhouse gas, while large bodies of water act as thermal reservoirs; together they act to regulate global temperatures and weather patterns. The second important function is hydroecological regulation, whereby water sustains ecosystem integrity and biodiversity. This is well illustrated by the wetlands that filter pollutants and improve water quality while providing critical habitats to many species. Water's presence in other ecosystems ensures their resilience to environmental stresses and maintains the complicated web of life dependent on stable water resources. The third core function is storage, as in the environment, there are several forms in which water exists: surface water, soil moisture, groundwater, and frozen in glaciers. It is through this storage function that the availability of some water during periods of deficit can be assured. Groundwater aquifers act as important reservoirs during droughts, whereas melting glaciers, in the warmer months, provide a steady supply. The fourth function—transport—allows for the movement of water, nutrients, and sediments from one ecosystem to another. Water, in both its atmospheric and surface routes, fulfills global moisture distribution and nutrient cycling. Rivers and streams transport sediments downstream, enriching floodplains and deltas, while atmospheric water vapor forms clouds that deliver precipitation across various climatic regions.

The role that water plays in climate regulation, ecosystem support, storage facilitation, and transportation is divided into five distinct water reservoirs: surface water, atmospheric water, soil moisture, groundwater, and frozen water. See fig.1.2 for an illustration of how these five main reservoirs interact with each other. Each acts as a different part of the hydrological cycle, providing unique functions to ecological and climatic functions.

Surface water—rivers, lakes, wetlands, and oceans—forms a basic source of accessible freshwater and plays a very important role in the four key functions. As regulators of hydroclimatic processes, such water bodies regulate themselves as thermal buffers by absorbing solar radiation and releasing heat slowly, tempering extreme variations of temperature. Moreover, surface water provides critical ecological habi-

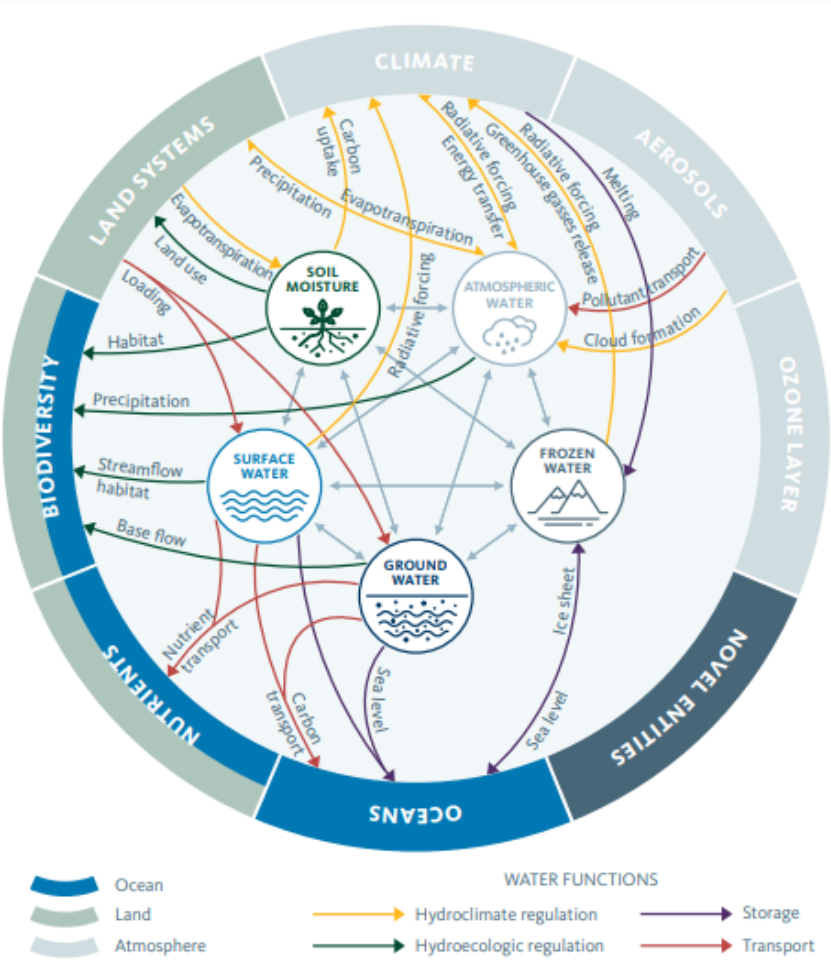

Figure 1.2: Four core Earth system functions of freshwater. The five major stores of water (soil moisture, atmospheric water, frozen water, groundwater, and surface water) interact substantially with all components of the Earth system. Source: Gleeson et al. (2020).

tats that host biodiversity and improves hydroecological regulation. Surface water has a dual role as a medium for both storage and transport. This allows the seasonal retention of water along with the downstream transfer of nutrients and sediments, which are the main ingredients for soil fertility and food webs in aquatic and riparian ecosystems.

Soil moisture is the water retained in soil particles, which provides the basic hydration for terrestrial vegetation and the key component of hydroecological reg-

ulation. It helps with plant growth and productivity, thus affecting the structure of vegetation and, by extension, whole food webs. It also tempers surface runoff and infiltration, thereby affecting how water gets into or moves over the landscape, controlling storage and transport functions. Soil moisture sustains ecosystem services and enhances resilience to droughts and extreme weather by maintaining soil stability and supporting plant communities

One of the world's largest sources of readily accessible freshwater is groundwater, stored in aquifers beneath the Earth's surface; it plays a critical role in each of the four primary services. This hidden reservoir acts as a long-term storage system, providing a stable supply during droughts when the availability of surface water decreases. It supports base flows in rivers and streams, contributing to the hydroecological regulation of ecosystems during dry seasons. As an extremely important source of water for both human use and ecological use, it provides for transport, sustaining river flows carrying nutrients, sediments, and organisms downstream. Rates of recharge and availability are sensitive to the dynamics of atmospheric and surface water, indicating a strong coupling among stores.

Frozen water, primarily in the form of glaciers, ice caps, and permafrost, constitutes a significant portion of Earth's freshwater reserves. This store acts like a "climate buffer," where frozen reservoirs hold on to water in solid form and give it up slowly through meltwater that supplies rivers and ecosystems downstream. The cryosphere, by reflecting solar radiation, plays a role in modulating global temperatures and hydroclimatic conditions. The seasonal melt of glaciers and snowpacks provides a fresh water supply for the downstream regions, feeding agriculture, human consumption, and ecosystem health. Frozen water reserves thus bridge temporal scales, linking present water needs with long-term hydrological stability.

Atmospheric water, represented as water vapour, clouds, and precipitation, is a relatively minor but dynamically important reservoir of water. It is essential in hydroclimatic regulation since it enables atmospheric transport of heat and moisture, affecting the patterns of precipitation and modulating climates at the regional scale. The cycling of atmospheric water controls the soil moisture, recharges surface water bodies, and affects the rates of groundwater recharge and, therefore, is an integral component of water storage processes. Atmospheric water, through precipitation, also links distant ecosystems, allowing this transport function that distributes moisture and nutrients across the geographic regions and links ecosystems by hydrological flows.

The upcoming pages will focus specifically on this last store, with the aim of thoroughly examining the large-scale mechanisms that govern the atmospheric water cycle. From evaporation, through the transport of water particles in the atmosphere,

to their eventual precipitation, the processes that enable this vital flow to occur will be explored.

1.2 Evaporationsheds and precipitationsheds

Global, regional, and local climates are impacted by atmospheric moisture linkages, which shift water from evaporation sources to precipitation sinks. Understanding the significance of terrestrial evaporation for water availability requires an understanding of these relationships, which are essential to the global hydrological cycle. Since evaporated water can travel thousands of kilometres in the atmosphere before falling as precipitation, modification in the evaporation process can lead to transformation in these connections between sources and sinks (J. Theeuwen et al. 2023).

Moisture recycling is the process through which evaporated water travels through the atmosphere and returns as precipitation downwind. This phenomenon can be analyzed through both forward and backward tracking of atmospheric moisture flows. The first one follows moisture from its evaporation source to where it eventually precipitates, while the second one follows precipitation back to its various evaporation sources. These tracking methods help us understand two closely connected concepts: precipitationsheds and evaporationsheds.

These two elements are of fundamental importance when considering the atmospheric moisture tracking in the aim of understanding the complex spatial relationships in the atmospheric water cycle. Indeed, in an analogous way to river hydrology—where watersheds provide the surface water flow paths—these two concepts allow to map the atmospheric water pathways.

Precipitationsheds (Fig.1.3 (b)), revealed through the backward moisture tracking, represent the spatial footprint of moisture sources that contribute to precipitation events in a specific target region (P. Keys et al. 2012). In other words, a precipitationshed shows where atmospheric moisture originates before falling as precipitation. This concept is particularly interesting as it identifies critical source regions that provide moisture to a specific area, allows to quantify the relative importance of different moisture sources, and reveals the spatial extent of atmospheric moisture connections. Furthermore, it can consequently highlight how land-use changes, both near and far, can change local precipitation, helping understanding seasonal variations in moisture sources.

On the other hand, evaporationsheds (Fig.1.3 (a)), identified through the forward moisture tracking, show the final destiny of water that evaporates from a specific source region (J. van der Ent et al., 2013). In this way, these footprints map the spatial distribution of where the local evaporated moisture precipitates at the end of

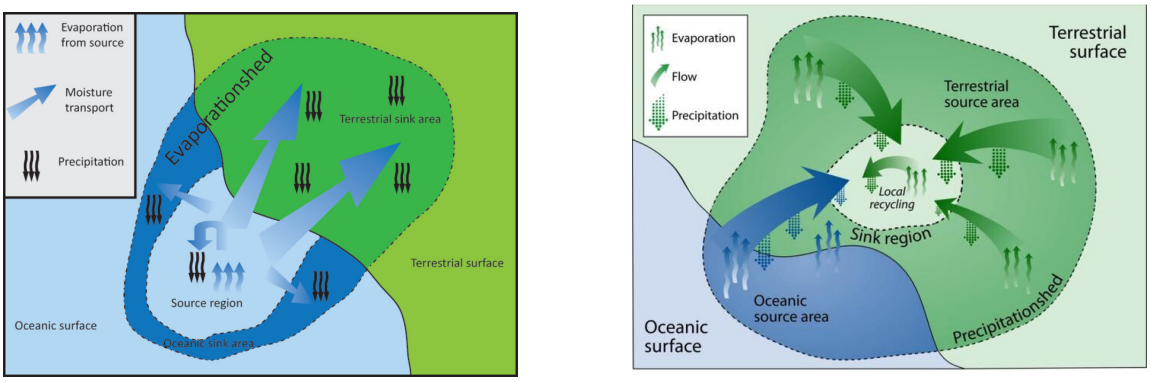

(a) Evaporationshed (b) Precipitationshed

Figure 1.3: (a) Conceptual image of an evaporationshed, with evaporation in the source region ending up on both terrestrial and oceanic sink regions as precipitation. Source: J. van der Ent et al. 2013. (b) Conceptual image of a precipitationshed, with precipitation in the sink region originating from both terrestrial and oceanic sources of evaporation. Source: P. Keys et al. 2012.

its journey, helping in revealing the downstream impacts of local land-use changes and quantifying the role of an area as a moisture source for other regions. As for the precipitationsheds, they also identify moisture transport corridors in the atmosphere and allow us to understand the extension of hydrological connections between different regions.

Together, these two complementary concepts give a comprehensive overview of atmospheric moisture transport. While precipitationsheds answer the question 'Where does a region's rain come from?', evaporationsheds answer the question 'Where does a region's evaporation go?' Many facets of resource and environmental management depend on this dual perspective. In water resource management, it helps to understand the dependencies of local precipitation on external sources, assess potential sensitivity to upstream land use changes, and organize plans for climate change adaptation. For policy making, it could allow to identify adequate stakeholders in atmospheric water resources, inform international water management policies, and lead to cross-boundary water resource agreements. Furthermore, in the context of climate studies, precipitationsheds and evaporationsheds are particularly important for identifying the impacts of land-use changes on regional precipitation, understanding intricate teleconnections in the water cycle, and assessing possible instabilities in the precipitation sources due to climate change (J. Rockström et al., 2023).

As we face growing challenges in water resource management in relation to an-

thropogenic stresses and global warming, the study and analysis of these atmospheric water pathways is becoming more and more crucial and of relevant importance.

1.3 Precipitation and evaporation recycling

Precipitationsheds and evaporationsheds serve as conceptual frameworks that help to understand moisture recycling patterns. Moisture recycling can be seen as a continuous cycle, where water moves through various stages, driven by evaporation and precipitation. This cycling process can be quantified through two key metrics usually expressed as percentages: the evaporation recycling ratio and the precipitation recycling ratio.

The evaporation recycling ratio is defined as the fraction of water that evaporates from a given area and subsequently precipitates within the same area, relative to the total evaporation from that area. Calculating evaporation recycling requires that moisture evaporated from the region of interest is tracked to determine where precipitation is generated. This computation is performed through the use of the forward tracking model.

On the other hand, the precipitation recycling ratio is defined as the fraction of precipitation falling in a given area that originated as evaporation from the same area, relative to the total precipitation in that area. To compute precipitation recycling, the path of precipitation in a given region must be tracked back to identify where the water was evaporated upwind. This is carried on through the backward tracking models which determine where the moisture that led to precipitation in a specific region originated.

Precipitation and evaporation recycling ratios can be read through various perspectives, each giving important interpretations into the regional hydrology and atmospheric moisture patterns. In particular, their computation may provide useful indicators of a region's hydrological self-sufficiency and its relations with external moisture sources. A high precipitation recycling ratio denotes that a considerable portion of local precipitation takes origin from the region itself, indicating a high hydrological autonomy and a reduced exposure to changes in external moisture transport. Conversely, a low precipitation recycling indicates a substantial dependence on atmospheric moisture imported from other regions, making the area more sensitive to changes in large-scale atmospheric circulation patterns or land-use changes in upwind regions.

Furthermore, from a meteorological perspective, precipitation recycling also shows the efficiency of local atmospheric processes in converting evaporated moisture back

into precipitation, giving perception of the strength of local convection and precipitation mechanisms.

While precipitation recycling can be considered as an indicator of a region's 'atmospheric water self-sufficiency', the evaporation recycling can be interpreted as a measure of moisture 'retention efficiency', that is how effectively a region retains its evaporated water within its boundaries. A higher evaporation recycling indicates that the area behaves as a more efficient 'moisture recycler,' successfully capturing and reusing its evaporated water. From an atmospheric transport perspective, evaporation recycling also point out the region's role as a moisture source - lower values suggest the area acts mainly as a moisture source for other regions, while higher values indicate more local moisture recycling. When interpreted together, these ratios can reveal complex regional characteristics. For instance, a region with high evaporation recycling but low precipitation recycling might be characterized as a 'moisture transformer,' efficiently processing atmospheric moisture but still requiring significant external inputs. Conversely, an area with low evaporation recycling but high precipitation recycling might be considered a 'moisture accumulator,' heavily dependent on local recycling despite losing much of its evaporated moisture to other regions. These interpretations are particularly valuable for understanding regional vulnerability to climate change, potential impacts of land-use modifications, and the interaction of regional water cycles.

This theoretical framework has been recently applied to practical cases. As shown by O. Tuinenburg et al.(2020), the analysis of recycling ratios across the world's 26 largest river basins reveals noticeable patterns in atmospheric moisture dynamics (Fig.1.4). The study found that evaporation recycling ratios typically exceed precipitation recycling ratios. This prevalent pattern suggests that most major river basins act as net moisture sources for other regions, exporting more of their evaporated moisture than they retain. The tropical river basins, particularly the Amazon and Congo, demonstrate the highest evaporation recycling ratios (63% and 60% respectively), highlighting the intense local water cycling in these regions. On the contrary, low midlatitude regions show the lowest recycling ratios (0-0.4). These patterns have important implications for understanding regional vulnerability to climate change and land-use modifications. Regions with high recycling ratios, like the Amazon and Congo basins, may be particularly sensitive to deforestation and land-use changes that could disrupt their efficient moisture recycling systems. Conversely, regions with low recycling ratios may be more vulnerable to changes in large-scale atmospheric circulation patterns and remote moisture sources.

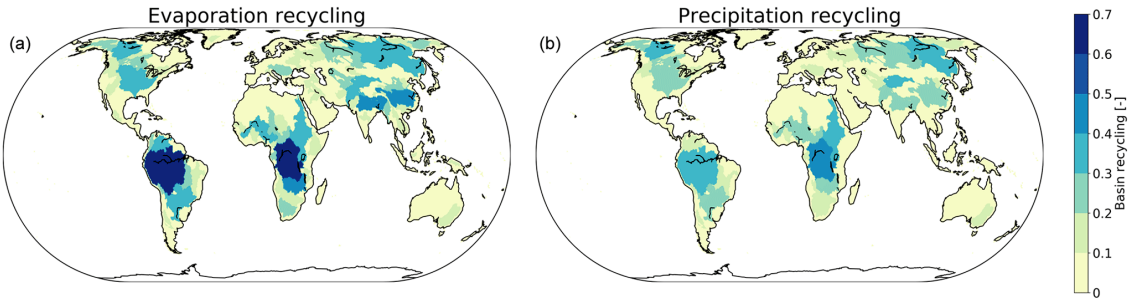

Figure 1.4: Average evaporation (a) and precipitation (b) recycling ratios for basins. Source: O. Tuinenburg et al., 2020.

1.4 Moisture-tracking models

Understanding the movement of water particles in the atmosphere, in particular how moisture recycles and flows through the air tracing complex trajectories, requires advanced computational methods that could be drawn from different datasets. In this respect, moisture-tracking models have raised as the most powerful tools to compute these patterns. These elaborated models use atmospheric reanalysis data to trace the water's journey in the sky, constantly updating their calculations based on basic factors such as evaporation rates, rainfall patterns, and wind behavior (speed and direction). See Fig.1.5 for a schematic representation. Through the processing of this information, it is possible to map out the whole moisture trajectory—from where it comes from to where it eventually precipitates.

The primary distinction between different moisture-tracking models resides in how they represent space. These models can be generally divided into two principle groups: Eulerian models, which are based on a fixed grid structure, and Lagrangian models, which are based on trajectories.

In Eulerian models, the area under study is divided into a two/three dimensional grid of cells. During each time step, the moisture content in each cell is updated based on estimated winds moving between cells, together with precipitation and evaporation data. The main advantage of Eulerian models is related to their efficiency, specifically for simulations where moisture is tracked across a large portion of the world. This efficiency is related to their scalability—every grid cell is updated at the same rate, regardless of how much moisture is present, making them well-suited for large-scale simulations.

On the contrary, in Lagrangian models, the internal state isn't defined by a grid but consists of a set of water parcels. As the simulation goes on, these parcels are

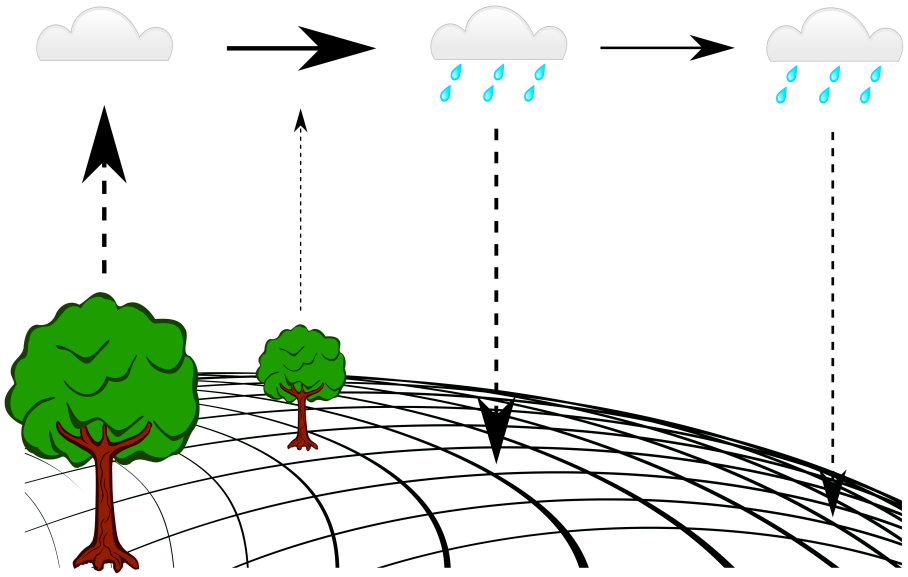

Figure 1.5: Moisture tracking from source to sink. Source: O. Tuinenburg and A. Staal, 2020.

released and carried by the wind field used in the model. Unlike Eulerian models, the position of these parcels isn't limited to the grid of the input data, allowing Lagrangian models to manage significant atmospheric moisture fluxes and to trace trajectories. This flexibility enables parcels to move across multiple grid cells of the forcing data in a single time step. A key advantage of Lagrangian models is their ability to avoid the numerical inaccuracies that is often associated with Eulerian models due to the grid structure.

1.4.1 ERA 5

The choice of the most appropriate model depends not just on the study's goals but also on the quality and detail of the data used to carry it on. Recently, the high-resolution ERA5 reanalysis dataset has set a new standard, permitting the development of a new surge of moisture-tracking models. With reanalysis data is intended a scientific method that combines real-world observations with computer model simulations to create a comprehensive, consistent picture of Earth's climate system over time. This means that it reconstruct the weather of the past using both historical observations and modern understanding of atmospheric physics.

In this respect, ERA5 stands as the fifth generation of atmospheric reanalysis data

produced by the European Centre for Medium-Range Weather Forecasts (ECMWF), developed by the Copernicus Climate Change Service (C3S). This innovative dataset represents a significant leap forward in climate and weather data assimilation, offering hourly estimates of atmospheric, land-surface, and sea-state parameters dating back to 1940. At its core, ERA5 operates at a horizontal resolution of 31 kilometers globally. This means that each grid cell covers a square of 0.25 degrees by 0.25 degrees on the Earth's surface, introducing a substantial enhancement from ERA-Interim's 79-kilometer resolution. The vertical structure spans 137 levels, reaching from the Earth's surface up to 80 kilometers into the atmosphere. Furthermore, ERA5 provides hourly data outputs, a significant improvement from the previous six-hourly intervals, enabling much more detailed temporal analysis.

When compared to its predecessor ERA-Interim, ERA5 demonstrates substantial improvements across multiple aspects. The tropospheric representation achieves higher accuracy, while the stratospheric circulation patterns show marked improvement. Precipitation patterns are captured with greater precision, and tropical cyclones are represented with enhanced detail. The physical processes modeling has also seen significant advancement, particularly in areas such as land-surface parameterization, radiation schemes, and cloud microphysics.

1.4.2 UTrack-atmospheric-moisture

The 2020 study by O. Tuinenburg and A. Stall developed and systematically evaluated a set of moisture-tracking models using ERA5 data. Following the introduction of this new dataset, determining the most suitable model for calculating atmospheric moisture flows became essential.

The study compared Eulerian and Lagrangian models, testing both with two- and three-dimensional forcing data to examine how vertical variability in atmospheric moisture flows affected tracking results. In the three-dimensional data simulations, horizontal transport (north-south/"northward" and east-west/"eastward" in ERA5) was driven by wind speed at the specific pressure level of each parcel (Lagrangian model) or grid cell (Eulerian model).

The moisture-tracking models were forced with ERA5 hourly atmospheric reanalysis data at 0.25×0.25 resolution. The analysis incorporated two-dimensional fields (total precipitation, evaporation, vertical integrals of northward and eastward water vapor flux, total column water vapor) and three-dimensional fields (specific humidity, U and V wind speed components, and vertical wind speed).

The study found that three-dimensional Lagrangian models provided superior accuracy and computational efficiency compared to Eulerian versions when tracking

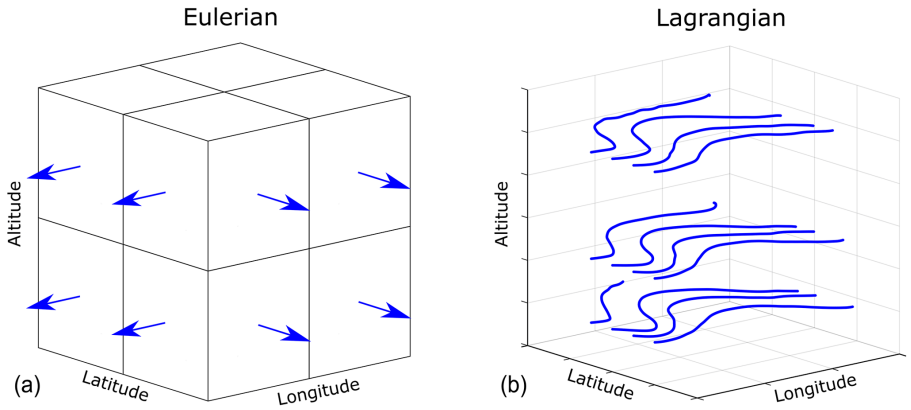

Figure 1.6: Differences between Eulerian and Lagrangian moisture-tracking models. Source: O. Tuinenburg and A. Staal, 2020.

water from single grid cells. The greatest source of uncertainty in moisture tracking stemmed from the rate of vertical mixing of moisture in the atmosphere. The researchers concluded that while the enhanced resolution of atmospheric reanalysis data enables more precise moisture tracking results in a Lagrangian framework, significant uncertainty persists regarding turbulent mixing. Their work introduced an efficient Lagrangian method for tracking atmospheric moisture flows globally using ERA5 reanalysis data. The model, named UTrack-atmospheric-moisture, was made publicly available with its accompanying code (DOI UTrack dataset: 10.1594/PANGAEA.912710, DOI UTrack support paper: 10.5194/essd-12-3177-2020).

In this study, the global atmospheric moisture connections from Tuinenburg et al. (2020) will be utilized. These moisture connections represent a 10-year climatology (2008–2017) of monthly averages at a 0.5° spatial resolution. This model's methodology involves the release of 100 moisture parcels for each millimeter of evaporation in each 0.25° grid cell. These parcels are transported horizontally and vertically through the atmosphere by wind. The vertical movement occurs across 25 atmospheric layers through a probabilistic scheme, where parcels are randomly distributed across each grid cell's vertical moisture profile. The moisture budget is calculated at 0.1-hour time steps using evaporation, precipitation, and total precipitable water.

Parcel tracking continues for up to 30 days or until only 1% of original moisture remains. While the average atmospheric moisture lifetime is 8-10 days (Sodemann, 2020), some moisture may persist beyond this period. By 30 days, most parcels have released all their original moisture through rainfall (Tuinenburg and Staal, 2020).

For complete model settings, tests, and underlying assumptions, readers should reference Tuinenburg and Staal (2020).

Chapter 2

Territorial Framework and methodology

2.1 Study areas

The present work focuses on the atmospheric moisture transport patterns of Italy, along with three diverse regions representing different geographical and climatological contexts in the Mediterranean basin: Piemonte (25.400 km^2) in the north, Lazio (17.203 km^2) in the central area, and Sicily (25.711 km^2) in the south.

The Italian boot-shaped peninsula extends from about 35°N to 47°N latitude and from about 6°E to 18°E longitude, covering an extension of 302.070 km^2. The country extends some 1.200 km north to south, with its width varying considerably from about 530 km across in the north to only about 100 km in the south.

The main features of the country include two principle mountain ranges: the Alps, stretching from west to east along the northern border, and the Apennines, extending from northwest to southeast, appearing as the backbone of the boot. This mountainous framework, combined with approximately 7.600 kilometers of coastline on three sides, results in a noticeable mix of climatic zones throughout the territory.

The regional climate variations across Italy display an interesting influence of geographical factors. In northwestern Piemonte, the Alpine backdrop leads to a continental climate with the presence of precipitation throughout the year, reaching its peak during spring and autumn. Going to central Italy, the Tyrrhenian coastal region of Lazio witness the classic Mediterranean presence of hot, dry summers with mild, wet winters, affected by the interplay of maritime and continental air masses. Further south, Sicily, the largest island in the Mediterranean, is characterized by a more pronounced Mediterranean climate with rather prolonged hot summers marked

Figure 2.1: Map of Italy. Areas in red represent the study regions: Piemonte (nord), Lazio (center), Sicilia (south).

by arid periods and mild winters, with rainfall primarily concentrated in the winter months.

This vast geographical and climatic variability makes Italy a very special natural case study for investigating precipitation, moisture recycling, and intricate relationships between local and remote water sources in the Mediterranean region. The unique configuration of the country provides an insight that is particularly valuable in understanding how topographical features and varying climatic regimes affect moisture transport and recycling in the Mediterranean basin and beyond.

2.2 Precipitation and evaporation in Italy

Fig.2.2 presents the spatial distribution of cumulative annual precipitation (a) and evaporation (b) over Italy for the period 2007-2018. The data were taken from ERA5 monthly averaged reanalysis (total precipitation and total evaporation). Originally in meters per day, these data were processed through multiple steps to obtain meaningful annual accumulations. First, monthly accumulations were calculated by multiplying the daily means by the number of days in each month. Indeed, in the ERA5 dataset, the accumulations in monthly means of daily means have been originally

scaled to have units that include "per day". This procedure was applied to both precipitation and evaporation data.

To account for interannual variability, the analysis was performed for each month during the 10-year period (2008-2017). Cumulated monthly values were then averaged across years to obtain characteristic monthly accumulations representative of the study period. Finally, these monthly averages were summed to produce the mean annual accumulations shown in the Fig.2.2.

Since ERA5 provides precipitation and evaporation data at 0.25° resolution while UTrack operates at 0.5° resolution, a regridding process have been performed on the ERA5 data in order to ensure consistency. This regridding was performed using Climate Data Operators (CDO), a collection of command-line tools developed by the Max Planck Institute for Meteorology to process climate and meteorological data. The command to perform this operation was:

```
cdo remapcon,r720x360 input.nc output.nc
```

where 720 is the number of longitudes and 360 the number of latitudes.

This conservative interpolation in CDO is a regridding method specifically designed to preserve the integrals of meteorological variables when transitioning from one grid to another. This is particularly important for variables like precipitation and evaporation, where the mass balance must be conserved.

Both precipitation and evaporation reveal distinct patterns in the two representative plots, exhibiting a complementary trend. Indeed, annual precipitation shows a higher accumulations in the northern regions, particularly along the Alpine arc, with Valle d'Aosta and Friuli Venezia Giulia the most affected regions, showing values exceeding 2.0 m. Rather intense rainfall can be also noticed along the Apennine arc, especially in the western side.

Conversely, evaporation patterns show a notable gradient, with higher values over the Mediterranean Sea and lower accumulations over the mainland, ranging from 0.4 to 1.4 m annually. As oppose to precipitation, the lowest values are visible along the Alpine arc.

At the national scale, Italy shows an average annual precipitation of 1.08 m and an evaporation of 0.68 m, indicating an overall positive water balance. However, this national average is characterized by a significant regional heterogeneity, as noticed by analyzing the three study regions. Piemonte, while maintaining relatively low evaporation (0.62 m), exhibits the highest precipitation among the studied regions, with an average value of 1.4 m. This substantial precipitation surplus (0.78 m) can be ascribable to its proximity to the Alps and the associated orographic effects, while

the lower evaporation rates is a reflection its more temperate continental climate and higher latitude position.

Lazio, in central Italy, shows values closer to the national average, with 1.13 m of precipitation and 0.73 m of evaporation. This region's moderate surplus, that is 0.40 m, represents a transitional position between northern and southern climatic regimes and demonstrates the simultaneous influence of both Mediterranean and continental air masses. Sicily presents an evident contrast, as it is the only region among those studied with a negative water balance: 0.63 m of precipitation versus 0.80 m of evaporation, resulting in a deficit of 0.17 m. This pattern is characteristic of south of the Mediterranean basin, where high summer temperatures and intense solar radiation lead to substantial evaporation rate, while precipitation is limited and concentrated only in some periods of the year.

The highlighted north-to-south gradient in these patterns is particularly noteworthy: precipitation decreases southward (from 1.40 to 0.63 m) while evaporation increases (from 0.62 to 0.80 m). This inverse relationship makes evident the transition from the water-abundant northern regions to the water-limited southern regions, reflecting the tight interaction between latitude, topography, and Mediterranean influences in impacting the hydrological regime of the peninsula.

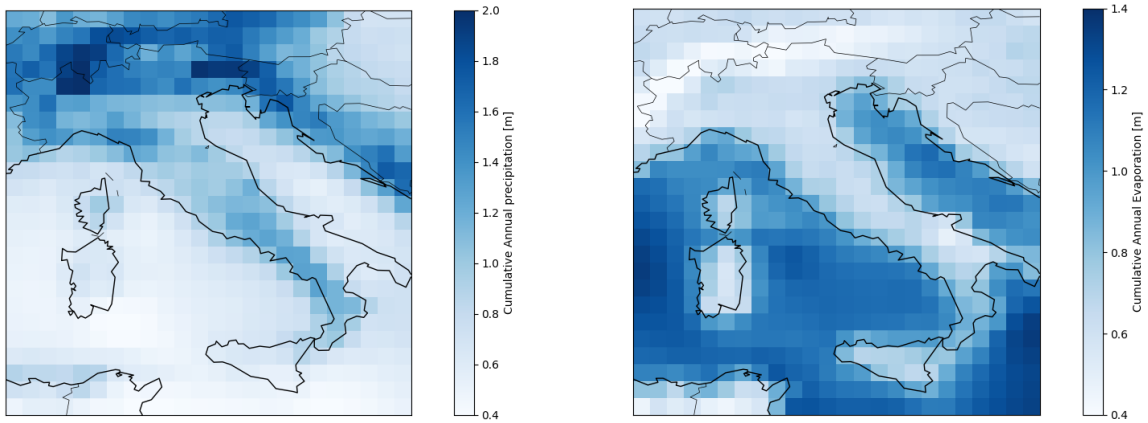

(a) (b)

Figure 2.2: Cumulative annual precipitation (a) and cumulative annual evaporation (b), 0.5 degrees of resolution. Plots are obtained averaging the ERA 5 values of precipitation and evaporation in the reference period 2008-2017.

2.3 Utrack processing

The UTrack dataset offers data for a mean reference year y for the years 2008-2017 at a monthly resolution (m) and at 0.5° and 1° resolutions. In this case, the dataset is used for analysis at a spatial resolution of 0.5°. Within the data set, the choice of a source cell s (point of evaporation) gives a detailed matrix that illustrates the monthly forward footprint of atmospheric moisture, $p_f(s,t,m)$. The matrix is meant to express the proportion of evaporation from the specified cell s that is transported to each target cell t during the month m. In contrast, the identification of the target cell t (the precipitation site) produces the monthly backward footprint of atmospheric water, $p_b(s,t,m)$, the proportion of precipitation in cell t contributed by upwind evaporation in each of the source cells s (reference article in DOI: https://doi.org/10.21203/rs.3.rs-4177311/v1).

Annual atmospheric moisture forward and backward flows (m^3/y) are reconstructed by sourcing, for each month, the forward footprint $p_f(s,t,m)$ and the backward footprint $p_b(s,t,m)$. Since the footprint of atmospheric moisture is dimensionless, and evapotranspiration $ET_c(c)$ and precipitation $P_c(c)$ are provided in meters per day, the area of each cell $a(c)$, in square meters, and the number of days in each month $d(m)$ are considered to compute the cumulative atmospheric moisture volumes in cubic meters. Hereafter, the generic cell c is referred to as s when acting as a source cell and t when acting as a target cell. In the forward approach, the average annual atmospheric moisture flow, $ff(s,t)$, from a source cell s (evaporation) to a matrix of target cells t (precipitation) is evaluated as:

$$ff(s,t) = \sum_{m=1}^{12} ET_{ERA5}(s,m) \cdot pf(s,t,m) \cdot d(m) \cdot a(s) \tag{2.1}$$

where:

- $ET_{ERA5}(s,m)$ is the **evaporation rate** in meters per day for month m at cell s.
- $pf(s,t,m)$ is the **forward footprint**, representing the fraction of evaporation from s that reaches t as precipitation.
- $d(m)$ is the **number of days in month** m.
- $a(s)$ is the **area of source cell** s (in square meters).

In the backward approach, the average annual atmospheric moisture flow, $f_b(s,t)$, from a target cell t to a matrix of source cells s is evaluated as:

$$fb(s,t) = \sum_{m=1}^{12} P_{ERA5}(t,m) \cdot pb(s,t,m) \cdot d(m) \cdot a(t) \tag{2.2}$$

where:

- $P_{ERA5}(t,m)$ is the **precipitation rate** in meters per day for month m at cell t.
- $pb(s,t,m)$ is the **backward footprint**, representing the fraction of precipitation in t that originates from evaporation in s.
- $d(m)$ and $a(t)$ are the same as above but applied to the target cell.

2.4 Utrack correction and RECON dataset

The UTrack dataset is an efficient means of observing atmospheric moisture motions, supplying informative data on endpoints of evaporation and precipitation sources. While displaying skill in recreating paths of moisture, there exist systematic disparities between the mentioned dataset and ERA5's atmospheric reanalysis data. The variations require application of post-processing correction for enabling usage of the dataset in hydrological research without raising concerns regarding credibility. This correction hss been carried on by the Department of Environment, Land and Infrastructure Engineering, Politecnico di Torino, leading to the releasing of the RECON dataset (available at 10.5281/zenodo.14191920).

The ERA5 reanalysis data provide a physically constrained estimate of the global atmospheric state, mixing observational and numerical weather prediction inputs. The comparison of UTrack-based estimates of evaporation and precipitation at national and regional levels with ERA5 reveals large differences.

One of the significant sources of inaccuracy in the UTrack dataset is the imbalance between the global total recorded precipitation and evaporation. While ERA5 data is constrained by empirical observations, small inconsistencies are present in its comprehensive water budget. To negate this problem, in the RECON dataset a correction factor α has been applied to achieve long-term coherence of total atmospheric moisture flowes.

First, the global annual totals of ERA5 evaporation $ET_{\mathrm{ERA5,g}}$ and precipitation $P_{\mathrm{ERA5,g}}$ over the reference period (2008–2017) are computed.

These quantities are then adjusted to achieve the balance. This ensures that the total atmospheric moisture input (evaporation) and output (precipitation) are equal

in the long term, complying with mass conservation. The application of α does not alter the spatial distribution of atmospheric moisture flows but helps correct systematic biases, improving the dataset's reliability for hydrological studies.

Through the application of this correction, the discrepancy between total precipitation and evaporation in ERA5 data is fixed, reaching a closed 10-year water balance.

Despite the use of the α correction, discrepancies at the local and regional levels persist between the UTrack and ERA5 datasets. To correct these discrepancies in a systematic way, the Iterative Proportional Fitting (IPF) method is employed in the RECON dataset.

The IPF method works by adjusting the bilateral atmospheric moisture flows (evaporation $\rightarrow$ precipitation connections) so that each country's total evaporation and precipitation match ERA5 data.

This is accomplished while preserving the structural coherence of the dataset. Each pass of the algorithm adjusts the matrix values step by step, bringing them closer to the physical bounds expressed by the reanalysis data.

A key advantage of the IPF approach is that it introduces only minimal distortions to the dataset. Indeed, the total moisture flow adjustments are small ensuring that the fundamental spatial patterns and connections within the dataset remain intact. This correction enhances the reliability of the UTrack dataset by resolving inconsistencies with ERA5 data while maintaining the original topology of atmospheric moisture flows.

Once these modifications have been applied, to provide the continuity with the Utrack dataset data format and reduce the RECON dataset weight, moisture flow volumes are stored as integers [0, 255] and must be converted to cubic meters, as followed:

$$y = 10^{\frac{z-1}{254}\cdot[\log_{10}(y_{\max})-\log_{10}(y_{\min})]+\log_{10}(y_{\min})} \tag{2.3}$$

Where: z is the volume retrieved from RECON, $y_{\max} \approx 122079329\,m^3$ is the maximum volume in m^3 contained in RECON, and $y_{\min} = 10^{-3}\,m^3$ is the minimum threshold chosen to consider a moisture volume.

2.5 Italian and regional moisture volumes computation

The elaboration of the UTrack model has enabled the tracking and computation of atmospheric moisture flows on the global scale, allowing for a detailed analysis of two important aspects of the hydrological cycle. Through the application of this model, it has been possible to develop both precipitation basins and evaporation basins, which provides a precise understanding of moisture pathways in the atmosphere. In the case of the forward footprint (evaporationsheds), the model identifies the final destination (a matrix of target cells) for moisture evaporating from each geographic cell on the Earth's surface (the source cell), quantifying these flows in volumetric terms (cubic meters per year or per month, depending on the reference period analyzed). This volumetric quantification enables the reconstruction of a global 2D map (at 0.5° resolution) for each source cell, where each of the 360×720 target cells is assigned the volume of water that evaporated from the source cell and later precipitated in that specific location. This allows for a detailed spatial representation of precipitation originating from a given evaporation source. Similarly, through the analysis of the backward footprint (precipitaitonshed), the model identifies and quantifies volumetrically the contributions of all source areas that feed precipitation in a given geographic cell, allowing the reconstruction of the origins of local precipitation and the quantification of the contribution from each source area to the target cell.

The determination of precipitationsheds and evaporationsheds for the selected study areas—Italy, Piedmont, Lazio, and Sicily—involved a methodology developed in the following phases. Initially, a spatial analysis was perfomed to identify all the grid cells that intersects each region of interest. This analysis returned the identification of a specific number of cells for each area: 234 for the entire Italian territory, 23 for Piedmont, 20 for Lazio, and 32 for Sicily.

To improve the accuracy of the analysis, a weighting coefficient was assigned to each intersected cell, calculated as the ratio between the area of the region effectively contained within the cell and the total area of the cell itself. This procedure allowed to get a more precise representation of the spatial distribution: cells fully contained within the region of interest were assigned a coefficient of 1, while partially intersected cells were given a coefficient between 0 and 1, proportional to the fraction of the regional area actually present in the cell. Fig. 2.3 displays the detected intersecting cells, with colors proportional to their weighting coefficient .

The methodology for calculating the weighting coefficients was carried on using the EPSG:3035 reference system (ETRS89-extended / LAEA Europe), a choice par-

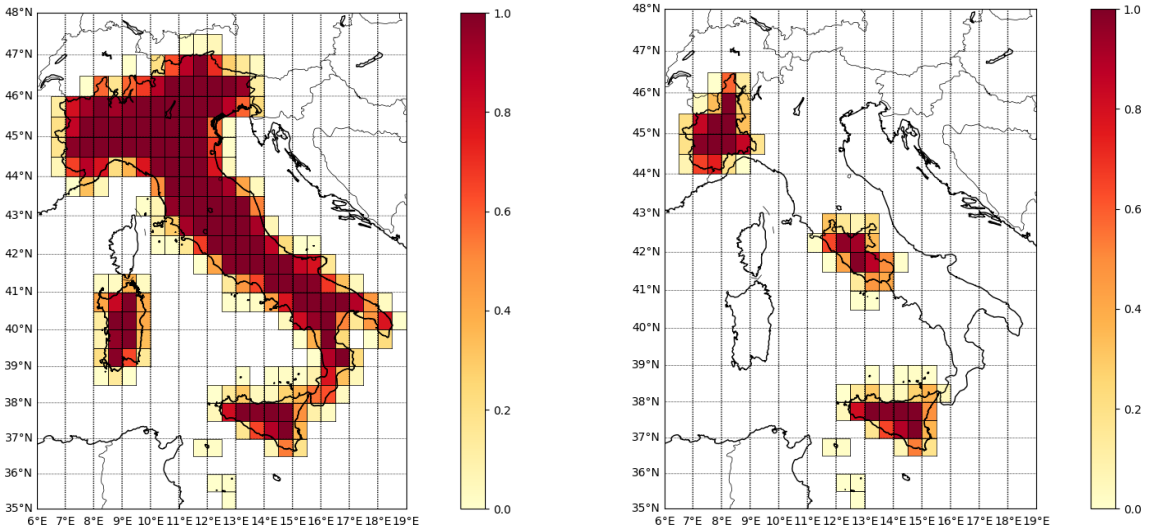

(a) (b)

Figure 2.3: Intersecting cells for Italy and regions. The intensity of the red tone is proportional to the weighting coefficient

ticularly suitable for spatial analysis in the Mediterranean area. This Lambert Azimuthal Equal Area projection was specifically designed for Europe and has optimal characteristics for calculating geographic areas in this context. It's based upon an equal-area approach which ensures that areal proportions are preserved, minimizing distortions in surface measurements.

Once the weighting coefficients were defined, the calculation of precipitationsheds and evaporationsheds for each study area was carried on through a weighted aggregation process. For the precipitationsheds, the backward footprint of each intersected cell was multiplied by its respective weighting coefficient; similarly, the forward footprint was used for the evaporationsheds. The sum of these products generated a two-dimensional matrix representing the global spatial distribution of precipitationsheds (or evaporationsheds) for the entire study area. This methodological approach allows to obtain an accurate representation of atmospheric moisture flows, taking into account the actual geographic extension of the analyzed regions within the geographical grid.

For the forward analysis, the atmospheric moisture forward flow (Equation 2.1) is computed for each cell intersecting the study region and multiplied by its corresponding weighting coefficient. The weighted values from all intersecting cells are then summed to determine the total atmospheric moisture forward flow of the study

region. The same process was applied for the backward analysis using Equation 2.2.

The total atmospheric moisture forward flow for a study region is computed as:

$$FF(R) = \sum_{s \in R} w(s) \cdot ff(s,t), \quad \forall t \in \text{World} \tag{2.4}$$

where:

- $FF(R)$ represents the **total atmospheric moisture forward flow map** for the study region R.
- The equation is computed for **all target cells** t across the world.
- $w(s)$ is the **weighting coefficient** for each intersecting source cell s.
- $ff(s,t)$ is the **atmospheric moisture forward flow** from each source cell s to every target cell t.

2.6 Statistical analysis

The calculation of precipitationsheds and evaporationsheds in volumetric terms for the selected study areas (Italy, Piedmont, Lazio, and Sicily) provided a detailed representation of atmospheric moisture flows on a global scale. This volumetric quantification forms the basis for an in-depth analysis of moisture exchange patterns between different regions and countries.

In the specific case of evaporationsheds, obtained through forward analysis, it is possible to determine the volumetric contribution of evaporation from the reference region to precipitation at a global level. This enables an evaluation of the percentage of such evaporation that returns to land versus oceans. This distinction between terrestrial and marine precipitation is essential, as the ecological and management implications differ significantly: water that precipitates on land can be directly used by natural and socioeconomic systems, while water that ends up in the oceans is effectively removed from the continental hydrological cycle.

Subsequently, the amount of water precipitated over each country in the world that effectively comes from the reference region can be determined, pointing out the main recipient countries of the evaporation from a specific area. This kind of detail allows deeper understanding of hydrometeorological connections among various regions, showing which countries depend most on the moisture evaporated from the study region. This information becomes important in the planning and management

of water resources, since it could help identify areas that could be more vulnerable in the case of changes in the patterns of evapotranspiration.

The sum of all evaporationsheds for the reference area allowed the calculation of total evaporation in cubic meters occurring within the area over the selected time period. This value was subsequently compared with total evaporation data provided by ERA5 reanalyses to verify consistency between the two datasets.

These analyses were conducted using QGIS, which enabled the overlaying of the 2D map of evaporationsheds with the world administrative boundaries shapefile, to compute specific statistics. This allowed for zonal analyses, summing evaporationshed values within each country and sea to quantify the contribution of the reference region to precipitation in each nation and sea.

A particularly significant result of this process was the determination of moisture recycling, which represents the proportion of precipitation within the reference region that originates from the evaporation of the same area, compared to the region's total evaporation. This quantity, for a specific region, can be calculated through the ratio of the sum of the evaporationsheds masked in the reference regions to the total evaporation of the region.

Similarly, the analysis of precipitationsheds, obtained through the backward analysis, allowed the identification of source areas for the moisture that precipitates in the regions of interest. Using QGIS and zonal statistics, it was possible to differentiate the proportion of precipitation deriving from terrestrial evaporation versus the one from the oceans. Consequently, this made it possible to identify the countries and seas that contribute most, through their evaporation, to the precipitation in the study areas, thus highlighting the main hydrometeorological dependencies.

The sum of all precipitationsheds for the study areas provided the total precipitation volume within these regions over the specified time period. This value was then compared with ERA5 reanalysis data to check for consistency between the two datasets.

Finally, the ratio between the volume evaporated from the reference area that precipitates within it and the total volume precipitation in the reference area allowed for the calculation of precipitation recycling. This indicator quantifies the ability to regenerate precipitation from local evaporation, thus providing essential information on the hydrological resilience and self-sustainability of the analyzed regions.

Chapter 3

Results

The main focus of this chapter is the analysis of atmospheric moisture flow patterns, taking as a basis the unique geoclimatic profile of Italy, along with the regional case studies of Piemonte, Lazio, and Sicilia. This strategic choice is intended to give an overall picture, viewed spatially and in latitude-oriented variations, about the atmospheric moisture patterns related to Italy. It thus intends to investigate water evaporation, its different trajectories, and its subsequent precipitation taking also into account the effect of geographical position of the region of interest. This is the first scientific study to take this approach in this geographical area.

In the effort to explain the hydrological profile of atmospheric moisture, two main investigative tools are proposed — "forward footprints" or "evaporation sheds and "backward footprints" or "precipitation sheds". Modeling these footprints leads to the mapping of downwind regions that receive precipitation from the source areas of interest (forward footprints) and upwind regions that contribute evaporation to precipitation in the mentioned area (backward footprints). These cutting-edge concepts quantify the dynamics of water-vapor exchange and provide a high resolution picture of the moisture paths from and to Italy.

The first part of this chapter will focus on the forward footprint analysis for Italy, presenting the overall pattern and then narrowing down to the regional point of view. This section thus details the evaporation pathways from the different regions, mapping their downwind journeys to areas of precipitation. Data that is going to be obtained from this research could significantly enhance the capability to understand the spatial characteristics of moisture transfers and the resultant regional climate impacts.

In the second part a similar structure is followed, but this time focused on the backward footprints. Using this tool, the source of the moisture leading to precip-

itation in Italy and the case-study areas can be clearly identified, along with those dominant upwind sources within the regional water cycle.

Subsequently, a similar analysis, both for the forward and the backward footprint, is carried on for the RECON model. Here, the outcomes are presented for the same study areas but only on the annual basis, that is without the seasonal development.

Once the results from RECON and Utrack are collected, the two models are compared to determine which is more reliable based on the consistency of specific hydrologic parameters.

Findings presented here could be useful to improve a better understanding of the diverse processes related to the atmospheric moisture transport over the nation as a whole and, more specifically, over its separate regions. Accordingly, this may enhance the scientific basis upon which water resource management and climate modeling improvements develop. Finally, these results could provide new perspectives for future researches, calling for an in-depth investigation in the field of atmospheric hydrology.

3.1 Utrack Forward footprint

3.1.1 Italy

In this subsection, the forward footprint, or evaporation shed, of Italy is revealed and interpreted, giving a presentation of the 'reservoirs' of the national precipitation. Output will be seasonal as well as annual.

The analysis begins by quantifying the amounts of evaporation that occur in the country for each season. The total volume of water, expressed in cubic meters, evaporating from Italy at the different seasons are indicated as "Total" (Table 3.1). The percentage of water which returns as re-precipitation above the landmass is also shown in the "to land" row. Such flowes contribute to the terrestrial circulation of water, helping the hydrological systems and ecosystems. It is an important resource for a variety of biological and human activities that depend upon fresh water. In contrast, the "to ocean" column shows how much of this water has evaporated into the atmosphere to then re-precipitates in the marine environment i.e., seas and oceans. From the table, it is clear that a smaller amount has evaporated overall from the winter and then rises to a peak in summer — warmest months of the year. This variability is mainly driven by the volume re-precipitating in land, whose value nearly triples from winter to summer. The volume ending up in the marine realm remains quite constant during the year instead, and it oscillates from 1.06E10 to 1.36E10 m^3.

For a better understanding of the distribution between landmasses and oceans,

Table 3.1: Italian evaporation volumes and their destination according to the seasons. Values are expressed in m^3.

	Total	to Land	to Ocean
Winter	3.57×10^{10}	2.23×10^{10}	1.34×10^{10}
Spring	5.84×10^{10}	4.48×10^{10}	1.36×10^{10}
Summer	7.49×10^{10}	6.43×10^{10}	1.06×10^{10}
Autumn	5.14×10^{10}	3.73×10^{10}	1.41×10^{10}
Annual	2.20×10^{11}	1.69×10^{11}	5.18×10^{10}

refer to Fig.3.1. This line graph illustrates the proportion of water that, once evaporated from Italy, ends up in land or ocean areas. The percentages, obtained from dividing the water volume destined to go either to land or ocean by the total evaporated volume per season are shown together with the data presented in Table3.1.

There are two different lines plotted in this graph: the green line corresponds to the fraction of water that re-precipitates over land masses whereas the blue line represents the fraction of water which falls back into the ocean. It can be clearly realized that the fraction of water that re-precipitates on land shows a peak during summer, when it reaches the 85 % of total evaporated water. Contrary to this, minimum fraction of water able to return to land is recorded during the winter, when it falls to about 60 %.

Given the complementary behavior of water quantities re-precipitating over land and ocean, the trend for oceanic re-precipitation must be reversed. The fraction of evaporated water that rains back into the ocean is, indeed, minimal during summer. This opposite behavior indicates that most of the Italian moisture evaporating in the hot summer months ends up over land, so a relatively smaller percentage of that can precipitate to eventually rejoin the oceanic water cycle.

Setting the foundations at the quantitative level, attention can then turn to visual depictions of these evaporation sheds (fig.3.2).

The annual evaporation shed plot, fig.3.2e, reveals a clear tendency for Italian evapotranspiration to re-precipitate mainly in Italy and along the Balkan coast. Indeed, one can identify a clear path of moisture advection to the east, crossing the Adriatic Sea, and ending with precipitation along the southeastern European shoreline. The summer visual (fig.3.2c) shows a more intense local re-precipitation over Italy, especially next to the Alps, and at the same time a weaker contribution to the Balkan coast compared with the other seasons.

Seasonal variations affect the centroid of the evaporation sheds (represented in the map with a red dot), which indicates the average location of re-precipitation. It is

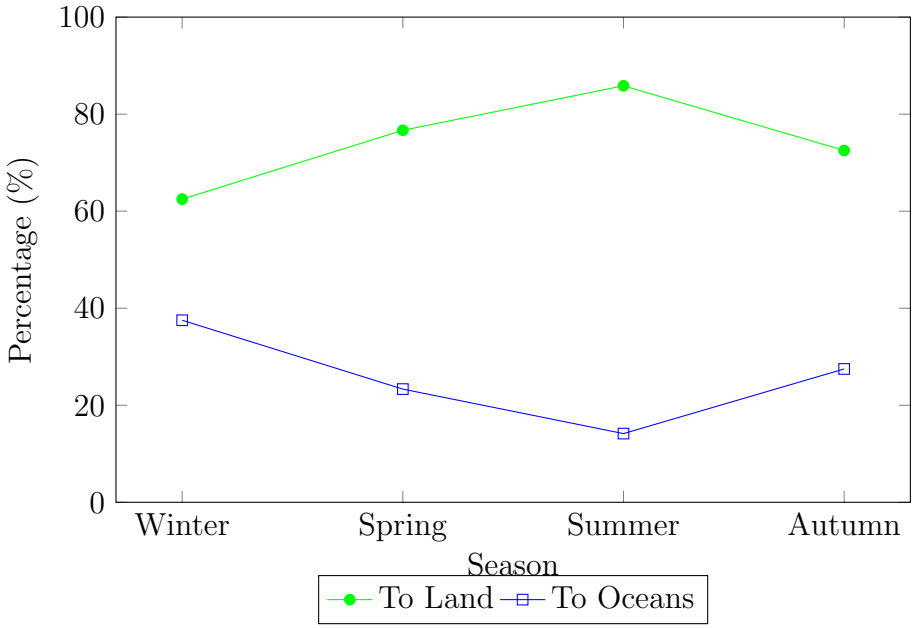

Figure 3.1: Seasonal Distribution of Italian Evaporation Re-precipitation in Ocean and Landmasses.

over Puglia in the summer, which means that water vapor that has evaporated during this time of year undergoes a swift re-precipitation. However, it moves to Greece in the winter, covering a greater distance before re-precipitation occurs. These summer evaporation sheds have revealed some interesting observations, one of which is the re-occurrence of precipitation in Africa, notably in the belt between the Equator and the Tropic of Cancer. Since none of the other seasonal portrayals include this intriguing component of moisture movement, it adds a particular perspective to the current knowledge of Italy's summer hydrologic processes.

To uncover the climatological mechanisms at the heart of these atmospheric moisture channels, these atmospheric patterns will be further analyzed in the Subsection 3.1.3.

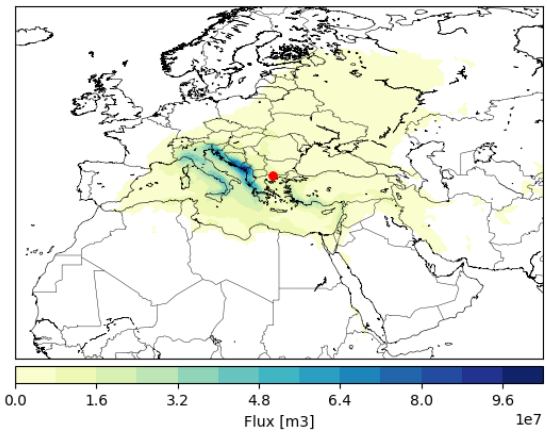

(a)

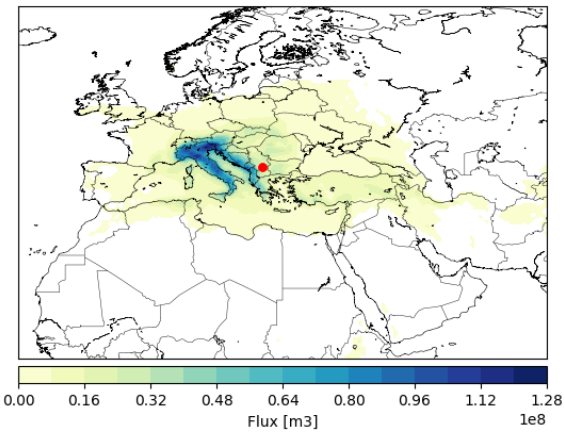

(b)

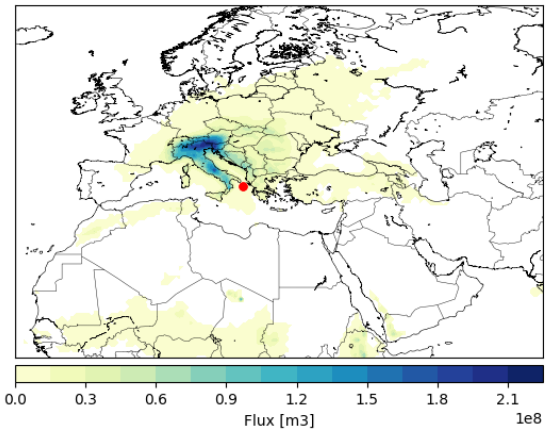

(c)

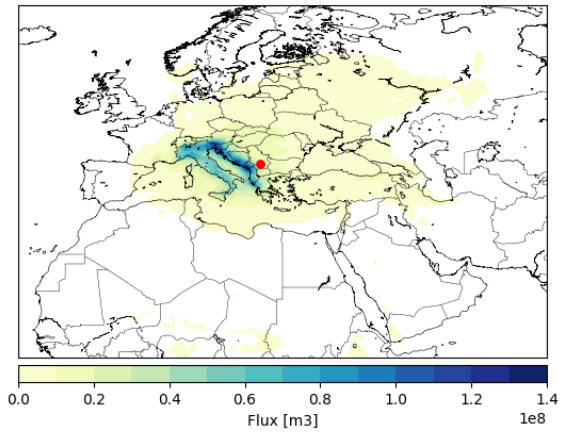

(d)

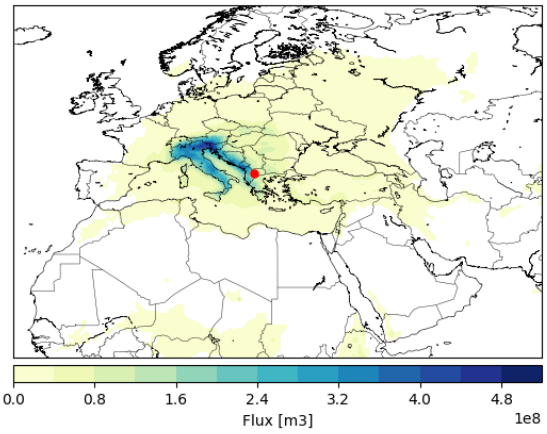

(e)

Figure 3.2: Italy evaporation sheds: winter (a), spring (b), summer (c), autumn (d), annual (e).

The following tables attempt to identify and rank the main beneficiary recipients for Italy's annual evapotranspiration, focusing on both the terrestrial and marine perspective. A more thorough examination of these beneficiaries can be achieved by reviewing Table 3.2 and 3.3, which provide the top ten countries and oceans, respectively, where Italy's evaporated water re-precipitates. The item 'others' refers to all the other countries, for Table 3.2, and seas, for Table 3.3.

Table 3.2 lists the major receiving countries of the moisture that originates from Italy. For each country it shows these values: the quantity of evaporated Italian moisture that it receives, the proportion of this received quantity to the total evaporation of Italy, and the proportion of this received quantity to the sum of the Italian originating moisture that re-precipitates on land.

Italy tops the list, getting approximately 13% of its own evaporated moisture, indicating a noteworthy tendency to moisture recycling. Following Italy, about 15% of the redistributed national evapotranspiration is accounted for by Russia, Turkey, and Austria combined. Separately, Romania and Ukraine record a little less than 3% individually. Interestingly, the only country west of Italy to receive Italian evapotranspiration is France.

Table 3.3, which uses a similar methodology, outlines the primary marine recipients of Italy's evapotranspiration and complements Table 3.2. The table shows, for each sea: the amount of evaporated Italian water that is received, the ratio of this volume relative to the overall volume of evaporation in Italy, and the ratio of this volume relative to the total amount of moisture originating in Italy that re-precipitates on seas. The Adriatic Sea comes out on top, taking in 4.22% of all the water that evaporates from Italy; that is, about 18% of all the Italian moisture that ends up in the sea. After then, the eastern Mediterranean Sea basin receives 3.8% of Italy's evapotranspiration.

Of particular note, the North Atlantic, Black Sea, and North Sea are the only bodies of water that are not included within the Mediterranean Basin.

These tables explain the spatial dispersal patterns of Italian atmospheric moisture, helping in a better understanding of regional and global moisture exchanges. In summary, the results demonstrate the connectedness of regional climates with respect to each other and the role that Italy plays within these hydrologic networks. Further climatological interpretation of these patterns is explored within the following subsections of this chapter.

The principal terrestrial and marine receivers of Italian evapotranspiration are included in Fig. 3.3, which further demonstrates this assumption.

This figure shows the major recipient countries (a), seas (b). For these specific

plots, intensities of colours had been used as a visual to present the fraction of moisture that each specific country or sea throughout the world receives from Italy. The darker the tone, the bigger the proportion of received moisture. These values are calculated through the percentages names as "flow/Tot flow to countries" and "flow/Tot flow to seas", in Table 3.2 and 3.3, respectively.

These images support the study that has been done so far, giving an extensive overview of Italy's atmospheric moisture dispersal patterns and rapid insights into the spatial migration of the water particles throughout the territory and its surrounding areas.

Table 3.2: Main receiving countries.

Countries	**flow** $[m^3/y]$	**flow/tot flow**	**flow/tot flow to countries**
Italy	2.97×10^{10}	13.46%	17.58%
Russia	1.69×10^{10}	7.66%	10.01%
Turkey	1.01×10^{10}	4.59%	6.00%
Austria	8.22×10^{9}	3.73%	4.87%
Ukraine	6.26×10^{9}	2.84%	3.71%
Romania	6.10×10^{9}	2.77%	3.62%
Bosnia and Herz.	5.40×10^{9}	2.45%	3.20%
France	4.73×10^{9}	2.15%	2.81%
Greece	4.38×10^{9}	1.99%	2.60%
Croatia	4.26×10^{9}	1.93%	2.53%
Others	7.27×10^{10}	32.96%	43.08%

Table 3.3: Main receiving seas.

Seas	**flow** $[m^3/y]$	**flow/tot flow**	**flow/tot flow to oceans**
Adriatic Sea	9.31×10^9	4.22%	17.98%
Mediterranean Sea - Eastern Basin	8.45×10^9	3.83%	16.33%
North Atlantic Ocean	5.93×10^9	2.69%	11.45%
Tyrrhenian Sea	5.79×10^9	2.63%	11.18%
Ionian Sea	5.32×10^9	2.41%	10.28%
Mediterranean Sea - Western Basin	4.06×10^9	1.84%	7.85%
Black Sea	2.70×10^9	1.22%	5.21%
Aegean Sea	2.15×10^9	0.98%	4.15%
Ligurian Sea	9.88×10^8	0.45%	1.91%
North Sea	7.05×10^8	0.32%	1.36%
Others	6.36×10^9	2.88%	12.29%

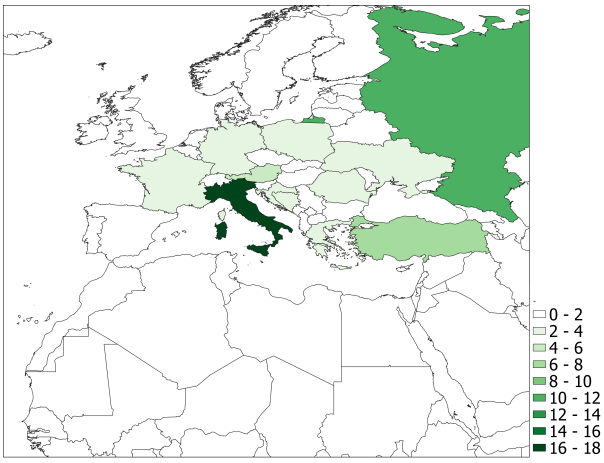

(a)

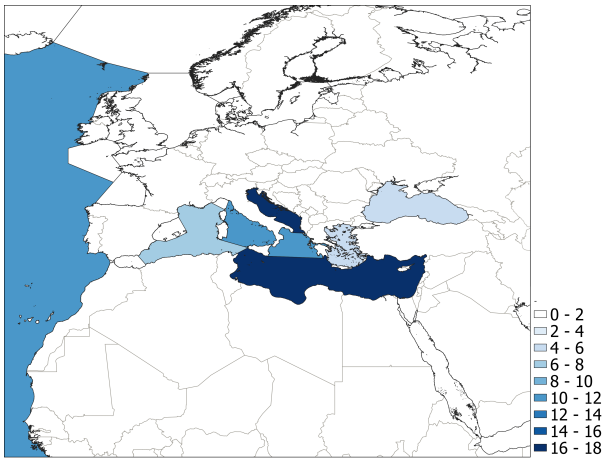

(b)

Figure 3.3: Main receiving countries (a) and seas (b). The percentage is using the values 'flow/Tot flow to countries' for (a) and 'flow/Tot flow to oceans' for (b), retrievable in Tab.3.2 and 3.3, respectively.

3.1.2 Pemonte, Lazio, Sicilia

After reviewing Italy's national forward footprint, the attention is focused on analyzing regional variations in moisture flows. Piemonte, Lazio, and Sicilia are the regions picked for this in-depth analysis; they are located in the northern, central, and southern regions of Italy, respectively. This distribution throughout the nation provides a chance to compare and contrast the impacts of geographic location on evapotranspiration dynamics.

Table 3.4 presents the seasonal and annual volumes of water evaporated in Piemonte, Lazio, and Sicilia respectively. Each table includes three columns: 'total' represents the volume of water evaporated within the region for a specific season, 'to land' indicates the volume that re-precipitates on terrestrial landmasses, and 'to ocean' quantifies the volume that re-precipitates in the marine realm. The annual values of these quantities are collected in the bottom row of each table.

In this dataset, it is possible to notice discernible patterns of behavior. Taking the regions of Piemonte (a) and Lazio (b), both show a marked increase in the volume of evaporation during summer, which corresponds to a respective decrease witnessed in winter.

In the case of Piemonte, for example, the evaporation volume surges from a winter low of 1.25×10^9 m^3 to a summer high of 7.09×10^9 m^3. In a similar trend, Lazio rises from 3.44×10^9 m^3 during winter to 4.04×10^9 m^3 in the summer months.

It is important to point out that although both series reflect the same seasonal pattern, the amount of evaporation volume changes by season varies in magnitude. Piemonte has more dramatic fluctuations; it rises steeper in the summer and falls steeper in the winter. On the other hand, Lazio experiences a more moderate seasonal variation.

Conversely, Sicilia (c) follows a different evolution, with the greatest evaporation volume recorded in the fall and the lowest in the summer. In addition, Sicilia experiences relatively small seasonal variations in evaporation volume, much like Lazio.

The assessment proceeds with an analysis of the land evaporation recycling, also referred to land recycling, which is defined as the fraction of evaporation from terrestrial surfaces that subsequently precipitates over land areas. Fig.3.4 offers a visual representation of this process together with the fraction of evapotranspiration that re-precipitates in the marine realm.

An interesting observation arising from this representation is the consistent seasonal trend observed across all three regions, that reflects also the Italian one (Fig.3.1). This trend captures the fluctuations in land recycling and marine precipitation contri-

Table 3.4: Evaporation volumes according the seasons - Piemonte (a), Lazio (b), Sicilia (c). Values are expressed in m^3.

Piemonte	**Total**	**To Land**	**To Ocean**
Winter	1.25×10^9	7.63×10^8	4.85×10^8
Spring	4.18×10^9	3.09×10^9	1.09×10^9
Summer	7.09×10^9	5.99×10^9	1.11×10^9
Autumn	3.02×10^9	2.14×10^9	8.72×10^8
Annual	1.55×10^{10}	1.20×10^{10}	3.56×10^9

(a)

Lazio	**Total**	**To Land**	**To Ocean**
Winter	3.44×10^9	1.96×10^9	1.47×10^9
Spring	3.46×10^9	2.42×10^9	1.04×10^9
Summer	4.04×10^9	3.26×10^9	7.86×10^8
Autumn	4.07×10^9	2.70×10^9	1.36×10^9
Annual	1.50×10^{10}	1.03×10^{10}	4.65×10^9

(b)

Sicilia	**Total**	**To Land**	**To Ocean**
Winter	5.65×10^9	2.91×10^9	2.74×10^9
Spring	5.25×10^9	3.55×10^9	1.71×10^9
Summer	5.03×10^9	3.87×10^9	1.16×10^9
Autumn	6.02×10^9	3.56×10^9	2.46×10^9
Annual	2.20×10^{10}	1.39×10^{10}	8.07×10^9

(c)

bution across the four seasons. Regardless of the region, land recycling is consistently lower during winter months, elevating gradually to reach its zenith in summer, and then subsequently decreasing in autumn. This cyclical pattern suggests a strong correlation between seasonal changes and the trajectory of evaporated moisture.

Although the general pattern is regular, the regional land recycling, however, shows to be quantitatively different across the seasons. Piemonte display the highest rates of land recycling in each of the seasons, while in Sicilia they obtain the lowest. Lazio is placed in a central position, and it occupies an intermediate position between these two extremes.

These differences could probably be related to the geographical position of the regions within the country. Land recycling is more intense in Piemonte, which is not touched by seas and is closer to the continental mass. Sicilia, an island region, shows a lower rate, probably due to the greater influence of its proximity to the sea. Following this reasoning, Lazio, being in the middle of the peninsula, displays a land recycling rate that falls between the other two. In the chapters that follow, these elements will be examined more specifically.

The detailed regional analysis, therefore, shows minor but important variations of the moisture transport processes across the Italian landscape, strongly pointing out geographical position as the influential factor in these patterns. This perspective gives an overview of how climatological processes interface with regional landscapes in shaping the pattern of moisture flows.

The study continues by exploring the regional evaporation sheds of Piemonte, Lazio, and Sicilia. These are graphically depicted throughout the seasons and on an annual scale, in their respective plots shown in Fig.3.5, 3.6 and 3.7.

Starting with Piemonte (Fig.3.5), a striking aspect of its evaporation sheds is the confinement of the most intense footprints to northern Italy, their extent largely constrained by the Alpine arch. Interestingly, the centroid of these evaporation sheds exhibits stability in the Balkan coast, predominantly situated on the Croatian coast. The maximum distance from Turin is recorded during the winter season, with the centroid located approximately 1011 km away, on the southern border of Serbia.

Moving on to Lazio, as represented by Fig.3.6, the pattern of evaporation shows a different trend. The intensity of the evaporation-shed is mostly restricted to the Italian peninsula's center, with evident concentration in correspondence of the west coast. The other main destination of precipitation influenced by Lazio's evaporation is the Balkan coast, where some high-intensity evaporation sheds clearly show up. This general pattern shifts somewhat in the summer, when the sheds seem more concentrated in the Lazio region itself, though a noticeable footprint extends into

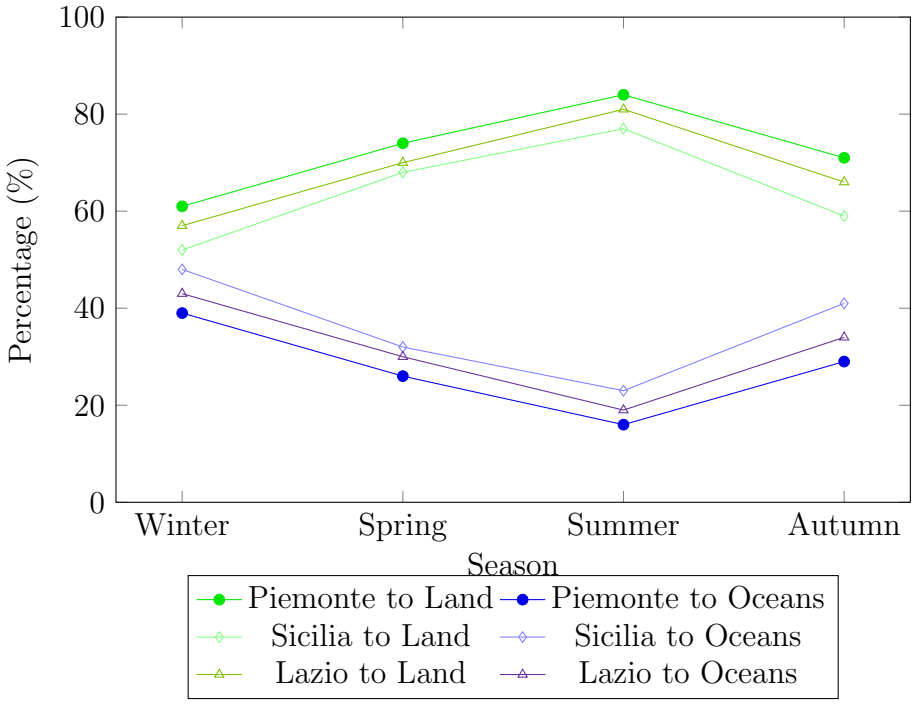

Figure 3.4: Seasonal Distribution of Evaporation Re-precipitation in Ocean and Landmasses for Piemonte, Lazio and Sicilia

Africa between 0 and 15 degrees latitude. Similar to Piemonte, the centroid of the Lazio sheds is located furthest from Rome during the winter season, at approximately 883 km. It is notable that across all seasons, except summer, the centroid resides near the northern border of Greece, shifting southward to the Ionian Sea during summer months.

Moving the focus to Sicilia (Fig.3.7), the distribution of evaporation sheds follows yet another distinctive pattern. The intense footprints primarily encompass Sicilia itself and the western coast of Greece, with southern Turkey also showing some influence during winter (a) and spring (b). Of particular interest is the behaviour of the sheds during the summer season (c). During this period, high-intensity evaporation sheds are mostly confined to Sicilia, while several smaller sheds scatter across the African tropical belt. This change is reflected in the centroid's position, which migrates to the center of Libya in summer, a stark contrast to its position around the Aegean Sea during the other three seasons.

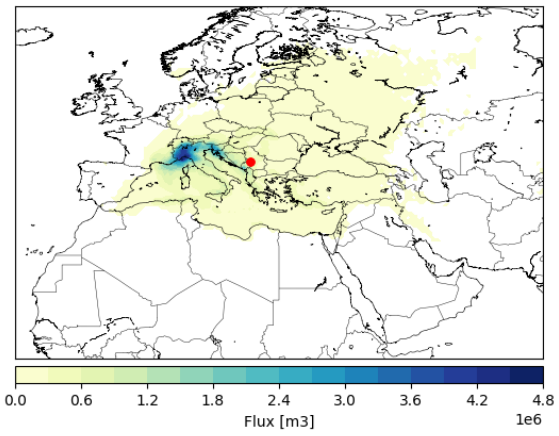

(a)

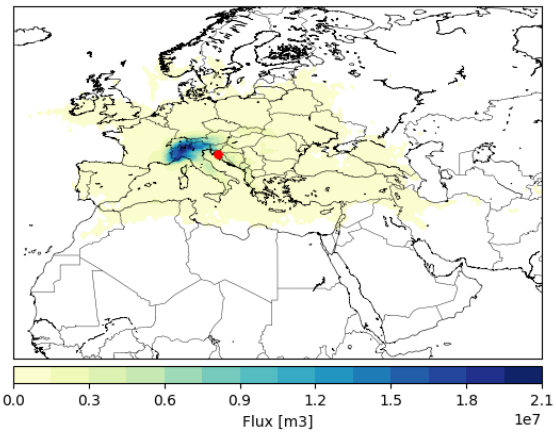

(b)

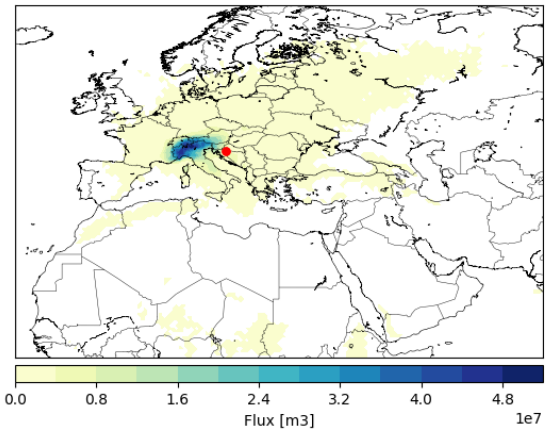

(c)

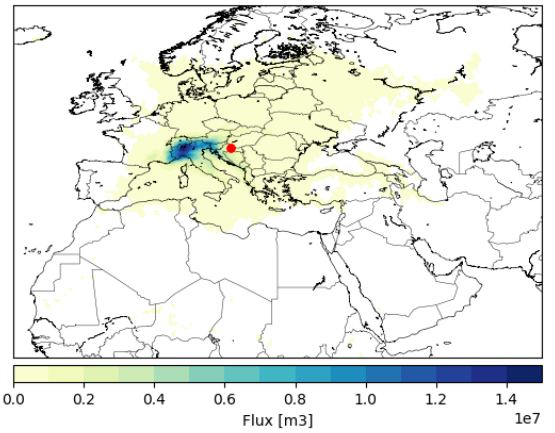

(d)

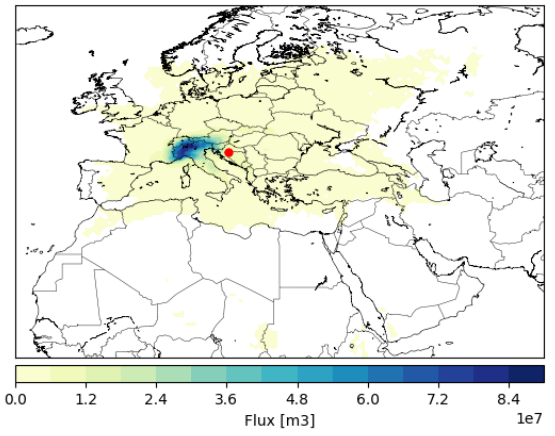

(e)

Figure 3.5: Piemonte evaporation sheds: winter (a), spring (b), summer (c), autumn (d), annual (e).

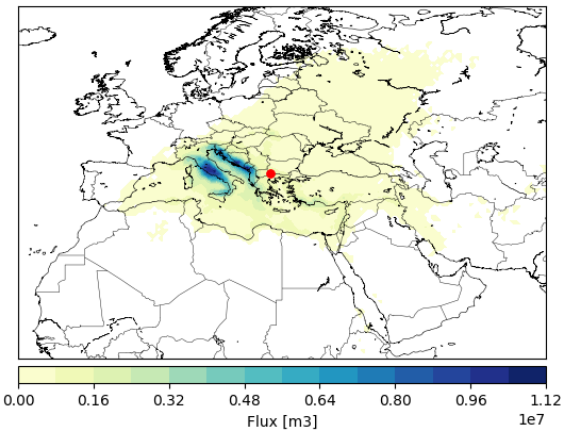

(a)

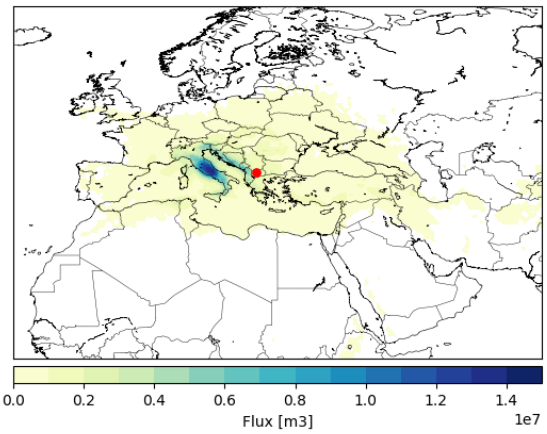

(b)

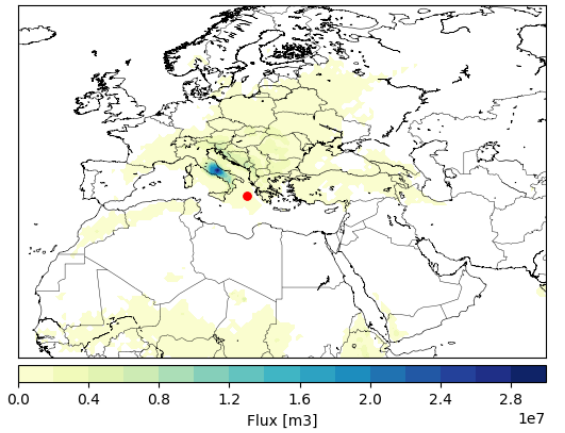

(c)

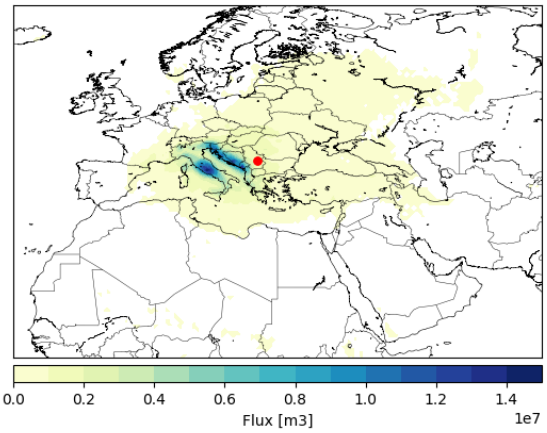

(d)

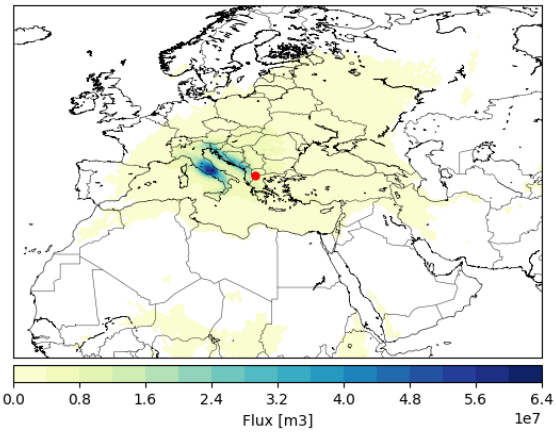

(e)

Figure 3.6: Lazio evaporation sheds: winter (a), spring (b), summer (c), autumn (d), annual (e).

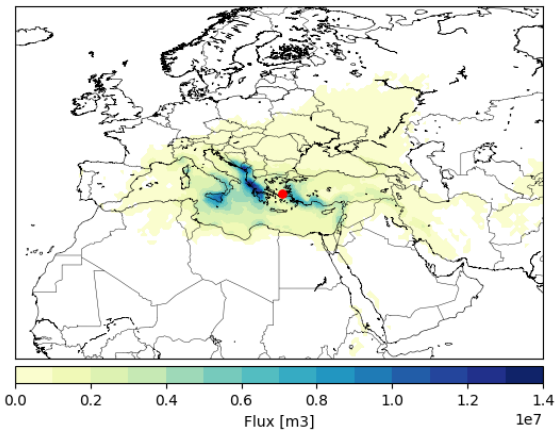

(a)

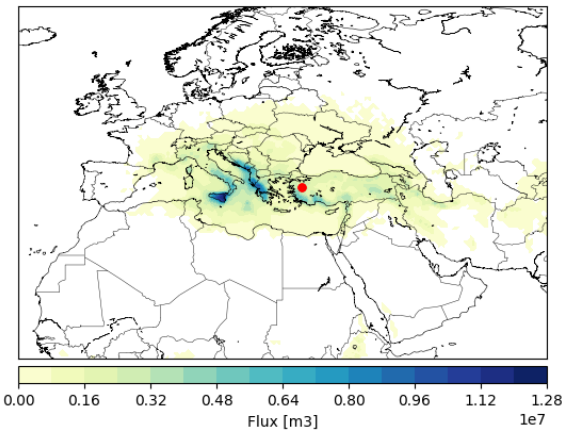

(b)

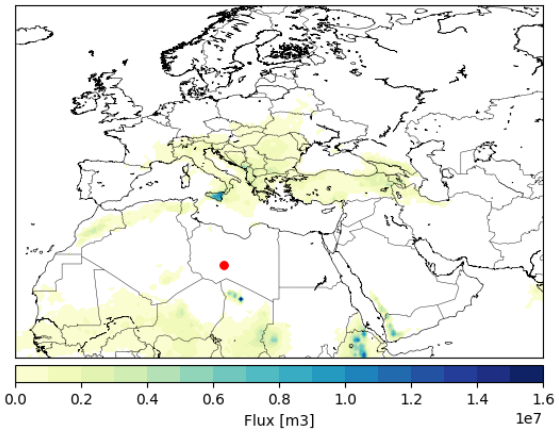

(c)

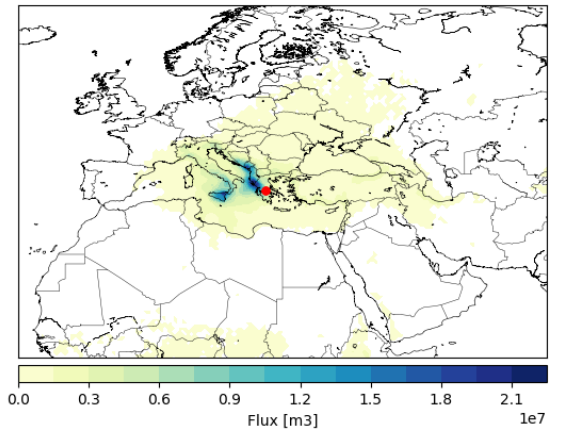

(d)

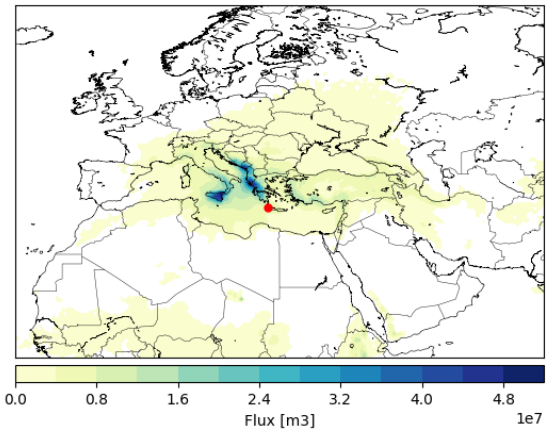

(e)

Figure 3.7: Sicilia evaporation sheds: winter (a), spring (b), summer (c), autumn (d), annual (e).

Regarding the estimation of the annual evaporation to precipitation patterns for these three regions of interest—Piemonte, Lazio, and Sicilia—the most significant terrestrial recipients of their evaporated water have been recognized and presented through Tables 3.5, 3.6, and 3.7 respectively. Similarly, the primary marine receptors are elaborated in Tables 3.8, 3.9 and 3.10.

Beginning in Piemonte, it is striking to find that almost 20% of the region's evaporative output once again falls over the area of Italy, indicating a very strong mechanism of moisture recycling. This means that practically one third of Piemonte's evaporative flow, which ultimately precipitates over land, does so within the nation's boundaries. Beyond Italy, the main recipients are the Eastern European countries, among which Russia stands out, receiving 6.6% of the humidity from Piemonte. Interestingly, France, taking up 5% of Piemonte's humidity, is the only country located westwards in the top ten receivers, likewise with the pattern discovered for Italy.

Turning the attention to Lazio in Table 3.6, it's possible to retrieve a common pattern relative to some aspects. Italy remains a primary recipient, though the extent of local moisture recycling is somewhat reduced—indeed, just less than 14% of Lazio's evaporated water precipitates within the region. Similar to the case of Piemonte, Russia featured the second most prominent recipient, with very close proportions. However, contrary to Piemonte, the evaporation footprint of Lazio spills over to Europe, with Iran featuring as a noteworthy receiver, although with a percentage slightly below the 2%.

Examining Sicilia's evaporation distribution reveals divergent patterns, likely due to its distinct geographical location. In this case, Turkey emerges as the primary recipient, receiving over 8% of Sicilian evaporative output, while Italy holds the second position at 5%. Russia remains a key player, albeit with proportions marginally lower than Italy's. Notably, Sicilia's evaporation footprint reveals a meaningful contribution to precipitation within Africa, as evidenced by its impact on Ethiopia, Chad, and Algeria—though each receive between 1.4% to 1.8% of Sicilian evaporative flow, it marks a distinctive pattern compared to the other regions.

Now turning to the marine receptors of regional evaporative output, it is expected that lower percentages of moisture received compared with the terrestrial recipients should appear. This already concurs with the previous observation of the high land recycling ratios.

As expected, the Mediterranean Basin appears as an important receiver over all regions. In the case of Piemonte, more than 32% of the evaporative outflow that precipitates over marine domains does so within the Western Basin of the Mediterranean

Sea and the Adriatic Sea; these regions almost share equal portions.

For Lazio, the Mediterranean influence is even stronger. Almost 40% of the region's evaporative output that ultimately precipitates over oceans falls within the Tyrrhenian and Adriatic Seas, with both sea's receiving roughly equal amounts.

Beyond the Mediterranean, both Piemonte and Lazio make some contributions to precipitation over the far northern seas—that is, the North Sea for Piemonte and the Barents Sea for Lazio. In addition, all three regions contribute massively into the Atlantic Ocean, although the contribution by Sicilia becomes prominent as the Atlantic turns out to be the third major receiver of Sicilian moisture.

Speaking of Sicilia, about one-third of its evaporative yield that subsequently precipitates over oceans falls in the Eastern Basin of the Mediterranean Sea, and a sixth is received by the Ionian Sea.

These patterns therefore emphasize that regional evaporative cycles are deeply interlinked with the broader systems of marine hydrology. While the Mediterranean Basin dominates as the greatest sink, contributions to more distant marine environments underscore that the processes are truly interlinked and that the influence of these regions goes far beyond the immediate geographic confines.

A more detailed and descriptive representation of the major recipients of evaporated water vapor by the three involved regions is given by Fig. 3.8. This plot is placed in the special form of a cartographic display and points out the main terrestrial and marine recipients of the regional evaporation annual dispersal, allowing a clearer and diversified visualization of the intricate interaction between the selected Italian regions and the rest of the world.

Each country and body of water is assigned a different shade within the green and blue spectrum, respectively. On that basis, this color-coding system creates an easily interpretable visual key to the distribution of moisture, with each shade correlating directly to the percentage of received moisture from each region under consideration.

These percentages are based on the earlier discussed figures displayed for Italy. For terrestrial recipients, the ratio of the flow received to the total flow destined for land is considered, while for marine recipients, the ratio is drawn between the flow received to the total flow directed towards the oceans.

Table 3.5: Piemonte - main receiving countries.

Countries	**flow** $[m^3/y]$	**flow/tot flow**	**flow/tot flow to land**
Italy	3.84×10^9	24.74%	32.08%
Russia	1.03×10^9	6.60%	8.56%
France	8.05×10^8	5.18%	6.72%
Austria	6.07×10^8	3.91%	5.07%
Romania	3.49×10^8	2.25%	2.92%
Ukraine	3.46×10^8	2.23%	2.89%
Switzerland	3.43×10^8	2.21%	2.87%
Slovenia	3.29×10^8	2.12%	2.75%
Germany	3.26×10^8	2.10%	2.72%
Croatia	3.20×10^8	2.06%	2.67%
Others	3.68×10^9	23.71%	30.76%

Table 3.6: Lazio - main receiving countries.

Country	**flow** $[m^3/y]$	**flow/tot flow**	**flow/tot flow to land**
Italy	1.98×10^9	13.23%	19.18%
Russia	1.06×10^9	7.05%	10.22%
Turkey	6.13×10^8	4.09%	5.93%
Romania	4.49×10^8	3.00%	4.35%
Ukraine	3.97×10^8	2.65%	3.84%
Croatia	3.42×10^8	2.28%	3.31%
Greece	3.35×10^8	2.23%	3.24%
Bosnia and Herz.	3.17×10^8	2.11%	3.06%
Iran	2.44×10^8	1.63%	2.36%
Serbia	2.19×10^8	1.46%	2.12%
Others	4.38×10^9	29.23%	42.38%

Table 3.7: Sicilia - main receiving countries.

Countries	**flow** $[m^3/y]$	**flow/tot flow**	**flow/tot flow to land**
Turkey	1.79×10^9	8.15%	12.89%
Italy	1.13×10^9	5.13%	8.11%
Russia	1.09×10^9	4.97%	7.86%
Greece	8.16×10^8	3.72%	5.88%
Iran	6.79×10^8	3.09%	4.89%
Ethiopia	5.14×10^8	2.34%	3.70%
Chad	4.11×10^8	1.87%	2.96%
Ukraine	3.30×10^8	1.50%	2.38%
Romania	3.15×10^8	1.43%	2.27%
Algeria	3.14×10^8	1.43%	2.26%
Others	6.50×10^9	29.61%	46.82%

Table 3.8: Piemonte - main receiving seas.

Seas	**flow** $[m^3/y]$	**flow/tot flow**	**flow/tot flow to ocean**
Mediterranean Sea - Western Basin	5.95×10^8	3.83%	16.73%
Adriatic Sea	5.89×10^8	3.79%	16.56%
Ligurian Sea	4.28×10^8	2.75%	12.02%
Tyrrhenian Sea	3.79×10^8	2.44%	10.65%
North Atlantic Ocean	3.74×10^8	2.41%	10.51%
Mediterranean Sea - Eastern Basin	2.86×10^8	1.84%	8.04%
Ionian Sea	1.52×10^8	0.98%	4.26%
Black Sea	9.76×10^7	0.63%	2.74%
North Sea	8.89×10^7	0.57%	2.50%
Aegean Sea	8.02×10^7	0.52%	2.25%
Others	4.89×10^8	3.15%	13.75%

Table 3.9: Lazio - main receiving seas.

Seas	**flow** $[m^3/y]$	**flow/tot flow**	**flow/tot flow to oceans**
Tyrrhenian Sea	9.53×10^8	6.36%	20.50%
Adriatic Sea	9.20×10^8	6.14%	19.77%
Mediterranean Sea - Eastern Basin	8.06×10^8	5.38%	17.32%
Ionian Sea	4.15×10^8	2.77%	8.93%
North Atlantic Ocean	3.87×10^8	2.58%	8.33%
Mediterranean Sea - Western Basin	3.11×10^8	2.07%	6.68%
Aegean Sea	1.80×10^8	1.20%	3.86%
Black Sea	1.75×10^8	1.17%	3.76%
Ligurian Sea	8.06×10^7	0.54%	1.73%
Barentsz Sea	3.93×10^7	0.26%	0.84%
Others	3.85×10^8	2.57%	8.28%

Table 3.10: Sicilia - main receiving seas.

Seas	**flow** $[m^3/y]$	**flow/tot flow**	**flow/tot flow to oceans**
Mediterranean Sea - Eastern Basin	2.70×10^9	12.29%	33.45%
Ionian Sea	1.21×10^9	5.53%	15.05%
North Atlantic Ocean	9.80×10^8	4.46%	12.15%
Tyrrhenian Sea	7.68×10^8	3.50%	9.52%
Adriatic Sea	6.69×10^8	3.05%	8.30%
Aegean Sea	4.63×10^8	2.11%	5.74%
Mediterranean Sea - Western Basin	3.39×10^8	1.54%	4.20%
Black Sea	3.31×10^8	1.51%	4.10%
Ligurian Sea	7.27×10^7	0.33%	0.90%
Arabian Sea	7.20×10^7	0.33%	0.89%
Others	4.61×10^8	2.10%	5.71%

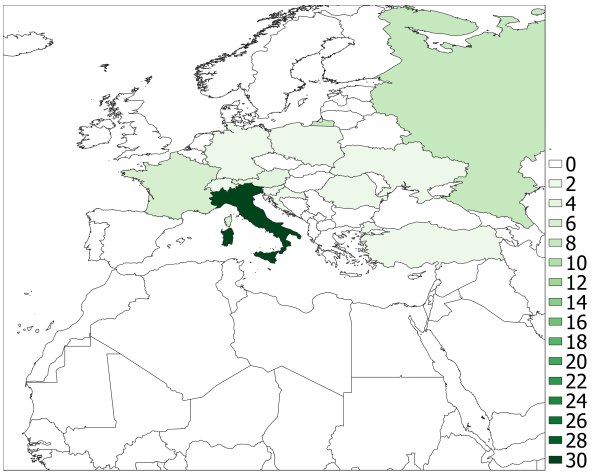

(a)

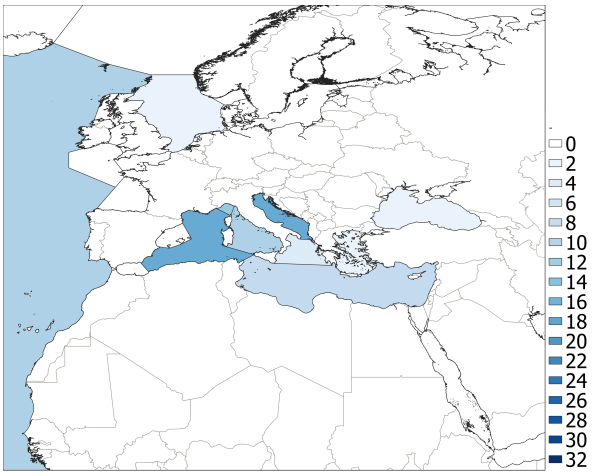

(b)

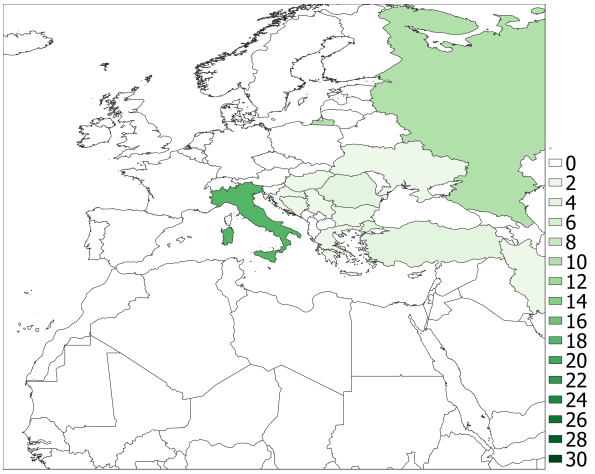

(c)

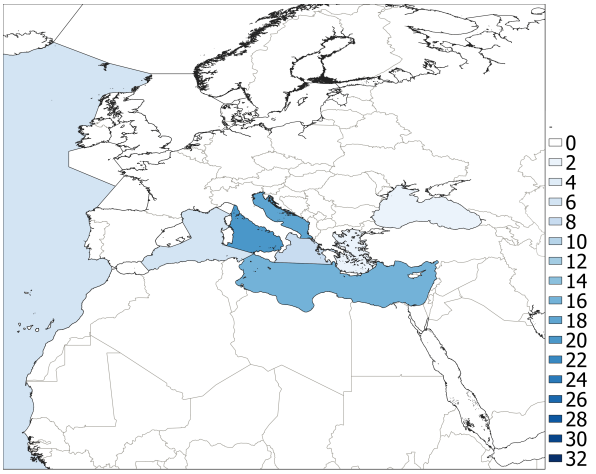

(d)

(e)

(f)

Figure 3.8: Main receiving countries and seas for Piemonte (a) and (b), Lazio (c) and (d), Sicilia (e) and (f).

3.1.3 Forward footprint: climatological framework

The findings gathered so far may need an explanation that can be located within climatological and geographical dimensions. This shall be done by analyzing the variety of plots and tables developed to shed light on complicated and interlinked patterns. Beginning with a detailed study of the forward footprint of moisture transport over Italy and its various regions, could help to try to explain some of the interesting happening dynamics and provide valuable insight into evapotranspiration redistribution processes and consequent precipitation in different regions. This critical review takes a central role in deciphering the influence of different climatological factors through the moisture transportation cycle.

Indisputably, the geographical and topographical features of the country greatly influence its wind and moisture patterns, thus making the study particularly interesting in terms of moisture transport mechanisms within the atmosphere. In fact, its geographical disposition, being close to the African continent in the south and the vast landmass of Eurasia in the north, no doubt makes an interesting blend of atmospheric patterns, which can be studied in relation to the wind directionality and circulation of moisture. Its southern part is exposed by its proximity to Africa with possible exchanges of warm and dry air masses carried above the the Mediterranean Sea. This could have some potential influences on the wind patterns, which in certain time-of-year periods might be carrying air that is leaving the Italian Peninsula for the continent of Africa, on the basis of certain season-related conditions that will be described shortly in this chapter. By contrast, the northern parts of Italy are relatively close to the broader Eurasian continent. This sets up somewhat different wind dynamics than in the south, with cooler continental air sometimes pulled across the Alpine regions. This kind of airflow may take moisture northwards from Italy, therefore contributing to precipitation in areas beyond the Alps. Nonetheless, against the backdrop of these regional disparities, some common patterns and trends emerging across the earlier presented visualizations can be detected.

Two fundamental characteristics are largely found in these visualized plots: the eastward displacement tendency of the evaporation sheds and the large terrestrial moisture recycling. Strive to the eastern preference first. This feature indicates that there is a dominant atmospheric pattern, such as winds or atmospheric circulations, that would favour eastward advection of moisture. As Italy is situated within the middle latitudes of the Northern Hemisphere, it is affected by the action of the westerlies, whose general direction is from west to east. These winds, created by the differential air pressure between subtropical high-pressure zones and subpolar low-pressure belts, are steered further east in both hemispheres because of the Coriolis

effect. This aspect generally leads to an eastward flow of air masses and weather systems, which eventually feeds into the eastward flowes of water vapor from Italy. This trend is further underscored by the generally eastward placement of evaporation shed centroids in all the visualized plots, reflecting their large paths of evaporated moisture, even into vast areas of Russia.

Secondly, a more detailed analysis of the high level of terrestrial moisture recycling deserves some explanation. This could be related to two factors: convective instability and orographic lifting. In fact, the first one is that turbulence, marked by an intensified upward motion of warm, buoyant air, which is larger over land than over water. This phenomena is related to the differential heating: under insolation, land heats at a more intense rates and creates localized warm-air zones that start to rise, forming atmospheric instability. This will then enable the development of convective clouds and later increase the potential for precipitation. Orographic lifting, instead, refers to the elevation of air over mountains. In this phase, adiabatic cooling comes to play an important role. This is the process in which, as air gets elevated, it expands and becomes cold as a result of a reduction in pressure at higher levels. The moistures condense into clouds at the dew point temperature where condensation occurs. This, in conjunction with the growth of water droplets or ice crystals within the clouds, favors precipitation in the form of rain, snow, or drizzle. Argumentatively, these two processes, convective instability and orographic lifting, contribute significantly to recycling over the land, thus leading to high terrestrial precipitation.

Beside this brief explanation about the presence of high-land recycling, another visible aspect, whose importance is probably the most relevant, needs to be taken into account. Given the geographical position of Italy and the presence of the aforementioned westerlies, the moisture that is released by the nation and that will prefer to move towards the east will tend to meet areas mostly occupied by mainlands, as it encounters the east of Europe and Asia. In fact, the only sea that touches the Italian oriental coast is represented by the Adriatic Sea, whose extension is rather limited. This straight-forward consideration plays a fundamental role in the re-precipitation of the Italian humidity over the land.

Many of the forward footprint plots, particularly those for Italy (Fig3.2), agree with the ideas discussed above. Apart from the major evaporation sheds over Italy, there are big ones on the Balkan coast. Italian evaporated moisture, indeed, pushed eastward by the westerlies, meets the Dinaric Alps, then condenses and precipitates. This trend is equally evident in the plots for Lazio (Fig3.6). For Sicilia, (Fig3.7) the plots bring out the dense evaporation sheds particularly along the western coast of Greece and this effect could be attributed to the orographic lifting in the Pindus Mountains. In continuation, Sicilian moisture precipitates again along the southern

coast of Turkey (Fig3.7 (a) and (b)), where the Taurus Mountains come into play.

When considering Piemonte, evaporation shed on the east coast of the Adriatic is, however, somewhat less marked. This evidence could be connected with the higher latitude of its location, its proximity to the Alpine arch to the north, and other correlated local circulation patterns. In particular, the presence of the mountains, which embrace the region from the North, creates opportunities for the lifting and condensation of moist air, heightening precipitation over Piemonte and neighbouring regions. Thus, a larger fraction of evaporated moisture is recycled as precipitation within Piemonte, instead of being transported to precipitate in other more distant areas. Indeed, Piemonte exhibits the highest land moisture recycling rate of all the case studies considered here. Moreover, the evaporation shed centroid is generally located closer to Piemonte itself than in the other case studies: a consideration which strengthens this argument.

The other important point which has to be kept in view is the similar pattern followed for land moisture recycling in all the regions under study, depicted by Fig.3.1 and 3.4. It was found that the minimum land recycling is during winter, followed by gradual increase attaining a maximum during summer and then decreasing. This variation is due to the difference in land-sea heat absorption, which becomes maximum during summer. In summer, land surfaces warm up much faster and to higher temperatures compared to the sea. This difference in thermal absorption makes the land-sea system a condition of marked thermal contrast. The heated surface of the land creates convective instability that drives the rapid ascent of air with condensation, leading to rainfall. Differential heating, together with atmospheric circulation patterns and moisture convergence, favors the concentration of precipitation over land during the summer. More convective activity and rainfall over the mainland are made possible by its thermal properties, causing land to heat up and cool down more rapidly than water.

In addition, an interesting pattern is observed when looking at the plots for Italy, Piemonte, and Lazio: winter and autumn appear to be the seasons during which the centroids of evaporation sheds are situated at the greatest distance from the area of interest. In the colder months of the year, the difference in average air temperatures between high-latitude polar regions and mid-latitude zones become maximally pronounced, leading to a strong temperature gradient. This increased temperature contrast can enhance pressure gradients and hence strengthen the westerly winds even further. This is supported by the analysis carried out for the whole of Italy. The maximum distance is in winter (Fig.3.2 (a)), with the centroid standing at 950 km away from Rome, while the minimum is in summer (Fig.3.2 (c)), with the distance Rome-centroid falling down to below 650 km. The westerlies show variations

both in strength and patterns with latitude, and their configuration would depend on the pressure systems. Thus, the case of Piemonte, the northernmost region considered, falls within the middle latitudes and close to the core of the westerlies. This is confirmed by the forward footprint plot of Piemonte, which shows the highest centroid distance difference between colder and warmer seasons. In winter (Fig.3.5 (a)), the centroid lies 1011 km from Turin; in spring (Fig.3.5 (b)), this distance is almost halved, decreasing to 573 km. The trend in Lazio, being a lower latitude region, is much the same but not quite as pronounced. In the winter (Fig.3.6 (a)) the centroid is located 870 km from Rome. In the spring, it's about 130 km closer (Fig.3.6 (b)).

However, this general pattern does not apply to Sicilia. The southern parts of Italy are at lower latitudes and much closer to the subtropics. The westerlies in these areas are much weaker than elsewhere in the country, especially in summer when subtropical high-pressure systems dominate. The weaker the westerlies, the less able they are to bring moisture to the east. The summer plot for Sicilia (Fig.3.7 (c)) shows a unique scenario: it breaks the usual trend of long eastward moisture transport. Instead, a significant amount of moisture is tunneled southwards. The centroid indeed lies over Libya, almost at the same longitude as Sicilia. As shown in Fig. 3.9, in summer, most of Sicilia's evaporationsheds are located around 15°N. This anomalous behavior calls for a finer investigation, which naturally leads to the study of the Hadley Cell dynamics.

The Hadley cell includes a rising process of air near the equator, being transferred towards the poles at high altitudes, and then descending inside subtropical regions. At about 30° latitude in both hemispheres are the subtropical zones where this transported air starts to fall. The trade winds are formed as the descending air in these subtropics rushes back towards the equator near the surface. In the Northern Hemisphere, these trade winds blow from the northeast. The Hadley Cell enlarges toward the poles during the summer months because of increased equatorial heating. On the other hand, recent studies have found that global warming would affect the size of the Hadley cell to expand toward the poles. Consequently, the moisture evaporated from Sicilia could be trapped by the trade winds and transported toward the African countries. In support of this assertion, one can consider the evaporation sheds of Sicilia during autumn and summer seasons. Indeed, according to studies by Grise et al., 2018; Hu Y. et al., 2018; and Staten et al., 2018, the Hadley cell undergoes a larger widening during the summer and autumn seasons for each hemisphere. This is consistent not only with the summer plot, which marks the most intense evaporation shed in Africa, but also with the autumn forward footprint plot (Fig.3.7 (d)), where pale but noticeable evaporation sheds in Africa can be observed. When Hadley Cellis is not so extended, in winter and spring, the contribution to Africa is not visible

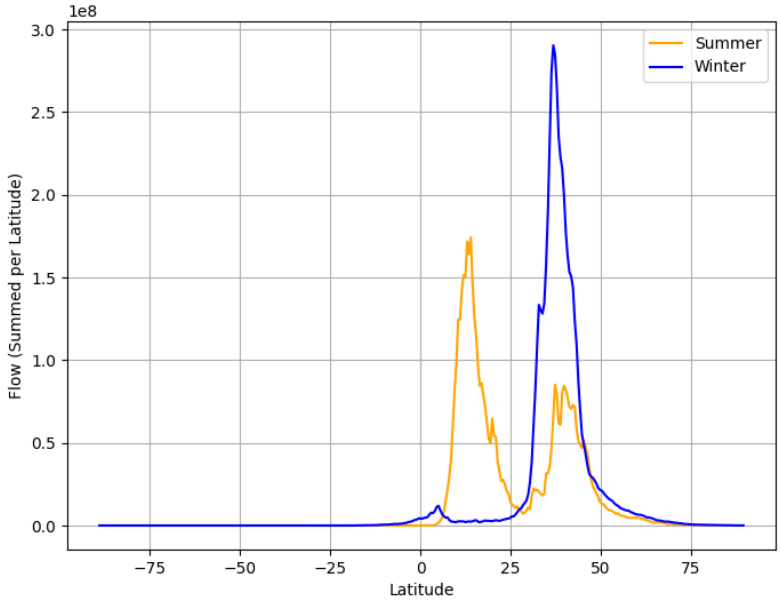

Figure 3.9: Zonal distribution comparison between Sicilia's winter and summer evaporationsheds.

(Fig.3.7 (a), (b)).

Such interactions of climate warming, Hadley Cell expansion, and trade wind dynamics, however, are nonlinear and of outstanding complexity in reality. It is, in fact, an interplay of several factors that symbolizes the intricate and multi-dimensional nature of our climate system. All the understandings about these interactions are, in fact, constantly evolving. More detailed research on the process and its implications for a broader, complete, and accurate understanding is thus indispensable in all respects.

3.2 Utrack Backward footprint

3.2.1 Italy

This section deals specifically with the Italian backward footprint, intended here as the source area of moisture for Italy. As for subsection 3.1.1, it is unveiled and explained through a procedure that will be described in the following. It provides a meteorological description of the origin of the country's precipitation, considered on a seasonal and a annual basis.

At this regard, the reference table is 3.11. Here, the column 'Total' refers to the volume of moisture that, once evaporated throughout the world in a specific season, reaches Italy to re-precipitates. The column 'From land' refers to the portion of that volume that comes from landmasses evaporation and the column 'from ocean' the portion of that volume that comes from the marine realm. The last row, 'Annual', aggregates these quantities over the years. By analyzing this table, the contrast in the seasonal contributions between seas/oceans and land can be clearly detected. The sea's or ocean's contribution volume of moisture remains almost the same in every season. However, the percentage coming from land shows rather acute changes. This means that, while the marine realm continually supplies a constant amount of moisture, land offers a dynamic contribution, reacting drastically to varying conditions brought by the different seasons. This discrepancy in behavior thus underlines the distinct roles that these two kinds of sources play with regard to the atmospheric hydrological cycle.

Table 3.11: Italian precipitation volumes and their origin according to the season. Values are expressed in m^3.

	Total	**From land**	**From ocean**
Winter	5.55×10^{10}	9.80×10^{09}	4.57×10^{10}
Spring	7.99×10^{10}	3.21×10^{10}	4.78×10^{10}
Summer	9.63×10^{10}	4.68×10^{10}	4.95×10^{10}
Autumn	6.63×10^{10}	1.66×10^{10}	4.97×10^{10}
Annual	2.98×10^{11}	1.05×10^{11}	1.93×10^{11}

The other remarkable observation that could stand out is the disparity in the volume of precipitation that originates from oceans versus landmasses. Data reveals a much higher contribution coming from the oceans, where nearly 2×10^{11} m^3 of water end up to Italy per year compared with slightly over 1×10^{11} m^3 from landmasses. This implies that the marine realm represents a more important source for Italian precipitation, providing nearly twice as much water as the land.

To further explain this large difference, one must consider the plot shown in Fig.3.10. This plot is used to display the seasonal variation of the sources of Italian precipitation, clearly distinguishing terrestrial versus marine evaporation sources. The plot gives an illustrative view of the seasonality in the oscillation between these two sources. Interestingly, one can see that the ocean evaporation fraction of precipitation maximizes during winter months and supplies more than 80% of Italy's total precipitation. However, this predominance weakens as the seasons enter into summer, and the oceanic sources contribution drops below 60%. Obviously, the share of moisture from land contributing to precipitation over Italy follows a complementary tendency. Its land-derived component strongly increases in the summer months, almost equaling the percentage that derives from the ocean. This input decreases with the onset of autumn, thus marking the variable impact of land-based areas on the precipitation patterns in Italy.

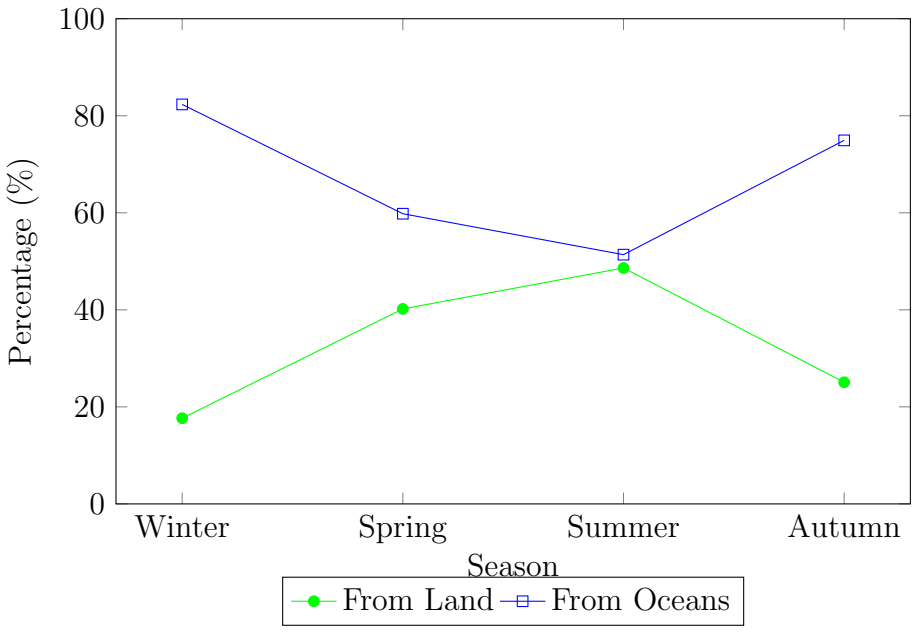

Figure 3.10: Seasonal Trends in Precipitation Origin for Italy.

After briefly glancing through these preliminary results, attention turns to the graphical displays of the precipitation sheds for the various seasons and the whole year, as plotted in Fig.3.11.

The first thing to be noticed from the preliminary examination is the dramatic western location of the sheds in all the graphs. More specifically, in winter and, in lesser measure, in autumn, the sheds located east of Italy experience a significant reduction.

The geographical position of the centroid of precipitation sheds in Italy has a notable variation with respect to seasonal shifts. In the winter period, the centroid is predominantly found in Portugal, reaching its southern latitude, as shown in Fig.3.11 (a). This centroid is shifted north during the summer, matching the alignment of the Pyrenees, as shown in Fig.3.11 (c).

Another interesting aspect that can be noted regards the location of the most intense sheds. In line with what has been noted in Fig.3.10, the eminently contributing sheds to Italian precipitation during the autumn (Fig.3.11 d) and even more so during the winter are the evaporation from the seas. In the winter months, the highest intensity areas are relevantly confined between the Gulf of Lyon (over the southern French coast) and the Ligurian Sea. So, considering autumn, this high-intensity region is extended southward, covering the whole western Mediterranean basin.

However, as the seasons change into spring (highlighted in Fig.3.11 b) and into summer, the pattern of precipitation sheds distribution greatly changes. The most extreme precipitation sheds begin to spread more variably around Italy, with an amplified accumulation in the northern regions and on the Italian west coast.

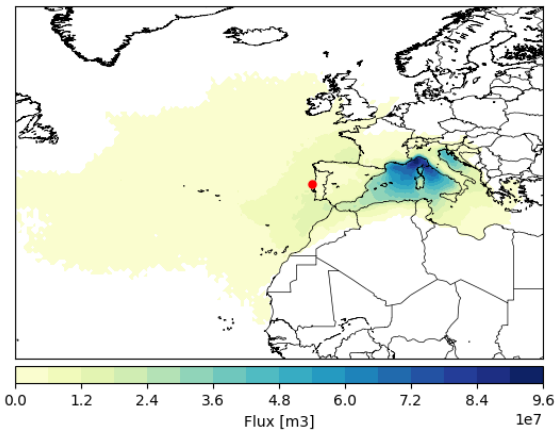

(a)

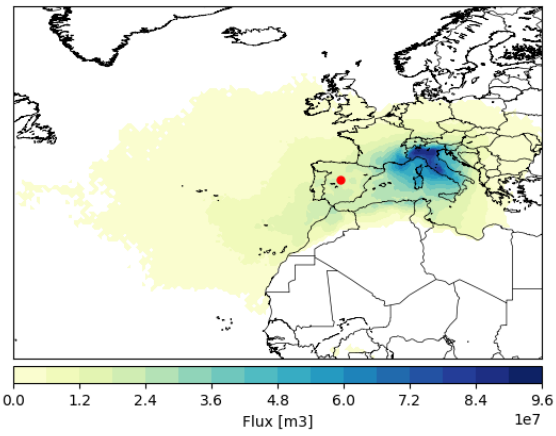

(b)

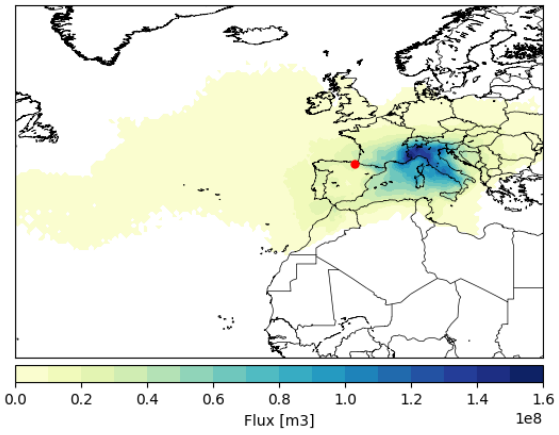

(c)

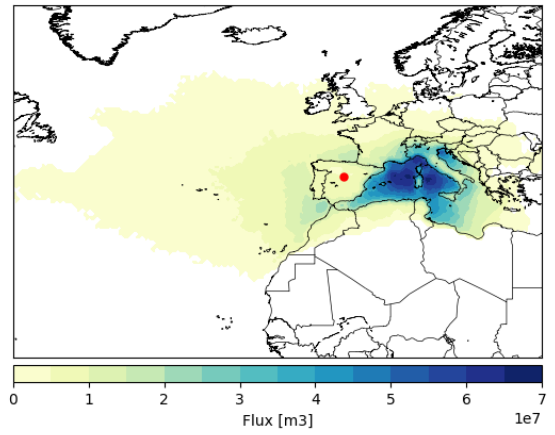

(d)

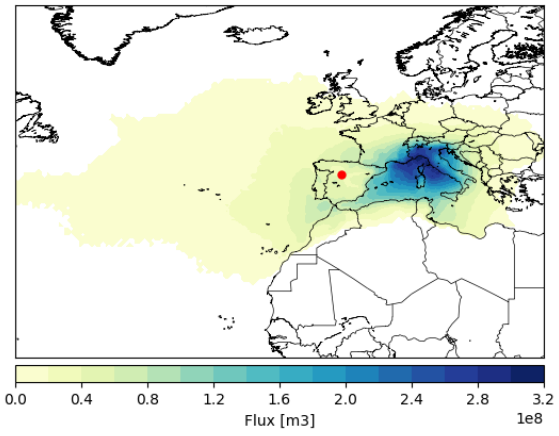

(e)

Figure 3.11: Italian precipitation sheds: winter (a), spring (b), summer (c), autumn (d), annual (e).

Tables 3.12 and 3.13 focus on the main countries and seas that contribute to the Italian annual precipitation through evaporation. Each table, in turn, reports the amount of moisture that evaporates from each country or sea, which is then re-precipitated in Italy (column 'flow').

In the table referred to countries (Table 3.12), the column 'flow/total flow' reflects the proportion of moisture evaporated from each country and that precipitates in Italy in relation to the total volume of moisture worldwide (both terrestrial and marine) precipitating in Italy.

Conversely, the 'flow/total flow from land' percentage demonstrates the ratio between the volume of evaporated moisture from each country that re-precipitates in Italy, compared to the total volume of moisture worldwide, but this time exclusively considering landmass evaporation, which re-precipitates in Italy.

Significantly, Italy is the main source of its own precipitation. About 9% of the precipitation recorded in Italy originates from its natural evaporation. This means, in other worlds, that one-fifth of all rainfall in Italy, initiated by terrestrial evaporation, can be accounted to originate from Italian evaporation itself. The French contribution ranks as the second most important source of precipitation to Italy, responsible for just over 6% of the worldwide evaporated water that eventually falls as rain in Italy. Spain is next largest contributor, with an input equal to half of that of France.

This is followed by the introduction of two African nations, namely Algeria and Morocco, whose combined contributions stand at approximately 3% of the total worldwide evaporation contributing to precipitation in Italy. The lower end of the top ten is completed by the nations of Germany, Austria, and Croatia, representing the first introductions in the list of a east-of-Italy nations.

The setting of the sea-related table (Table 3.13) is very similar to that of the nations. The table displays the two main ratios as the previous one, in addition to the 'flow' values. The first ratio, 'flow/total world flow', means the amount of water vapour evaporated by every sea that falls on Italy as precipitation, compared with the total global amount of water that evaporates - from land and seas - which falls back as precipitation on Italy.

The second percentage here, 'flow/total flow from seas', signifies the ratio of the volume of moisture which evaporates from each sea and then re-precipitates in Italy, with respect to the total volume of water which evaporates from all the seas around the world and then re-precipitates in Italy.

A preliminary evaluation shows the massive contribution from the Atlantic Ocean, which accounts for nearly a third of Italian precipitation. In the broader perspective, roughly half of the water vapor that evaporates from the world's oceans and falls

later as precipitation in Italy can be ascribed to the Atlantic. After the Atlantic's contribution, the Western basin of the Mediterranean Sea accounts for about 12% of the precipitation falling over Italy. Coming third is the Tyrrhenian Sea, but with nearly half the contribution of the Western Mediterranean.

So far, only seas/oceans located to the west of Italy appeared in the list. Nevertheless, some Mediterranean Basins contributes to the national precipitation, though on a much smaller scale. It is therefore the case of the Eastern Mediterranean basin, the Adriatic, and, lastly, the Ionian Sea. Interspersed between these last two mentioned seas are western bodies of water, that is the Balearic Sea and the Bay of Biscay, whose combined contribution amounts to about 3%.

The impact of different nations and bodies of water on precipitation patterns in Italy is illustrated more clearly in Fig.3.12. In this figure, each nation and sea is assigned a color that corresponds to the amount of evaporated water that eventually falls as precipitation over Italy. In particular, the ratios utilized for this graphical representation are sourced from Tables 3.12 and 3.13, designated as 'flow/total flow from land' and 'flow/total flow from seas' respectively.

Table 3.12: Main contributing countries.

Country	**flow** $[m^3/y]$	**flow/Tot flow**	**flow/Tot flow from land**
Italy	2.57×10^{10}	8.62%	24.38%
France	1.83×10^{10}	6.13%	17.35%
Spain	1.15×10^{10}	3.86%	10.91%
Algeria	5.43×10^{9}	1.82%	5.16%
Morocco	3.91×10^{9}	1.31%	3.71%
Germany	3.79×10^{9}	1.27%	3.60%
Austria	2.50×10^{9}	0.84%	2.38%
Croatia	2.38×10^{9}	0.80%	2.26%
Others	3.19×10^{10}	10.70%	30.26%

Table 3.13: Main contributing seas.

Seas	**flow** $[m^3/y]$	**flow/Tot flow**	**flow/Tot flow from seas**
North Atlantic Ocean	9.24×10^{10}	31.02%	47.98%
Mediterranean Sea - Western Basin	3.35×10^{10}	11.24%	17.39%
Tyrrhenian Sea	1.85×10^{10}	6.21%	9.61%
Mediterranean Sea - Eastern Basin	1.05×10^{10}	3.53%	5.46%
Adriatic Sea	8.61×10^{9}	2.89%	4.47%
Balearic (Iberian Sea)	4.72×10^{9}	1.59%	2.45%
Bay of Biscay	4.52×10^{9}	1.52%	2.35%
Ionian Sea	3.63×10^{9}	1.22%	1.88%
Others	1.62×10^{10}	5.43%	8.41%

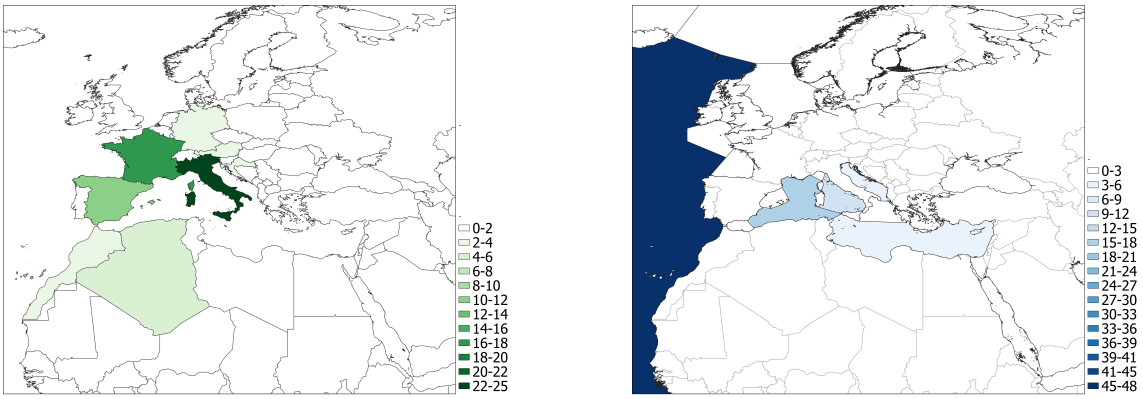

(a) (b)

Figure 3.12: Italian main contributing countries (a) and seas (b). Values are the percentages taken from 'flow/Tot flow from land' and 'flow/Tot flow from seas'.

3.2.2 Piemonte, Lazio, Sicilia

After the evaluation of the extensive backward footprint of Italy, the analysis shifts focus to a regional level. Table 3.14 presents the total volume of water that re-precipitates on a seasonal basis over the respective regions of interest and further quantifies this in terms of evaporating sources, distinguishing terrestrial (from land) and marine (from ocean) contributions.

The maximum recorded precipitation volume occurs for Piemonte, with an annual accumulation of 2.82×10^{10} cubic meters. Conversely, Sicilia receives approximately half of this volume, showing the lowest precipitation magnitude.

Table 3.14: Precipitation volumes according to the seasons and their origin - Piemonte (a), Lazio (b), Sicilia (c). Values are expressed in m^3.

Piemonte	**Total**	**From Land**	**From Ocean**
Winter	5.88×10^9	1.05×10^9	4.84×10^9
Spring	7.75×10^9	3.18×10^9	4.58×10^9
Summer	8.31×10^9	3.85×10^9	4.47×10^9
Autumn	6.24×10^9	1.77×10^9	4.46×10^9
Annual	2.82×10^{10}	9.85×10^9	1.83×10^{10}

(a)

Lazio	**Total**	**From Land**	**From Ocean**
Winter	2.82×10^9	4.36×10^8	2.38×10^9
Spring	4.37×10^9	1.44×10^9	2.93×10^9
Summer	5.55×10^9	2.37×10^9	3.19×10^9
Autumn	3.74×10^9	8.12×10^8	2.93×10^9
Annual	1.65×10^{10}	5.05×10^9	1.14×10^{10}

(b)

Sicilia	**Total**	**From Land**	**From Ocean**
Winter	2.37×10^9	4.46×10^8	1.92×10^9
Spring	3.97×10^9	1.51×10^9	2.46×10^9
Summer	5.82×10^9	2.35×10^9	3.47×10^9
Autumn	3.22×10^9	6.91×10^8	2.52×10^9
Annual	1.54×10^{10}	4.99×10^9	1.04×10^{10}

(c)

A striking similarity of the three regions concerns the ocean evaporation contribu-

tion to their total precipitation. On the annual period, the amount of precipitation contributed by ocean evaporation is roughly twice that one contributed by land evaporation, with Piemonte (a) registering a marginally smaller ratio and Lazio (b) and Sicilia (c) showing slightly higher proportions. Besides, the contribution to rainfall from land evaporation is lower in the cold period: it reaches the minimum during winter, while it attains its peak during summer. On the contrary, the sea evaporation contribution to Piemonte remains almost uniform throughout the year. For the other two regions, it follows the trend described for land contribution, although in a much less pronounced manner especially for Lazio.

To better appreciate the seasonal contribution of evaporation sources to regional precipitation, the reference is Fig.3.13. The percentage 'from land' is then calculated as the volume of water evaporated from land masses and then rained into the targeted region in a given season, divided by the total volume of water that precipitates in this region over the same season. The 'from ocean' percentage is calculated in a similar way, but this time utilizing the volume of water evaporated from oceans instead of landmasses. Evidently, the sums of these two quantities must give 100%.

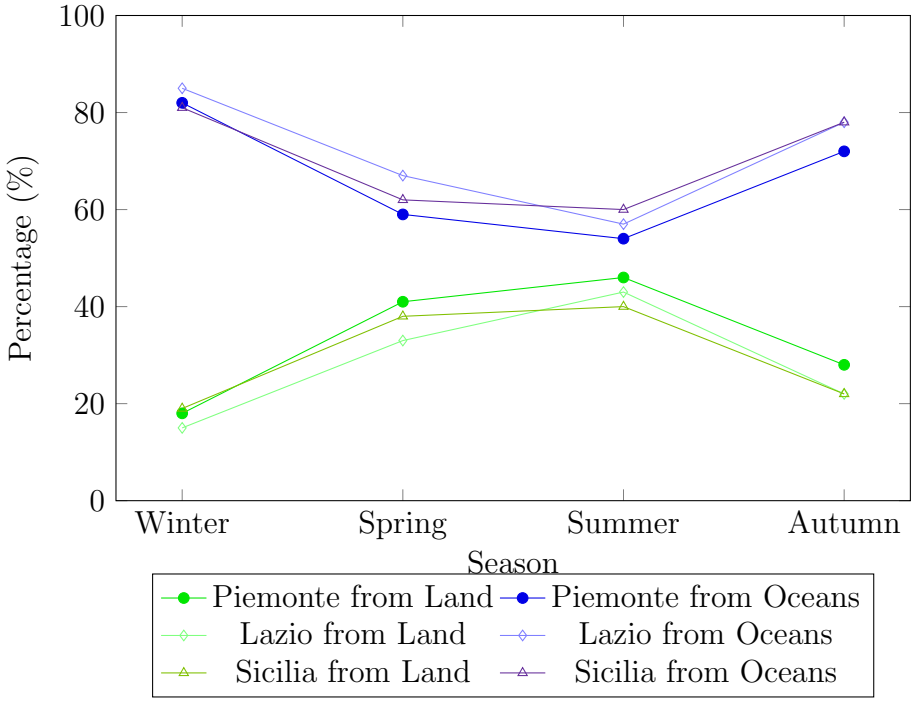

Figure 3.13: Seasonal Trends in Precipitation Origin for Piemonte, Sicilia, and Lazio.

All three areas essentially show the same pattern: the biggest contribution from ocean evaporation is visible in wintry precipitation—this is the case for all three regions, with values over 80% and with Lazio recording the highest levels. From this maximum, the percentage subsequently declines to its lowest point in summer, going below 60% for both Piemonte (54%) and Lazio (57%). When autumn comes, the proportion increases once again, returning to levels slightly under those recorded during winter – 72% for Piemonte and 78% for both Lazio and Sicilia.

Utilizing an analogous process as applied to the nationwide Italian backward footprint, Fig. 3.14, 3.15 and 3.16 showcase the regional precipitation sheds across each season as well as annually. These plots offer a clear representation of the distribution of the areas of evaporation contributing to precipitation for the individual regions throughout the different periods of the year.

Following exactly the same procedure performed for the backward Italian national-scale footprint, Fig. 3.14, 3.15 and 3.16 display the regional precipitation sheds by season, and on a yearly basis. These plots allow to offer a clear representation of the distribution of the areas of evaporation contributing to precipitation for the individual regions during the different periods of the year.

As happened in Italy, the precipitation sheds of the three regions are mainly westward of the regions for all the seasons. Consistent with this observation, the centroid of the sheds in each of the presented maps is found closely around Spain. The maximum distance between the centroid and the respective region is consistently recorded during the winter season. For example, the winter centroid for Piemonte emerges within the Atlantic near the Portuguese coast, while throughout the other seasons, it fluctuates within northern Spain. Moreover, during summer and spring, pale precipitaiton sheds extend eastward, a phenomenon which drops significantly through winter and autumn. Similarly, Lazio's winter centroid occupies the proximity of the Portuguese coast, transitioning towards the Pyrenees in summer. For Sicilia, the winter centroid is detected around the Strait of Gibraltar, then moving to the southern border of Spain and France during the summer months.

The other common features that need to be highlighted, as shown in Table 3.13, are predominance of the sheds located in seas in the colder seasons-winter and autumn-and the increasing contribution of the landmass evaporation in the warmer seasons.

With the winter plot of Piemonte (Fig.3.14 a) in consideration, the presence of high-magnitude precipitation sheds lie around the sea of Liguria. When entering the spring (b) and summer (c) seasons, these broad, high-magnitude sheds diffuse until they reach Piemonte itself and also the southeast coast of France. Extending into the autumn, while parts of the sheds remain around the Piemonte area, the great ma-

jority of them drift back towards the Mediterranean basin. However, these autumn sheds are scattered over a more extended region compared to winter, demonstrating a more dispersed pattern.

The plots from Lazio (Fig.3.15) illustrates a more uniform trend throughout the various seasons. The precipitation sheds are predominantly located within the Tyrrhenian region, in particular close to the coastline of Lazio. When spring (b) and summer (c) appear, a slight eastward movement can be seen, with the sheds gradually moving into the inland areas.

In the examination of precipitation sheds of Sicilia (Fig.3.16), a significant contribution from the Strait of Sicilia is evident in both winter and autumn, with a clearer dispersion observed in the latter season. In contrast, during the spring (b) and summer (c) months, regions exhibiting the highest evaporation rates, thereby creating the most intense sheds, appear to be confined within the geographical borders of the island.

A concluding observation, even if less visibly observable, relates to the geographic distribution of the precipitation sheds along latitudinal direction. Throughout all analyzed plots, including those representative of Italy in its entirety, one can observe a notable southward extension of the sheds during the winter and spring seasons in comparison with the autumn and, even more strikingly, the summer months. This phenomenon is especially evident in the plots associated with Sicilia. Here, the sheds reach the Senegal coastline during winter and spring and marginally intrude on the tropical regions, thus appearing in countries such as Ghana, Southern Mali, and Nigeria. During summer, on the contrary, the sheds extend only very slightly beyond the western coast of Morocco to barely reach the Canary Islands. Relating to Sicilia, it is possible to notice that the winter centroid stands at a latitude of 37.3, more than four degrees south of the summer centroid, which is at a latitude of 41.6. Such differences are evident in the other geographical locations as well, however the further north one travels, the less noticeable it become. In terms of latitudinal displacement, indeed, the winter centroid for Lazio is located about three degrees further south than it is in summer. The southward shift during the winter for Piemonte is partly smaller in comparison, about 2.5 degrees.

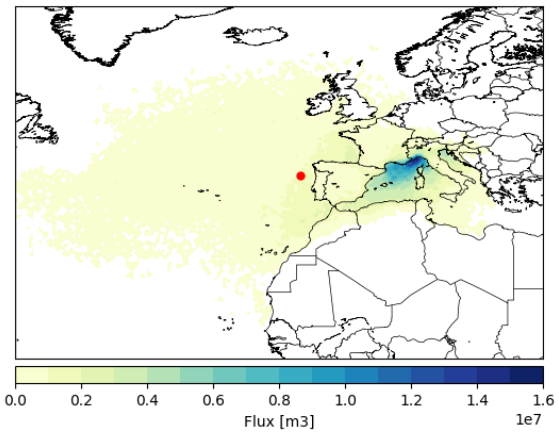

(a)

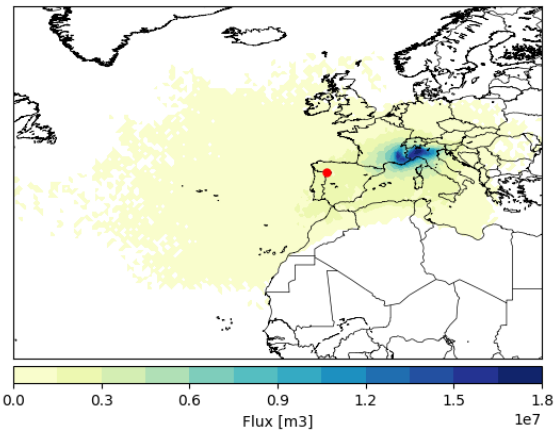

(b)

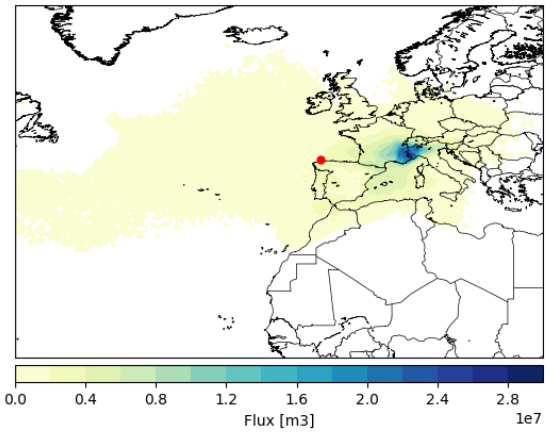

(c)

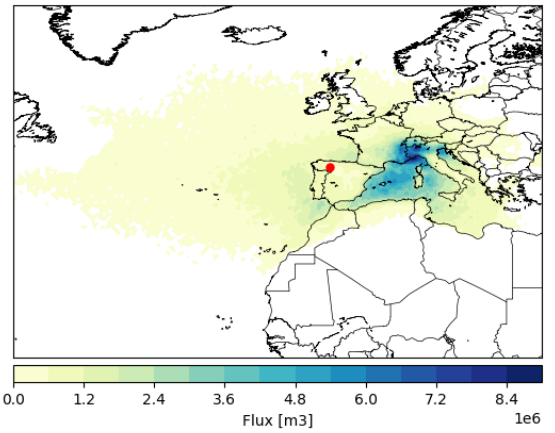

(d)

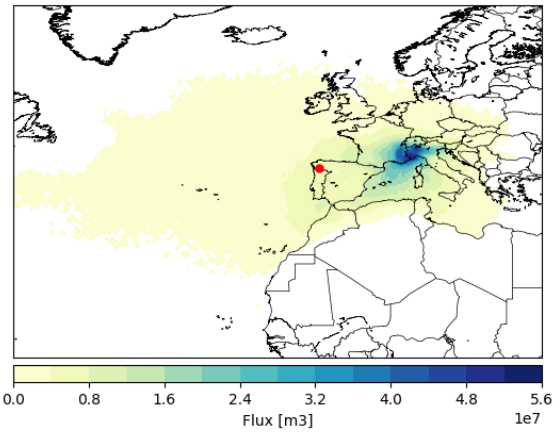

(e)

Figure 3.14: Piemonte precipitation sheds: winter (a), spring (b), summer (c), autumn (d), annual (e).

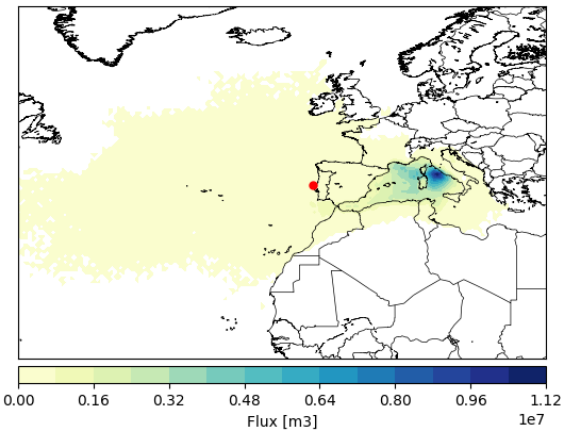

(a)

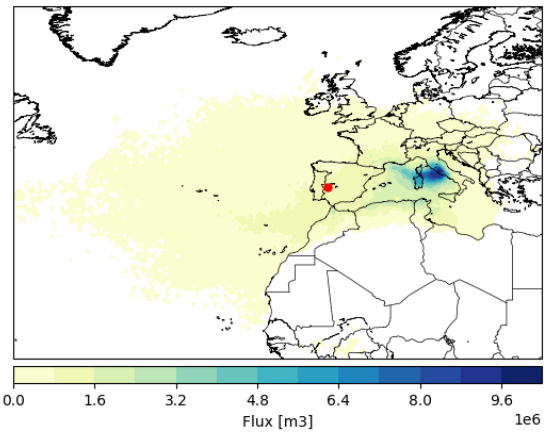

(b)

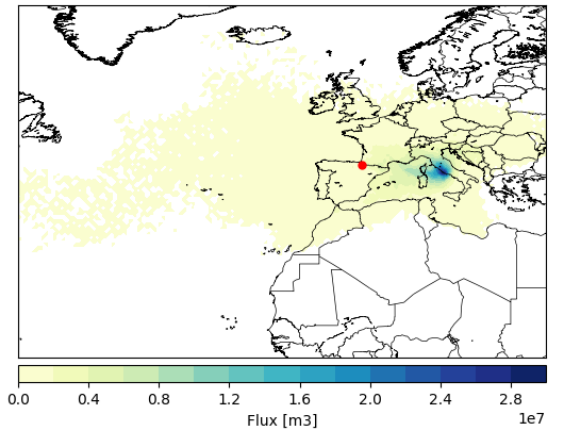

(c)

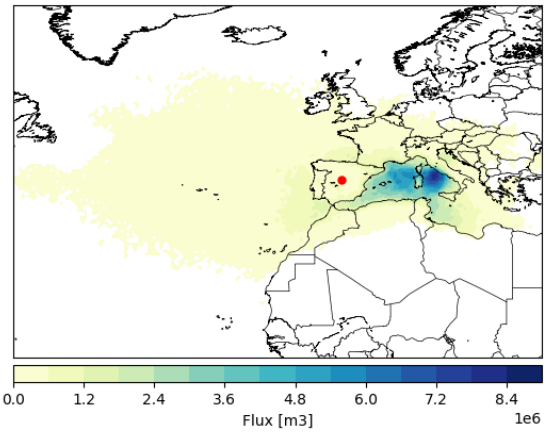

(d)

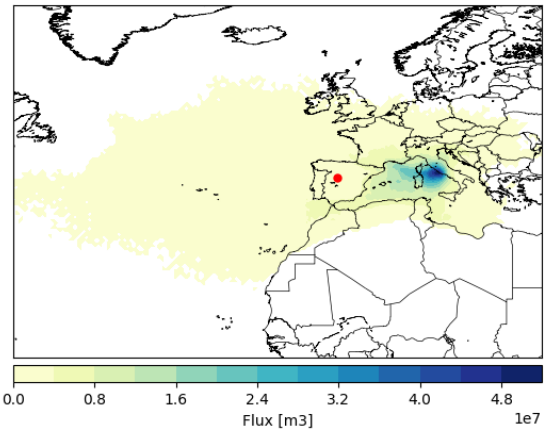

(e)

Figure 3.15: Lazio precipitation sheds: winter (a), spring (b), summer (c), autumn (d), annual (e).

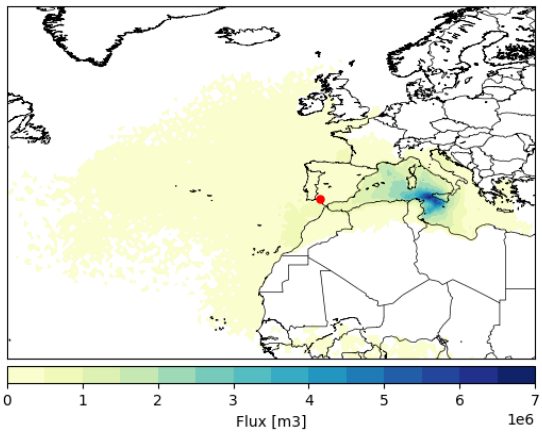

(a)

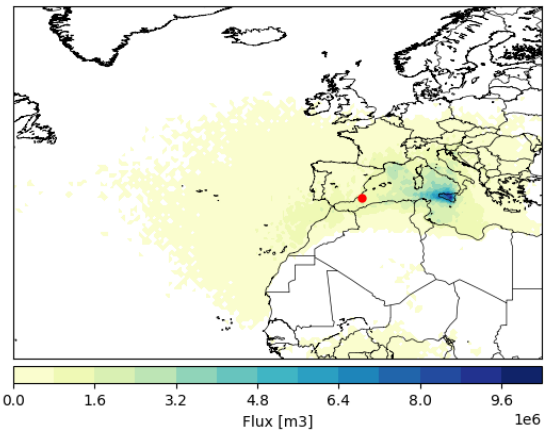

(b)

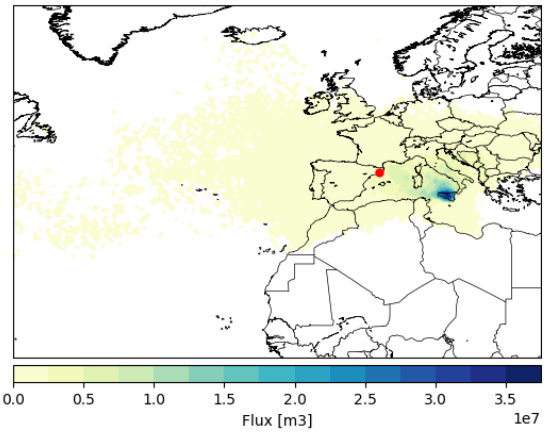

(c)

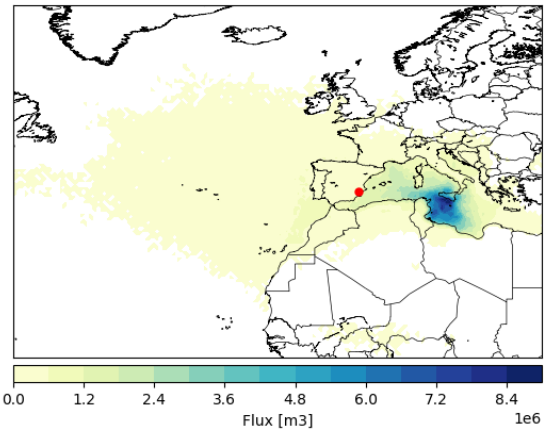

(d)

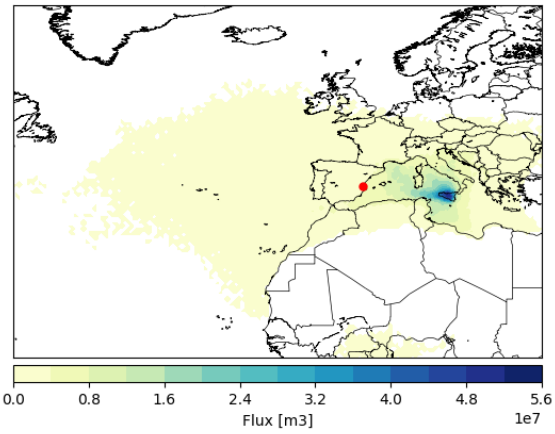

(e)

Figure 3.16: Sicilia precipitation sheds: winter (a), spring (b), summer (c), autumn (d), annual (e).

Following the evaluation of the regional precipitation shed plots, the primary countries and seas contributing to rainfall in the three regions under study have been identified. The respective data are presented in Tables 3.15 - 3.20. Each table specifies the volume of moisture evaporated from each respective country or sea and subsequently precipitated in the region under study (denoted as 'flow').

In the table corresponding to countries (Table 3.5, 3.6 and 3.7), the 'flow/total flow' percentage represents the ratio of moisture evaporated from a specific country that re-precipitates in the target region to the total global moisture volume (originating from both land and oceans) that re-precipitates in the same region. On the other hand, the 'flow/total flow from land' percentage indicates the proportion of moisture evaporated from a given country that precipitates in the target region, relative to the total global volume of moisture that re-precipitates in the same region, while this time considering only the evaporation from landmasses.

The major sources of precipitation for all regions include Italy, France, Spain, and Algeria, also as derived in the overall study for Italy. While the Italian evaporation steadily contributes about 6% to the total precipitation in all regions, the contributions from other countries display broader variation. Furthermore, North African countries, particularly those in the Maghreb region, appear stable and reliable contributors to the precipitation falling in the Italian regions.

In the case of Piemonte, as illustrated in Table 3.5, France appears to be the leading contributor, providing more than a quarter of the total precipitation due to land evaporation. The following main contributors are Italy and Spain, which provided contributions above one-sixth and one-eighth, respectively. Algeria follows with a contribution less than half of that from Spain, while Morocco contributed about one twentieth of the precipitation in Piemonte enabled by land evaporation. Interestingly, on the other extreme of the top 10, between Portugal, North American states of Canada and the USA appear. Together, they furnish roughly 4% of the global land evaporation that precipitates in Italy.

For Lazio, the reference is Table 3.6. Here, Italy plays the primary role, accounting for 6% of its precipitation, which is to say, one-fifth of the worldwide landmass evaporation that results in precipitation in Lazio originates from Italy. Following Italy, France comes in the second position, responsible for 4% of Lazio's precipitation, while Spain completes the podium, marginally under France's contribution. The middle-high ranks are filled by three Maghrebi countries—Algeria, Morocco, and Tunisia—whose combined contribution is comparable to that of Italy. Then, similar to Piemonte, Canada also plays a partial role in Lazio's precipitation. The list is rounded off by Germany and Portugal, along with Croatia, which is the first Eastern country to make an appearance.

For Sicilia (Table 3.7), as with Lazio, the dominant contribution to precipitation originates from Italy, in an almost identical manner. This time, Algeria claims the second position, supplying nearly 4% of Sicilia's rainfall. France and Spain, with contributions of around 2.5% each, play almost equivalent roles. After Morocco and Tunisia, Libya makes an appearance, responsible for 1.16% of Sicilian rainfall. Canada maintains its place in the lower ranks, and in an unexpected turn, two Eastern countries, Romania and Russia, conclude the top ten, contributing equally.

The sea-related table shares a similar format with the country table, not only featuring the 'flow' values but also two crucial ratios. The first, referred to as 'flow/total flow,' represents the proportion of moisture that evaporates from each sea and re-precipitates in the region of interest, relative to the total global evaporation volume (from both land and sea) that re-precipitates in the same region.

The second ratio, 'flow/total flow from seas,' demonstrates the proportion of moisture evaporated from each sea that eventually re-precipitates in the region of interest, against the total volume of sea-evaporated water globally that re-precipitates in the region of interest.

Every region records the Atlantic Ocean as the most important source of precipitation, indicating its broad-scale role in the Italian rainfall. Interestingly, moving southward, the role of the Atlantic appears to slightly decline: with a maximum importance in Piemonte, it becomes less predominant in Sicilia. Other important sea sources are the Western and Eastern Mediterranean basins, along with the Tyrrhenian Sea. Their relative importance varies from one region to the other, but they all share the common characteristic of being very far from challenging the leading role played by the Atlantic.

In the case of Piemonte (Table 3.18), more than one-third of precipitation is driven by Atlantic evaporation. This means that, on a global scale, more than half of the maritime evaporation that precipitates in Piemonte originates from the Atlantic Ocean. The following source of precipitation is from the Western basin of the Mediterranean Sea, accounting for nearly one-tenth of the region's precipitation. Remaining contributions descend gradually, the Tyrrhenian Sea accounts for about 3%, while the Eastern basin contributes around 2.5%. The other sources of Piemonte's precipitation are still seas belonging to the Mediterranean basin, including the Balearic Sea, the Adriatic Sea, and the Ligurian Sea. At the final tail of the rank, two northern seas (North Sea and the Celtic Sea) emerge, collectively responsible for approximately 2.6% of Piemonte's rainfall.

In Lazio (Table 3.19), the same four seas as Piemonte - the North Atlantic, Mediterranean Western Basin, Tyrrhenian Sea, and Eastern Basin - provide the largest contributions in the same order, although there's a shift in proportions. The

North Atlantic's contribution decreases by 5% when considering the 'flow/total flow' percentage. In contrast, the shares from the Mediterranean Western Basin, Tyrrhenian Sea, and Eastern Basin rise by approximately 3%, 8%, and 1% respectively. As with Piemonte, the Bay of Biscay, Balearic, and Adriatic Seas each contribute less than 2% to Lazio's precipitation, yet their order of contribution is reversed. A constrained moisture source is still detectable in the northern sea, with the Celtic Sea continuing its limited contribution and the Norwegian Sea making its initial appearance as the last of the rank.

In Sicilia (Table 3.20), the North Atlantic's contribution sees another reduction when considering the 'flow/total flow', though it still retains substantial influence, being responsible for 25% of Sicilia's precipitation. Notably, the Eastern Basin's share rises significantly, almost by 10% compared to Lazio, nearly matching the contribution of the Western Basin. The Tyrrhenian Sea and Adriatic Sea contribute around 7.7% and roughly a third of that, respectively. Thanks to its proximity, the Ionian Sea emerges as a source, despite with a restrained share below the 2%. The Balearic Sea, the Bay of Biscay and Alborean sea collectively account for about 2.5% of Sicilia's precipitation. Finally, even given Sicilia's lower latitude, a small contribution of less than 0.5% from the Norwegian Sea is still observed.

To deliver a more profound and visually appealing perspective on the main contributors to the precipitation in the three key regions under study – Piemonte, Lazio, and Sicilia – Fig.3.17 presents a clear geographic representation. This distinctive cartographic illustration underscores the principal land and sea areas that annually provide moisture to the regions of interest. The color intensity of the depicted countries and seas directly correlates with the 'flow/flow from land' and 'flow/flow from seas' values, previously elaborated from Table 3.15 to Table 3.20.

Table 3.15: Piemonte - main contributing countries.

Countries	**flow** $[m^3/y]$	**flow/tot flow**	**flow/tot flow from land**
France	2.63×10^9	9.33%	26.72%
Italy	1.73×10^9	6.14%	17.59%
Spain	1.29×10^9	4.57%	13.08%
Algeria	6.15×10^8	2.18%	6.24%
Morocco	4.83×10^8	1.71%	4.90%
Germany	3.44×10^8	1.22%	3.50%
Switzerland	2.38×10^8	0.84%	2.42%
Canada	2.15×10^8	0.76%	2.18%
Portugal	2.10×10^8	0.75%	2.13%
USA	1.84×10^8	0.65%	1.86%
Others	1.91×10^9	6.76%	19.36%

Table 3.16: Lazio - main contributing countries.

Country	**flow** $[m^3/y]$	**flow/tot flow**	**flow/tot flow from land**
Italy	1.01×10^9	6.11%	19.92%
France	7.58×10^8	4.60%	14.99%
Spain	6.21×10^8	3.77%	12.30%
Algeria	5.38×10^8	3.26%	10.65%
Morocco	3.53×10^8	2.14%	6.99%
Tunisia	1.49×10^8	0.90%	2.94%
Canada	1.26×10^8	0.76%	2.49%
Germany	9.83×10^7	0.60%	1.94%
Portugal	9.74×10^7	0.59%	1.93%
Croatia	9.07×10^7	0.55%	1.79%
Others	1.22×10^9	7.37%	24.05%

Table 3.17: Sicilia - main contributing countries.

Countries	**flow** $[m^3/y]$	**flow/tot flow**	**flow/tot flow from land**
Italy	9.23×10^8	6.01%	18.50%
Algeria	5.69×10^8	3.70%	11.40%
France	4.07×10^8	2.65%	8.15%
Spain	3.88×10^8	2.53%	7.78%
Morocco	3.08×10^8	2.01%	6.18%
Tunisia	2.06×10^8	1.34%	4.12%
Libya	1.78×10^8	1.16%	3.57%
Canada	1.17×10^8	0.76%	2.35%
Romania	1.10×10^8	0.71%	2.20%
Russia	1.08×10^8	0.71%	2.17%
Others	1.68×10^9	10.91%	33.58%

Table 3.18: Piemonte - main contributing seas.

Seas	**flow** $[m^3/y]$	**flow/tot flow**	**flow/tot flow from ocean**
North Atlantic Ocean	1.01×10^{10}	35.96%	55.27%
Mediterranean Sea - Western Basin	3.27×10^{9}	11.60%	17.82%
Tyrrhenian Sea	9.06×10^{8}	3.21%	4.94%
Mediterranean Sea - Eastern Basin	6.81×10^{8}	2.41%	3.71%
Bay of Biscay	5.30×10^{8}	1.88%	2.89%
Balearic (Iberian Sea)	4.59×10^{8}	1.63%	2.50%
Adriatic Sea	4.37×10^{8}	1.55%	2.38%
Ligurian Sea	3.18×10^{8}	1.13%	1.73%
North Sea	2.39×10^{8}	0.85%	1.30%
Celtic Sea	2.37×10^{8}	0.84%	1.29%
Others	1.13×10^{9}	4.01%	6.17%

Table 3.19: Lazio - main contributing seas.

Seas	**flow** $[m^3/y]$	**flow/tot flow**	**flow/tot flow from oceans**
North Atlantic Ocean	5.07×10^{9}	30.76%	44.37%
Mediterranean Sea - Western Basin	2.39×10^{9}	14.51%	20.93%
Tyrrhenian Sea	1.89×10^{9}	11.44%	16.50%
Mediterranean Sea - Eastern Basin	6.13×10^{8}	3.72%	5.36%
Adriatic Sea	2.57×10^{8}	1.56%	2.25%
Balearic (Iberian Sea)	2.49×10^{8}	1.51%	2.18%
Bay of Biscay	1.92×10^{8}	1.16%	1.68%
Alboran Sea	1.07×10^{8}	0.65%	0.94%
Celtic Sea	8.72×10^{7}	0.53%	0.76%
Norwegian Sea	7.64×10^{7}	0.46%	0.67%
Others	4.98×10^{8}	3.02%	4.36%

Table 3.20: Sicilia - main contributing seas.

Seas	**flow** $[m^3/y]$	**flow/tot flow**	**flow/tot flow from oceans**
North Atlantic Ocean	3.85×10^{9}	25.08%	37.16%
Mediterranean Sea - Western Basin	1.92×10^{9}	12.52%	18.54%
Mediterranean Sea - Eastern Basin	1.91×10^{9}	12.44%	18.43%
Tyrrhenian Sea	1.18×10^{9}	7.69%	11.40%
Adriatic Sea	3.27×10^{8}	2.13%	3.16%
Ionian Sea	2.72×10^{8}	1.77%	2.62%
Balearic (Iberian Sea)	1.68×10^{8}	1.10%	1.62%
Bay of Biscay	1.40×10^{8}	0.91%	1.35%
Alboran Sea	7.38×10^{7}	0.48%	0.71%
Norwegian Sea	6.59×10^{7}	0.43%	0.64%
Others	4.54×10^{8}	2.96%	4.38%

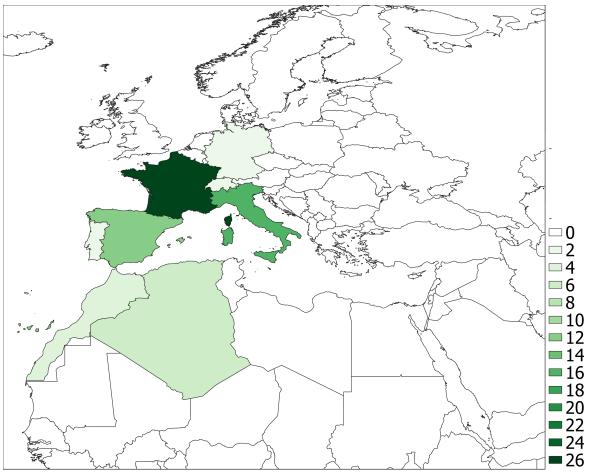

(a)

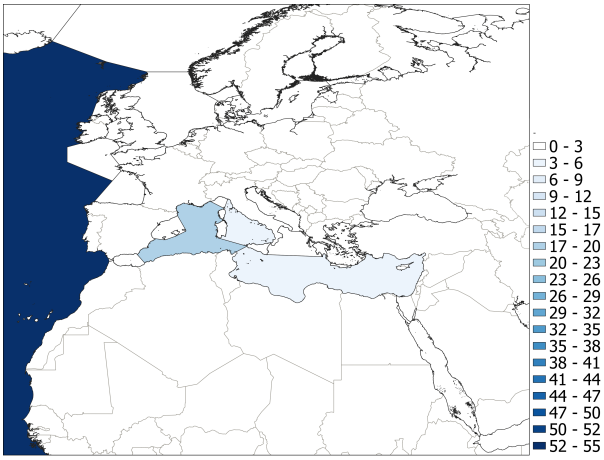

(b)

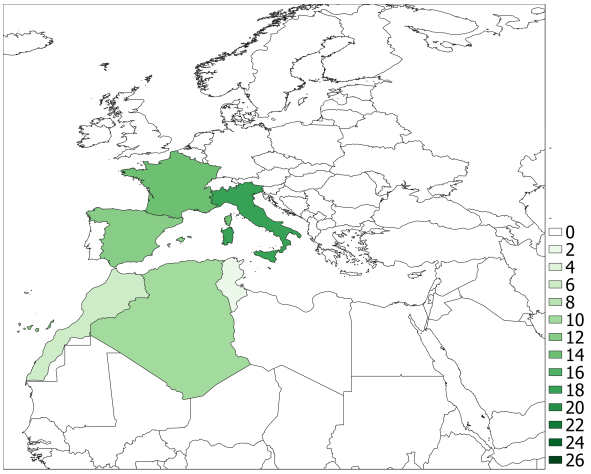

(c)

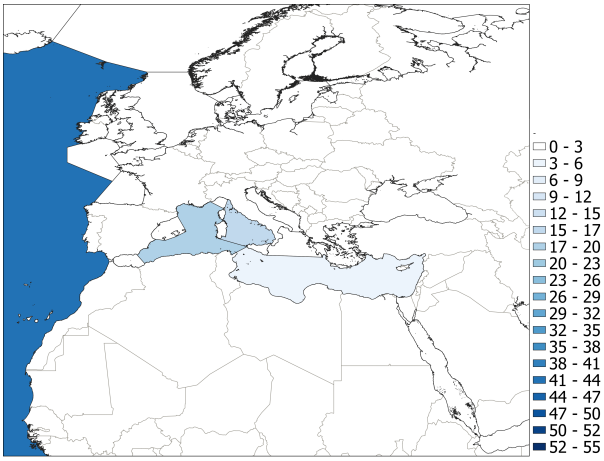

(d)

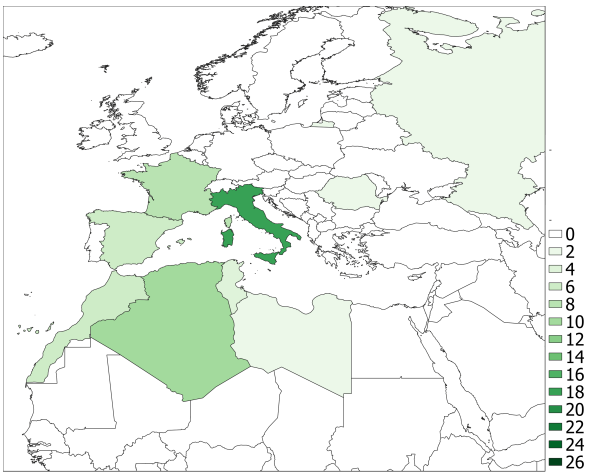

(e)

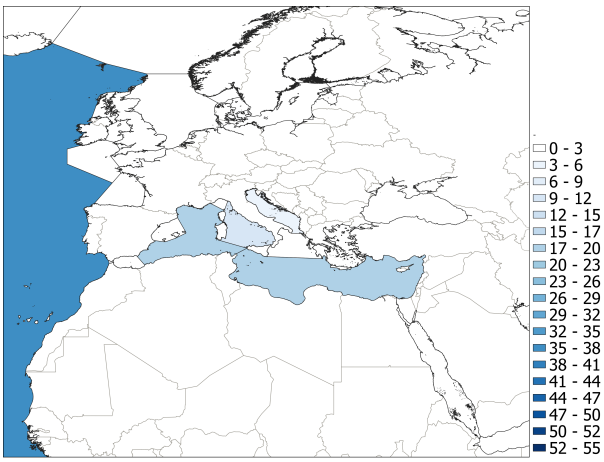

(f)

Figure 3.17: Main contributing countries and seas for Piemonte (a) and (b), Lazio (c) and (d), Sicilia (e) and (f). Values are taken from the percentages 'flow/tot flow from land' and 'flow/tot flow from oceans'.

3.2.3 Backward footprint: climatological framework

Similar considerations drawn from the forward footprint analysis can be pulled out here, where the aim is to identify recurring and divergent patterns in the distribution of precipitation sheds for both national and regional Italian plots.

The marked westward orientation of the precipitation sheds, as evidenced in the plots of Fig.3.11 and Figs.3.14 - 3.16, further confirms the impact of the prevailing westerlies. These winds, which, as already noted, blow from west to east, pick up substantial amounts of moisture from the Atlantic Ocean and from the western countries of Europe. Some of this moisture, when meeting favorable conditions in Italy, manifests as precipitation, thereby enhancing the rainfall within the regions. This trend can be clearly seen in all the graphical representations where the distribution of the precipitation sheds mainly shows a remarkable westward orientation.

Another interesting observation related to the seasonality of wind velocities could be drawn from the geographic location of the centroid. As seen above, the centroid in winter is generally located at a farther distance compared to its summer position. The reason for the increased separation can be explained again through the strength of the westerly winds (view Subparagraph 3.1.3 for a more detailed explanation): during its peak in winter, these are strong enough to carry moisture over longer distances before its eventual precipitation. As the seasons progress and the temperatures rise, the strength of the westerlies decreases, so does their capacity to carry moisture over greater distances.

For example, in the region of Piemonte, the centroid for winter (Fig.3.14 a) is located at a distance of roughly 1980 kilometers from Turin. Nevertheless, as spring arrives ((Fig.3.14 b), this centroid shifts closer, reducing the distance to approximately 400 kilometers. A similar trend is evident in Lazio, where the winter centroid (Fig.3.15 a) is situated about 1880 kilometers from Rome; however, by the summer season (Fig.3.15 c), this distance diminishes to nearly 1140 kilometers. This pattern is even more pronounced when analyzing Sicila. Here, the centroid distance in winter (Fig.3.16 a) from Palermo has a value of around 1780 kilometers, roughly double that expressed in its summer position by Fig.3.16 c.

Continuing with further reflection on where the centroid is located, it is relevant to discuss the larger dynamics of global atmospheric circulation. During winter, the Hadley cell — a key component of atmospheric circulation — contracts toward the equator. Simultaneously, the Intertropical Convergence Zone (ITCZ)—a low-pressure belt encircling Earth, where trade winds from the Northern and Southern Hemispheres converge—shifts toward the summer hemisphere. As a consequence of this phenomenon, the mid-latitude cell, where the westerlies dominate, extends southward in the Northern Hemisphere.

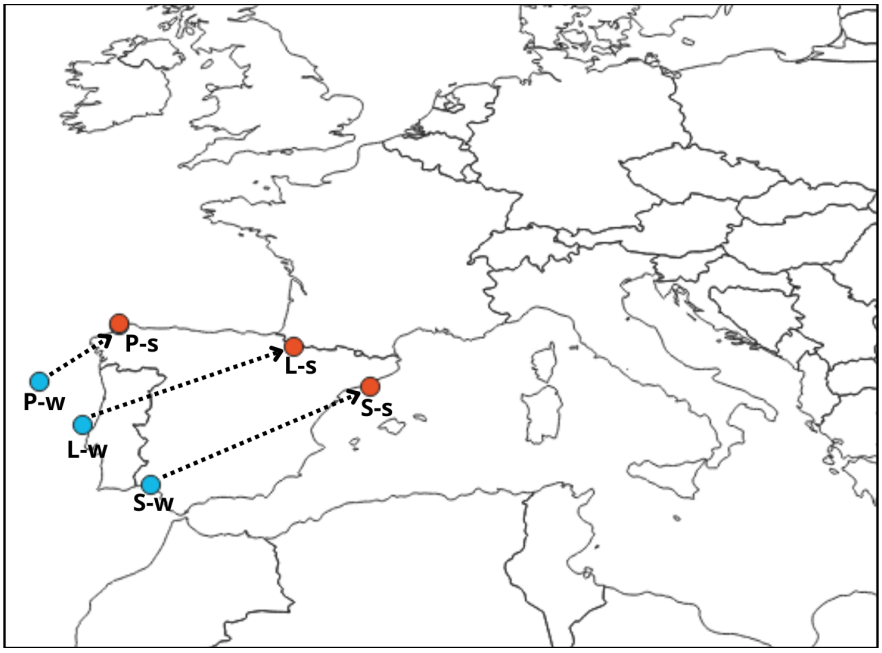

Figure 3.18: Precipitationshed centroids for Piemonte (P), Lazio (L), and Sicilia (S) shift seasonally between winter (w) and summer (s). Winter centroids are positioned further south and at greater distances from their summer counterparts, indicating seasonal variation in global moisture flow patterns.

These changes lead moisture-laden winds, such as the westerlies, to reach lower latitudes. Accordingly, the evaporation zones feeding the precipitation to Italy, represented by the centroids of the precipitation basins, also shift southward. This is evident from all graphical representations, where the winter centroids in all national and regional graphs are always farther south of their summer counterparts (see Fig.3.18 for a better visualization of this phenomena).

In addition, considering the distance between the centroid and its corresponding region, it should be notice a great latitudinal trend. In Piemonte, this distance, averaging all the seasons, is about 1680 kilometers, while in Lazio, it is about 1512 kilometers. Still, this reduction is more pronounced in Sicilia where it decreases to 1290 kilometers.

As outlined in the previous section, the intensity of the westerlies is observed to diminish with a southward progression. Sicilia, located at the boundary of the westerlies' impact zone, experiences a centroid of the precipitation sheds that is one-quarter closer compared to that in Piemonte.

In conclusion, a final observation relative to the centroid may need attention. It is evident that the centroid of precipitation basins consistently exhibits a greater distance than that of evaporation sheds throughout all seasons and geographical regions. This observation could be elucidated by the examined phenomena already seen so far, specifically the impact of the westerlies and the varying thermal exchange properties between aquatic and terrestrial environments, in addition to their distinct geographical distributions.

As discussed, a large part of the precipitation falling in Italy has a western origin due to the prevailing westerlies. The Atlantic Ocean dominates this area, acting as a substantial and constant moisture source for the rainfall over both Italy and Europe. The Atlantic, with its wide and homogeneous surface, allows for a continuous heat exchange between ocean and atmosphere; this favors stable environmental conditions. This stability in the atmosphere allows for the transport of water vapor over great distances, which explains why the centroid of the precipitation sheds is so far away from Italy. Even the western part of the Mediterranean Sea could play a similar role, obviously in a less extended manner.

In contrast, the moisture that evaporates from Italy and moves eastward tends to encounter mainly landmasses. The variable topography and greater fluctuations in heat flow of these terrestrial areas promote conditions of increased atmospheric instability, which speed up the processes of condensation and precipitation. Consequently, moisture is more predisposed to precipitate rapidly, reducing the distance covered by evaporation sheds and maintaining their centroid closer to Italy.

Now the focus shifts to Table 3.11 and Table 3.14. As mentioned earlier, most of the precipitation falling over Italy is of maritime origin. This is less surprising when looking at the global water distribution, whereby the oceans, making up about 71% of Earth's surface area, provide a vast area for evaporation, as opposed to the land. In addition, the ocean can continuously feed moisture to the atmosphere, while on land, its ability to supply the atmosphere with moisture is limited by conditions in arid/dry periods.

However, the introduction of seasonality into the analysis of precipitation shed origins can lead to the formation of varying patterns in sea and land contributions. In this regard, also Fig.3.10 and Fig.3.13 can offer a useful visualization.

During warmer seasons, like spring and summer, the higher temperatures lead to a rise in the evaporation rate from both land and oceans. Anyway, in cases where substantial amounts of water are available, such as rivers, lakes, or soil moisture, and where there is a considerable temperature rise, the surge in land-based evaporation can be particularly prominent. This would, in turn, lead to higher contribution portions of atmospheric moisture—and hence precipitation—originating from terrestrial

evaporation.

On the other hand, the sea's temperature fluctuations are less pronounced than those over land. Since water has a higher heat capacity than land, it requires more energy to achieve the same temperature increase. As a result, while rising temperatures during the hot months can enhance evaporation over the ocean, the effect is softer compared to the more abrupt increase observed over land.

All the graphical representations show this feature, whereby the most intense precipitation sheds are mostly found over the sea in the cold seasons. Contrarily, during the warm seasons, these precipitation sheds tend to go towards the land areas, enhancing the nature of the interplay between seasonality and the marine-terrestrial contribution to the precipitation process.

A more subtle but interesting observation is the variation in sea's contribution with region, as depicted by 3.14. In Piemonte, for instance, the sea's contribution to precipitation seems to remain fairly constant throughout the year. However, in Lazio and even more so in Sicilia, the sea's contribution appears to emulate the trend observed in land contributions - with a minimum in winter and a maximum in summer - though in a less pronounced manner. These differences can be explained through a plausible reason by analyzing the data in Table 3.18 - 3.20. The region of Piemonte is located in the northwestern part of Italy and is more directly influenced by the Atlantic Ocean, where the moisture carried by the westerlies receives the most substantial contribution from that vast body of water. The Atlantic Ocean, due to its vast dimensions and considerable depth, remains at a relatively stable temperature throughout the year. This also means that the ocean's evaporation rate tends to remains rather constant as well as, in turn, its contribution to the precipitation in Piemonte across all seasons.

Going on, Lazio and Sicilia, located further south, get a greater influence by the Mediterranean Sea, which behaves quite differently. In fact, the Mediterranean Sea is smaller and shallower than the Atlantic Ocean, and thus it heats up more quickly in the summer and cools down more rapidly in the winter. As a consequence, the rate of evaporation from the Mediterranean Sea (and consequently, its contribution to the precipitation in nearby regions like Lazio and Sicilia) varies more significantly across the seasons.

In the warmer months, when the Mediterranean Sea is hotter, the rate of evaporation increases. This moisture-laden air is then carried over Lazio and Sicilia, contributing to their precipitation. Conversely, in the colder months, the Mediterranean Sea cools down, likewise the rate of evaporation, and the contribution of the Mediterranean Sea to the precipitation in these regions diminishes. Subsequently, Lazio and Sicilia experience a more visible seasonal variation in their precipitation

sheds compared to Piemonte.

This climatological investigation tries to find some possible explanations of different nature to the results that have been collected in this research. Nonetheless, this effort could appear a somewhat simplified analysis of a deep and articulated system. The factors ruling over the transport of moisture in Italy and, even more specifically, in its different regions are dominated by a complex set of interconnected and multiple elements.

Variables including extensive global atmospheric circulation patterns, localized wind dynamics, topographical characteristics, variations in atmospheric parameters, as well as more short-lived meteorological events, collectively play an essential role in influencing where and when moisture is transported and precipitates. Additionally, alterations in land use and anthropogenic climate change may further complicate these dynamics by modifying these foundational parameters in ways we are only beginning to understand.

Though all these complications were recognized, the results in the above chapters find a good alignment with interpretations developed and provided in this subsection. Data confirm the underlying hypothesis that wind dynamics, especially those of the westerlies and their fluctuations in strength over the course of a year, together with other aforementioned factors, are key elements in determining how precipitation is distributed across Italy and how Italian evaporation is scattered throughout the world.

3.3 RECON and Utrack comparison

In this section, the annual forward and backward footprint developed through the RECON model will be shown and d. Furthermore, the results will be compared to the relative Utrack's outcomes in order to check analogies and inconsistencies between the two models.

3.3.1 Italian forward footprint

In Fig.3.19, the map of the annual evaporationsheds analyzed using the new RECON model is presented. Similar to the evaporationsheds obtained through the Utrack model (Fig. 3.2 (e)), a clear eastward shift is observed, with Italy and the Balkan coast being affected by the most significant evaporationsheds. Despite the first similarities between the two maps, some evident discrepancies that cannot be neglected emerge.

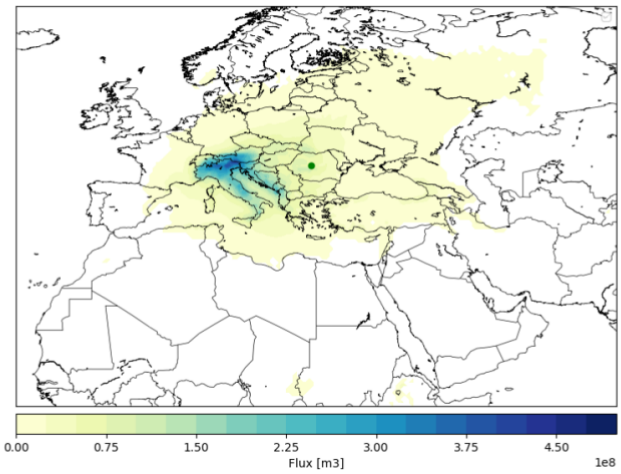

Figure 3.19: Annual Italian forward footprint according to RECON.

The differences between the two models are illustrated in Table 3.21. This table compares various parameters related to the annual forward footprint in Italy. Specifically, it analyzes: the total volume of water evaporated (total volume), the amount of water that ends up in the sea (volume to sea), and the amount that ends up on land (volume to land). The position of the centroid of the evaporationsheds is also

compared, both in terms of latitude and longitude, and in relation to the distance of this centroid from Rome. The "difference" entry for the centroid indicates the distance between the centroids calculated by the two models.

Additionally, the area containing 90% of the evaporationsheds is compared. In the last row, the percentage of overlap of this area for each model is provided, representing the overlap of the area calculated by RECON onto the area of Utrack and vice versa.

Table 3.21: Comparison of RECON and Utrack parameters in the Italin forward footprint processing.

Parameter	**RECON**	**Utrack**	**Difference**
Annual Evaporation Volume			
Total Volume (m^3)	2.00E+11	2.20E+11	-10.27%
Volume to Sea (m^3)	4.70E+10	5.18E+10	-10.16%
Volume to Land (m^3)	1.53E+11	1.69E+11	-10.25%
Centroid Location			
Latitude (°)	45.8	41.2	-4.7
Longitude (°)	24.5	21.2	-3.4
Distance from Rome (km)	1054	729	591
90% Evaporationshed Area			
Area (km^2)	2.73E+7	2.61E+7	4.60%
Area Overlap (%)	76.1	79.8	-

A first difference between the two models lies in the annual evaporated volumes over the territory. With 200 billion cubic meters, RECON's estimation is approximately 10% lower than the corresponding estimate from Utrack. This results in a reduction of about 10% in both the volume of water precipitating over land and that precipitating over seas/oceans.

In addition to the difference in quantity, a difference in spatial extent is also evident. Firstly, there is a slight difference in the area distributing 90% of the evaporated water. In the case of the RECON model, this area is estimated to be 4.6% larger than that of Utrack, indicating a slightly more dispersed or diffuse distribution. Consistent with this observation, the centroid of the evaporationsheds according to RECON is located more than 1,000 kilometers from Rome, compared to 729 kilometers for Utrack, indicating a distance of 591 km between the two centroids. In fact, in the case of RECON, the centroid is situated in Romania, over 4.5 degrees farther north and approximately 3.5 degrees farther east than the Utrack centroid, which

is located between Albania and North Macedonia. These differences in the distribution of evaporationsheds are further corroborated in the graph in Fig.3.20, which compares the zonal distribution (volume redistributed by latitude) of the evaporationsheds.

Both models show a similar trend, with a peak around 40-45° N latitude, a progressive decline to nearly zero toward 25° N, and a slight increase between 10-15° N latitude. A rather notable difference emerges when the curves are observed: the blue curve, associated with the RECON model, is positioned higher than the orange curve of the Utrack model above 50°, conversely, it is lower below 45°. This indicates that the RECON model tends to distribute the evaporationsheds more to the north of Italy and less to the south compared to the Utrack model.

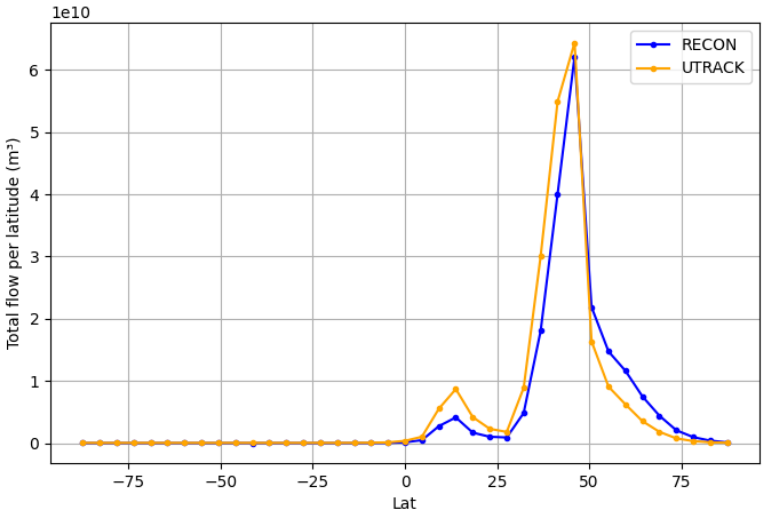

corr.= 0.948

Figure 3.20: Evaporationsheds zonal distribution comparison between RECON (blue line) and Utrack (Orange line).

Aligned with this discourse, the bar chart presented in Fig. 3.21 illustrates the ten principal recipient nations of water evaporated annually in Italy (in volumetric terms), as determined by the RECON model. For each of these nations, the outcomes derived from the RECON model are compared with the corresponding findings obtained through the Utrack model. It is important to point out that the Utrack data in this figure do not follow the top ten recipient countries of the model; instead, they match the same list of countries as found in RECON (to see the top ten receiving countries for Utrack, refer to Table 3.2).

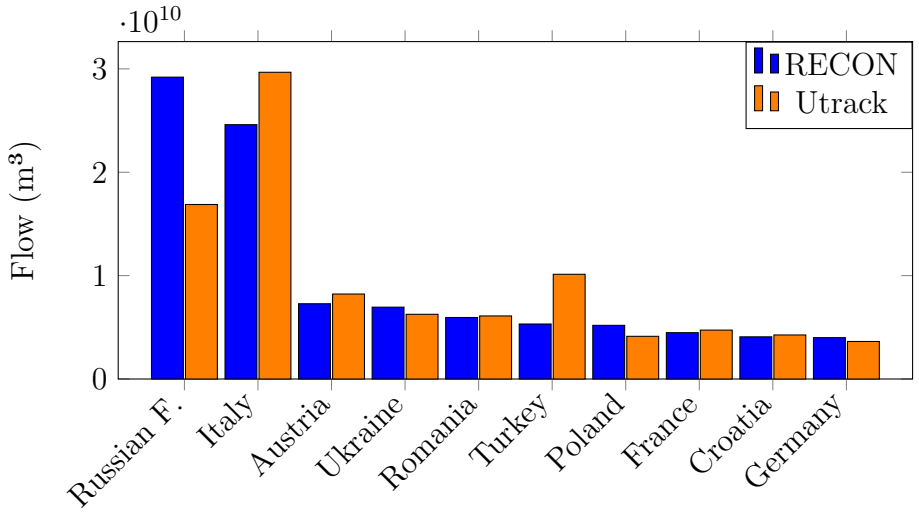

Figure 3.21: Top 10 receiving countries of water evaporated in Italy according to the RECON model, compared with the respective results obtained using the Utrack model.

With nearly 30×10^9 cubic meters received, Russia moves from second place in the Utrack model to first place in the RECON model, swapping positions with Italy. This inversion, which displays a discrepancy of the 40%, represents the most significant difference in this analysis.

Another important difference concerns Turkey, which receives almost twice the volume in Utrack compared to RECON. Regarding the remaining countries—Austria, Romania, Croatia, France, and Germany—the values in both models are comparatively close to each other. It should be noted that Bosnia and Herzegovina, as well as Greece, appear in the top ten of the Utrack ranking, do not appear in RECON.

In analogy to Fig. 3.21, Fig.3.22 shows the the top ten of receiving seas according to RECON, and the relative comparison with the Utrack's results. In terms of consistency, certain seas maintain their high rankings in both models. Both models recognize for the first four seas-Adriatic sea, Mediterranean western basin (WB), North Atlantic Ocean, Tyrrhenian- the main hierarchy. Anyway, the comparison of this ranking highlights notable differences in the estimated volumes of water received by various seas through evaporation from Italy. One important difference lies in the total volumes reported. In general, the Utrack model assigns higher values to most seas compared to the RECON model (as already seen in the row 'Volume to Sea' in Tab. 3.21). For example, the Adriatic Sea, which ranks first in both models, receives 8.63×10^9 cubic meters in the RECON model but 9.31×10^9 in Utrack. A similar

pattern is observed for the Eastern Basin of the Mediterranean Sea, which shows 5.80×10^9 cubic meters in RECON and 8.45×10^9 in Utrack.

Interestingly, the only seas receiving more volume according to RECON compared to Utrack are the Barents Sea and the North Sea, which are both located at high latitudes.

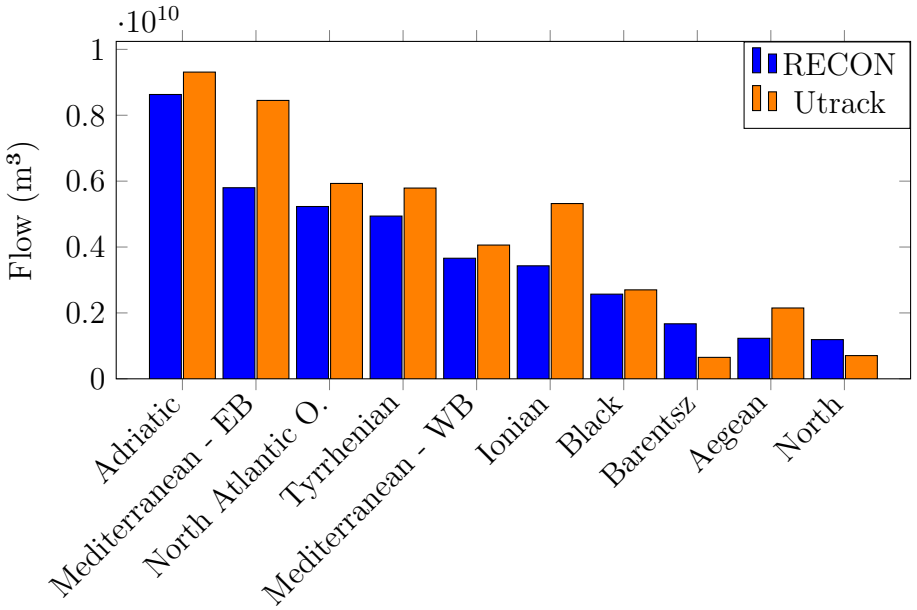

Figure 3.22: Top 10 receiving seas of water evaporated in Italy according to the RECON model, compared with the respective results obtained using the Utrack model.

3.3.2 Regional forward footprint

In this section, the outputs of the two models are analyzed and compared in terms of forward footprint for each reference region. RECON's maps for the annual regional evaporationsheds are shown in Fig.3.23. These results share some basic similarities to the corresponding maps in Utrack (Fig. 3.5 (e), 3.6 (e), 3.7 (e)) but exhibit significant differences in spatial localization and volumetric parameters.

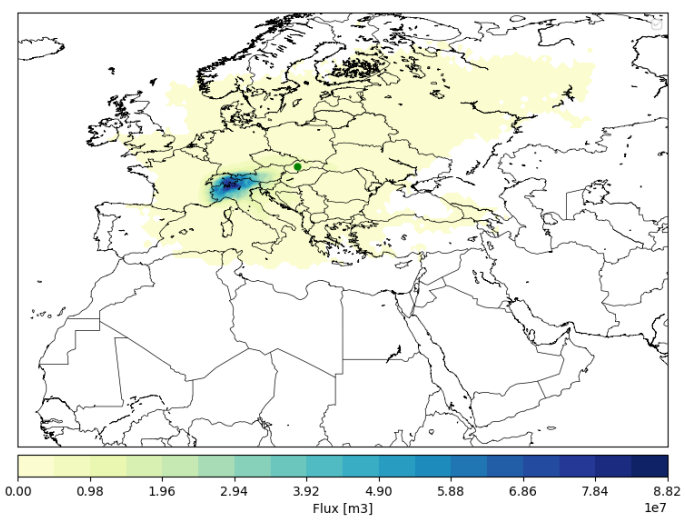

(a)

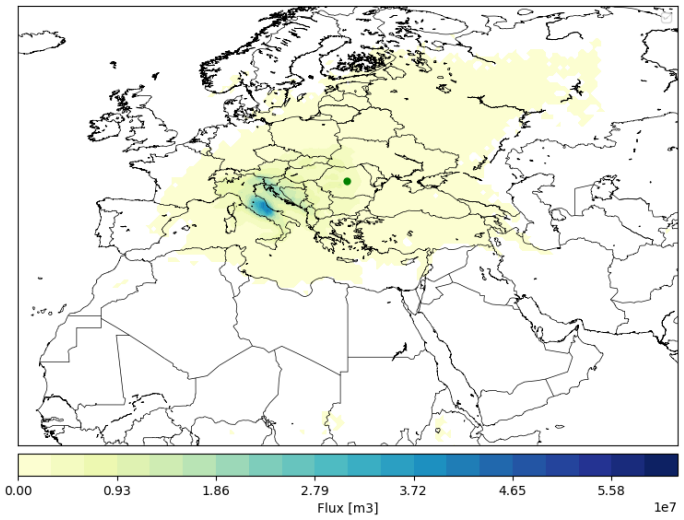

(b)

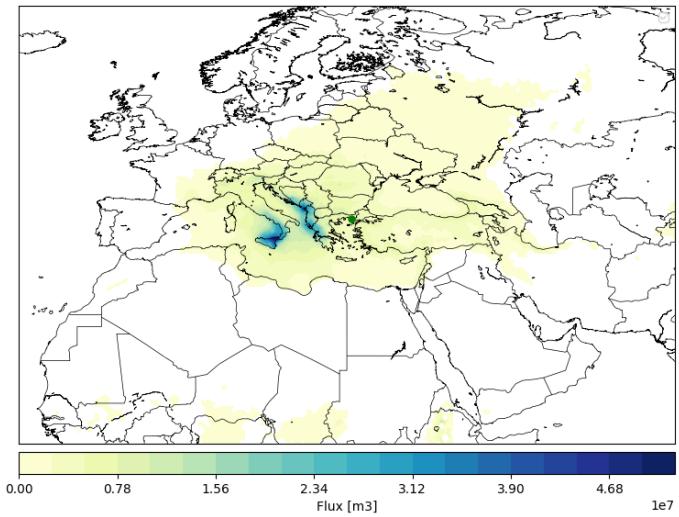

(c)

Figure 3.23: Annual forward footprint according to RECON. Piemonte (a), Lazio (b), Sicilia (c).

These discrepancies, while varying in intensity, follow recurring patterns that emerge across all analyzed regions and are consistent with the trends already observed at the national level for Italy.

The reference for a more precise comparison is Tab.3.22, whose construction is elaborated following the same reasoning described for Tab. 3.21. In all cases examined, the RECON model estimates a total volume evaporated from the region that is lower than the volume estimated by the Utrack model. The most significant difference is observed in Lazio, where RECON predicts a volume (1.22E+10 m3) that is 23% lower than Utrack, while Sicilia, with 2.03E+10 m3, shows the smallest discrepancy, approximately 7.5%. Both models agree in identifying a predominance of the volume that reprecipitates over land. However, for the three regions considered, the discrepancies between the two models regarding the volume that precipitates in marine environments are significantly greater than those related to the volume that precipitates over land, exceeding 35% in both Piemonte and Lazio.

Similarly to what was observed for Italy, the RECON model exhibits a broader distribution of evaporationsheds compared to the distribution estimated by the Utrack model in all analyzed regions. This behavior can be both evaluated through the area that distributes 90% of the total volume and through the position of the centroid.

Regarding the area, the results show that it is slightly larger for the RECON model, confirming its tendency to estimate more diffuse and less concentrated distributions. Concerning the centroid, it is observed that RECON consistently places it further east compared to Utrack, with the maximum difference recorded in Lazio, where the centroid estimated by RECON is shifted more than three and a half degrees eastward.

Additionally, it is noteworthy that the RECON model positions the centroid not only further east but also further north. The discrepancies in latitude are even more pronounced than those in longitude. Once again, Lazio shows the greatest difference, with the centroid estimated by RECON located about five degrees further north compared to Utrack.

These shifts are evident when examining regional cases: transitioning from the Utrack model to the RECON model, for Piemonte, the centroid moves from Croatia to Slovakia; for Lazio, from Macedonia to Romania; and, finally, for Sicilia, from Crete to the northern border between Greece and Turkey.

This trend is confirmed by the graphs shown in Fig. 3.26, which illustrate the zonal distribution of annual evaporated volume for each region. The blue curve represents the results of the RECON model, while the orange curve represents those of the Utrack model.

Similarly to what was observed for Italy, the three analyzed regions exhibit a sim-

ilar pattern: a maximum peak located between 45°N (Piemonte) and 30°N (Sicilia), followed by a rapid decrease to nearly zero at 25°N. Subsequently, a new increase is observed around 10°N, which is almost imperceptible for Piemonte but significant for Sicilia.

In all cases, the RECON model shows a less pronounced peak compared to Utrack. However, there is an increase in evaporationsheds at higher latitudes, i.e., to the right of the peak (blue curve higher than the orange curve), and a reduction at lower latitudes relative to the peak (blue curve lower). This behavior is consistent with previous observations, confirming that the RECON model generates a broader and less concentrated distribution, with a greater northward shift of evaporationsheds compared to the Utrack model.

In general, despite differences in details, there is a certain noticeable degree of compatibility between the two models. From Table 3.22, it can be observed that the area distributing 90% of the evaporated water volume is similar in size for both models. Moreover, despite the aforementioned differences, the geographic extent of these areas is also quite similar. Specifically, the overlap of this area between the two models is always greater than 70%, with higher values recorded for the overlap of Utrack with RECON, as the latter has a larger extent.

This similarity between the two models is also reflected in a high correlation coefficient for each region, with values in all three cases being very close to unity.

Meteorological explanation

It can be observed that both models highlight how the area in which 90% of the evaporated volume precipitates increases as latitude decreases. This area is smallest for Piemonte (less than $2 \times 10^7\,\mathrm{km}^2$) and largest for Sicilia (ranging between $3.4 \times 10^7\,\mathrm{km}^2$ according to the RECON model and approximately $3 \times 10^7\,\mathrm{km}^2$ according to the Utrack model). This indicates that Piemonte's evaporationsheds are more concentrated and less diffuse compared to those of Sicilia.

The origin of this difference can be traced to the analysis of the geographic and morphological characteristics of the three regions considered. As previously highlighted, the proximity of the Alps to Piemonte plays a "containing" role in the regional evaporative movement, promoting more rapid and localized water reprecipitation. Similarly, Lazio, being close to the Apennines, may exhibit a similar phenomenon, albeit to a lesser extent, given the lower elevation of this mountain range compared to the Alpine arc.

In contrast, in Sicilia, being an island characterized by predominantly flat terrain, evaporation transported by winds encounters fewer obstacles and tends to reprecip-

Table 3.22: Comparison of RECON and Utrack parameters in the forward footprint processing for Piemonte, Lazio, and Sicilia.

Parameter	**RECON**	**Utrack**	**Difference**
Piemonte			
Total Volume (m^3)	1.32E+10	1.55E+10	-17.38%
Volume to Sea (m^3)	2.25E+9	3.56E+9	-36.80%
Volume to Land (m^3)	1.10E+10	1.20E+10	-8.33%
Latitude (°)	48.4	44.9	3.6
Longitude (°)	18.9	16.5	2.4
Distance from Torino (km)	930	693	438
90% Area (km^2)	1.85E+7	1.63E+7	13.50%
Area Overlap (%)	74.3	83.9	-
Lazio			
Total Volume (m^3)	1.22E+10	1.50E+10	-22.97%
Volume to Sea (m^3)	2.93E+9	4.65E+9	-36.99%
Volume to Land (m^3)	9.31E+9	1.03E+10	-9.61%
Latitude (°)	45.8	40.8	5.0
Longitude (°)	25.0	21.4	3.6
Distance from Rome (km)	1090	752	633
90% Area (km^2)	2.46E+7	2.34E+7	5.13%
Area Overlap (%)	73.8	77.3	-
Sicilia			
Total Volume (m^3)	2.03E+10	2.20E+10	-7.55%
Volume to Sea (m^3)	6.85E+9	8.07E+9	-15.11%
Volume to Land (m^3)	1.35E+10	1.39E+10	-2.88%
Latitude (°)	40.5	35.5	4.9
Longitude (°)	25.8	23.3	2.6
Distance from Palermo (km)	1084	891	574
90% Area (km^2)	3.41E+7	2.99E+7	15.02%
Area Overlap (%)	74.3	84.5	-

itate in more distant areas. This is confirmed by the extent of the area where 90% of the volume precipitates, which is approximately double that of Piemonte.

This tendency is also evident from the analysis of the centroid position: in the case of Piemonte, it is closer (indicating a greater concentration of evaporationsheds), while in Sicilia, it is located at a greater distance. Furthermore, observing Fig. 3.26, it is noticeable that the peak relative to Piemonte is sharper and confined to latitudes typical of Italy, whereas the Sicilian peak appears broader and less pronounced, further confirming the greater diffusion of evaporationsheds in Sicilia.

An interesting observation emerges when examining the zoanl distribution trend of evaporationsheds below 30°N. The noticeable drop around 25°N can likely be attributed to the high-pressure subtropical zones, which are a result of descending air in the Hadley Cell.

Conversely, the increase around 10°N, particularly evident for Sicilia, may be linked to the fact that a portion of the water evaporated from the region is channeled into the trade winds, that is the equatorward, lower branch of the Hadley Cell. This effect could becomes more pronounced in the summer, as the Hadley Cell extends further north during this season. During summer, the ITCZ typically shifts to about 10-15°N, which aligns with the secondary peak observed for Sicilia and, to a lesser extent, Lazio.

In winter, the ITCZ shifts southward to approximately 10-15°S. The absence of evaporationsheds in these latitudes during this season suggests that this possible channeling of regional evaporated water into the trade winds is absent, or less relevant, in winter (as the Hadley Cell tends to be less extended in the North). Therefore, the peak at 15°N is likely attributable to a flow that occurs predominantly during the summer and spring months and which allows to some Italian moisture to be conveyed down to equator where, once reached the ascending branch of the Hadley Cell, finally lifts up and precipitates. As this secondary peak is almost absent in Piemonte, the mechanism described here may just involve primarily to the southern regions of Italy, which are closer to the trade winds influences, without applying to the areas located more northwards.

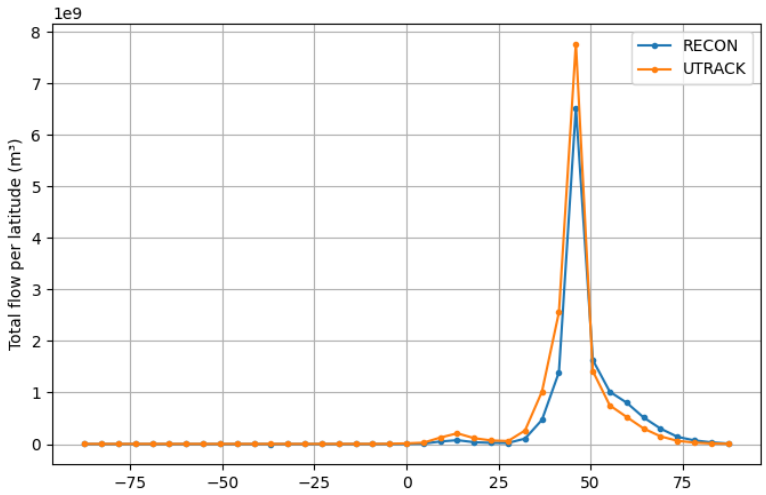

a) Corr: 0.960

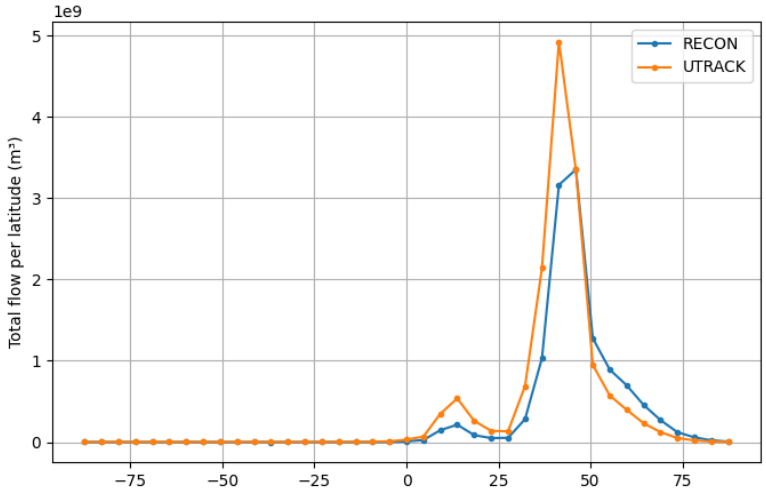

b) Corr: 0.945

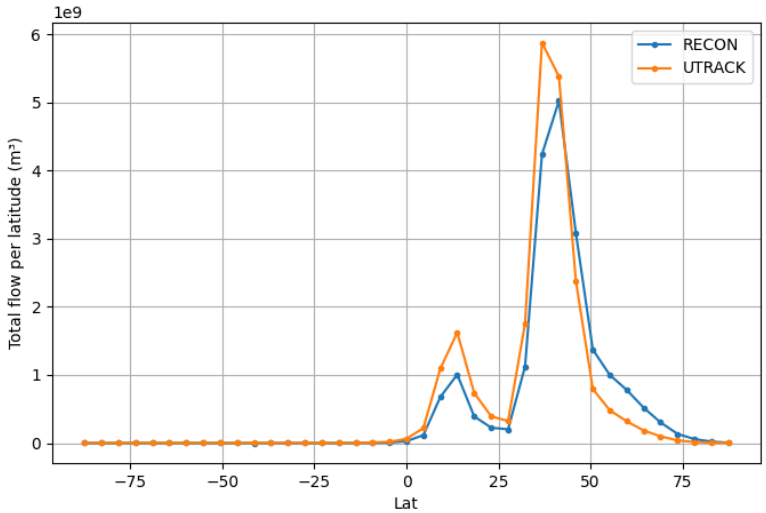

c) Corr: 0.940

Figure 3.26: Evaporationsheds zonal distribution comparison between RECON (blue line) and Utrack (Orange line) for Piemonte (a), Lazio (b) and Sicilia (c).

Main receiving countries comparison

Fig.3.27 displays the ten countries which receive the most the annual regional evaporation in cubic meters. These results are compared with the relative volumes computed with the Utrack model (refer to Tab.3.5, 3.6, 3.7 for the regional top ten according to Utrack).

Regarding Piemonte, both models identify Italy as the main destination of atmospheric moisture flowes generated by the region. However, the estimated volumes differ significantly, with Utrack attributing a value of 3.84×10^9 m^3/year, which is 45% higher than the 2.64×10^9 m^3/year estimated by RECON. This indicates greater internal recirculation according to Utrack.

Russia represents the second most important destination for both models, but with significant differences: RECON estimates a volume of 1.56×10^9 m^3/year, while Utrack reduces this estimate to 1.03×10^9 m^3/year, a decrease of 51%. For other European countries, such as Austria, Switzerland, France, and Germany, RECON presents higher estimates compared to Utrack, highlighting a greater concentration of evaporationsheds towards neighboring regions.

For Lazio, the differences between the two models are equally evident. The two models swap the position bewteen Italy and Russia. RECON identifies Russia as the main receptor with a flow of 1.81×10^9 m^3/year, a value that exceeds Utrack's estimate of 1.06×10^9 m^3/year by 71%. Conversely, the moisture destined for Italy is estimated higher by Utrack, which indicates a flow of 1.98×10^9 m^3/year, compared to 1.63×10^9 m^3/year from RECON, suggesting greater local recirculation in the latter model.

Another significant difference is observed in the flowes towards Turkey, which in Utrack are estimated at 6.13×10^8 m^3/year, more than double the 3.03×10^8 m^3/year from RECON. For Romania and Ukraine, the estimated volumes are comparable between the two models, with minimal variations indicating some consistency in the flowes towards these countries.

For Sicilia, the flow estimates towards Russia show one of the most marked differences between the two models. RECON attributes a volume of 2.59×10^9 m^3/year to this country, more tha twice the estimate provided by Utrack, which is 1.09×10^9 m^3/year. Conversely, the flows towards Italy are lower in Utrack, with an estimate of 1.13×10^9 m^3/year compared to 1.44×10^9 m^3/year in RECON.

Turkey emerges as an important destination for both models but with important different estimates. Utrack assigns a flow of 1.79×10^9 m^3/year to this country, 58% higher than RECON. Additionally, Utrack significantly increases the flowes to-

wards Greece (+63%) compared to RECON. An interesting aspect is the inclusion of African regions such as Ethiopia, Chad, and Algeria among the main destinations of the flowes according to Utrack, which are absent in RECON's estimates. Regarding Eastern European countries, such as Romania and Ukraine, RECON provides higher estimates compared to Utrack, indicating a greater emphasis on eastward and northern flowes.

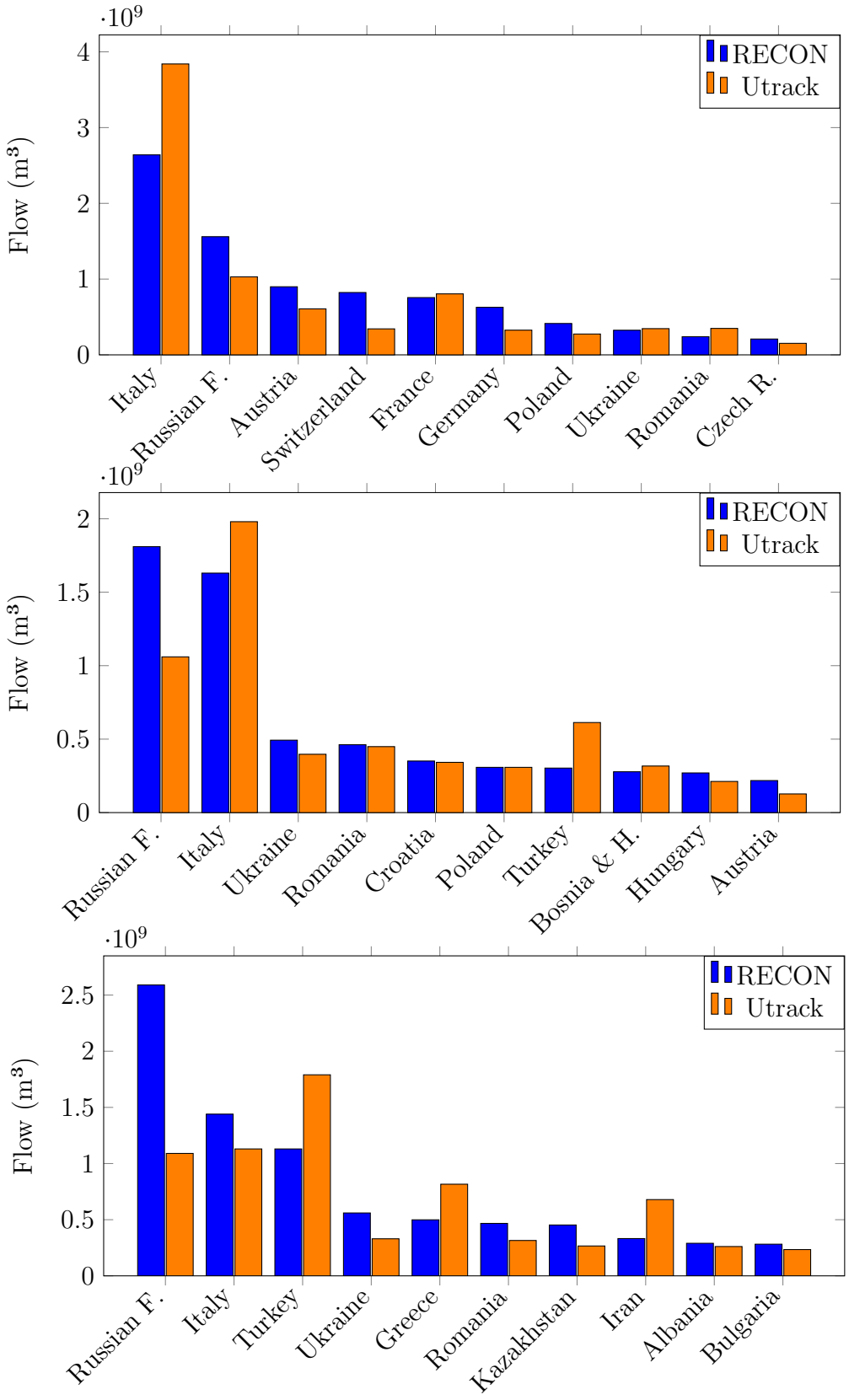

Figure 3.27: Top 10 receiving countries of water evaporated in Pimonte, Lazio ans Sicilia according to the RECON model, compared with the respective results obtained using the Utrack model.

Main receiving seas comparison

Fig.3.28 shows the main seas in which the evaporation from the regions of interest finally precipitates according to RECON (quantities expressed in cubic meters per year). These quantities are compared to the relative results elaborated with Utrack, whose top tan receiving seas is available at Tab.3.8, 3.9, 3.10. Regarding Piemonte and Lazio, all seas record a higher received volume according to Utrack, with the only exception for the Baltic and Barentsz Sea. Furthermore, the main five seas display rather great differences both in intensity and hierarchy.

For Piemonte, RECON places the Adriatic as the main receiver with 3.68×10^8 m^3/year, conversely, for Utrack, it stands in the second position, while exhibiting anyway a volume higher than the 50% compared to RECON. The most relevant discrepancy is visible for the Western Basin of the Mediterranean Sea which, with almost 6×10^8 m^3/year, ranks first for Utrack, almost tied with the Adriatic Sea, and is almost double than the respective value in RECON (2.53×10^8 m^3/year). A similar trend is visible for the Eastern Basin (EB) of the Mediterranean Sea. The only sea which shows a good consistency between the two models is the North Atlantic Ocean, which accounts for slightly less than 6×10^8 m^3/year for both RECON and Utrack.

For Lazio, RECON identifies again the Adriatic Sea as the main receiver with 6.97×10^8 m^3/year, 25% less than Utrack, in which it ranks the second position after the Tyrrhenian Sea. This sea shows one of the greatest difference between the two models, 4.38×10^8 m^3/year for RECON against 9.53×10^8 m^3/year for Utrack, a difference higher than the 100%. The other evident discrepancy is shown for the Eastern Basin of the Mediterranean Sea which, even if it ranks third for both models, highlights a deviation over 150%, 3.23×10^8 m^3/year in RECON and 8.06×10^8 m^3/year in Utrack.

While Piemonte and Lazio both reveal rather mismatch between the two models, Sicilia shows a better consistency. This finding is in line with Tab.3.22 according to which the island displays a difference of 15% in the row 'volume to the sea', while Piemonte and Lazio almost 40%.

For Sicilia indeed, almost all the seas follow a similar hierarchy and aligns in terms of received volumes, with a slight overestimation of Utrack compared to RECON (except for the Tyrrhenian Sea, Barentsz Sea and Norwegian Sea). The only considerable difference is evident for the Mediterranean-Eastern Basin which, even if it ranks first for both models, for Utrack it records almost 3×10^9 m^3/year while for RECON 1.6×10^9 m^3/year.

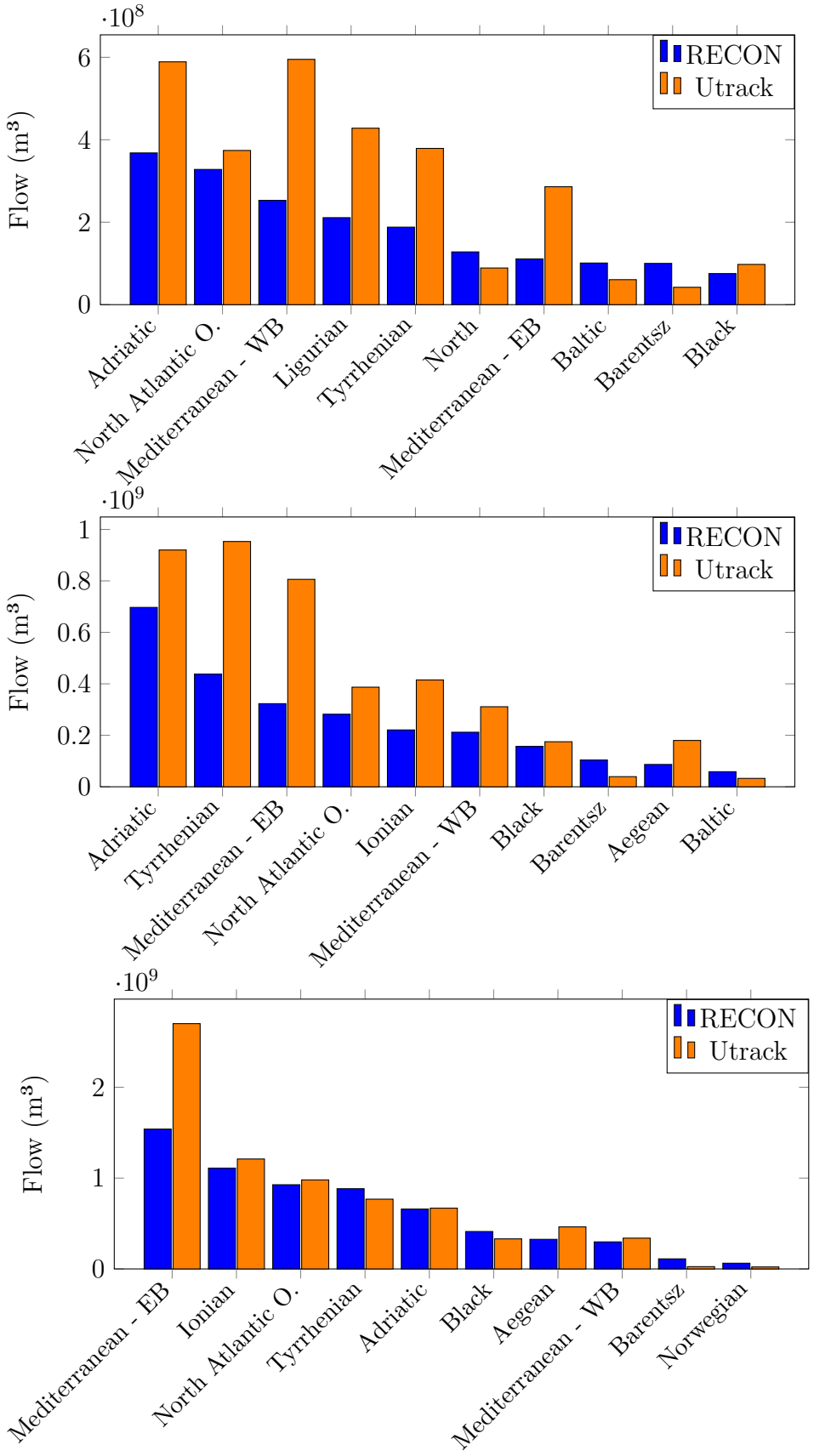

Figure 3.28: Top 10 receiving seas of water evaporated in Pimonte, Lazio ans Sicilia according to the RECON model, compared with the respective results obtained using the Utrack model.

3.3.3 Italian backward footprint

In Fig.3.29, the map of the annual precipitationsheds for the Italian territory is presented, obtained using the RECON model. As in previous cases, there is a noticeable similarity with the corresponding map derived from the Utrack model (Fig.3.11 (e)), particularly the substantial presence of precipitationsheds located west of Italy, with the highest intensity in the northeastern Mediterranean basin and northern Italy.

However, despite the apparent similarities at first glance, some significant differences between the two models start to become evident when analyzing Tab.3.23.

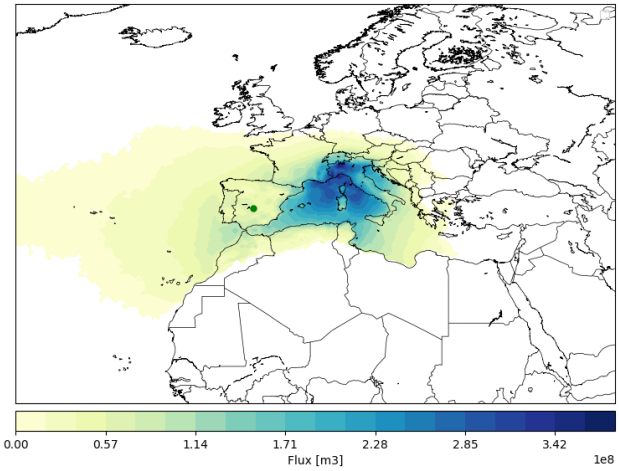

Figure 3.29: Annual Italian backward footprint according to RECON.

In this case, the RECON model estimates a precipitation volume that is 11% higher than that estimated by the Utrack model, with 3.31E+11 m^3 compared to 2.98E+11 m^3. It is noteworthy that the portion of the precipitation volume originating from land evapotranspiration ('Volume from the land') is consistent across both models, while the difference lies in the volume evaporated from the seas and oceans ('Volume from the seas'). Specifically, the RECON model estimates this at 2.26E+11 m^3 (68% of the total precipitated volume), which is 17% higher than the estimate from the Utrack model.

In addition to the differences in the intensity of the precipitationsheds, a variation in their extent is also observed. The area encompassing 90% of the precipitationsheds is slightly larger for the Utrack model, with an increase of just over 8%, suggesting a more dispersed distribution in this model.

Furthermore, when examining the centroids of the precipitationsheds, there is a clear agreement in terms of longitude, but a discrepancy of 2 degrees in latitude. The RECON model estimates the centroid's position at 39°N, located in the southern part of Spain near the border with Portugal. In contrast, the Utrack model estimates the centroid at 41.1°N, corresponding to northern Spain, close to the Bay of Biscay.

Table 3.23: Comparison of RECON and Utrack parameters in the Italian backward footprint processing.

Parameter	**RECON**	**Utrack**	**Difference**
Annual Precipitated Volume			
Total Volume (m^3)	3.32E+11	2.98E+11	11.39%
Volume from the Sea (m^3)	2.26E+11	1.93E+11	17.13%
Volume from the Land (m^3)	1.06E+11	1.05E+11	0.94%
Centroid Location			
Latitude (°)	39.0	41.1	-2.0
Longitude (°)	-4.1	-4.2	-0.1
Distance from Rome (km)	1438	1391	232
90% Precipitationshed Area			
Area (km^2)	2.07E+7	2.26E+7	-8.4%
Area Overlap (%)	93.6	85.8	-

This trend can be further observed in the graph shown in Fig. 3.30, which represents the zonal distribution of the precipitationsheds. It is evident that the two curves follow a very similar pattern, with slight differences. Both models exhibit a peak near 40°N, followed by a steep decline on either side. The decline is more pronounced north of 45°N compared to the more gradual decrease to the south (see Appendix A for the comparison between the precipitationsheds and evaporationsheds distribution in both models).

The RECON model, represented by the blue curve, estimates a slightly higher peak. Between 40°N and 50°N, the two curves converge, while Utrack shows higher values than RECON above 50°N. Conversely, RECON displays higher values than Utrack below 40°N, until both models approach zero at the equator. Despite these slight differences, it is possible to notice a close fit between the two curves, as also demonstrated by the high correlation value, which amounts to 0.985.

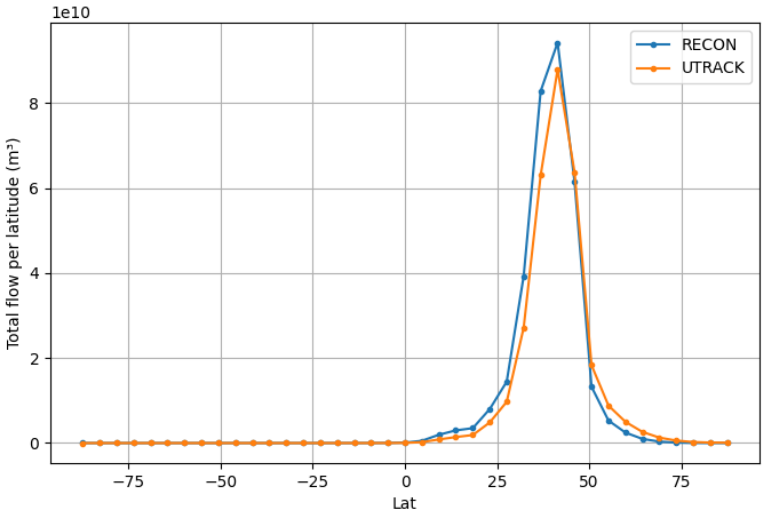

corr.= 0.985

Figure 3.30: Precipitationsheds zonal distribution comparison between RECON (blue line) and Utrack (Orange line) for Italy.

Main contributing countries comparison

In the comparison between the RECON and Utrack models (Fig.3.31), used to analyze the evaporative contribution to precipitation in Italy from ten countries, some significant differences emerge in both the estimated water volumes and the selection of the most relevant contributing states. For each of these countries, the RECON results are compared with the respective results obtained from the Utrack model. It is important to note that the Utrack data do not represent the top ten contributing countries, but rather correspond to the same set of countries as in RECON (see Tab.3.12 for Utrack's top ten contributing countries).

Both models agree on identifying Italy, France, Spain, Algeria, Morocco, and Germany as the six main contributing countries, listed in descending order, highlighting a greater alignment compared to the respective analysis performed for the forward footprint (Fig.3.21). RECON underestimates the contributions from Italy (2.37E+10 m^3) and France (1.66E+10 m^3) by less than 10% compared to Utrack. Conversely, it estimates Spain's contribution to be 10% higher and nearly doubles the contributions from Algeria and Morocco, with values of 9.96E+10 m^3 versus 5.43E+10 m^3, and 6.21E+10 m^3 versus 3.91E+10 m^3, respectively. For Germany, RECON returns to underestimating the contribution by approximately 40% compared to Utrack.

These results further confirm RECON's tendency to position the precipitation-

sheds further south compared to Utrack.

Regarding the minor contributors, there is a notable discrepancy with Tunisia and Portugal, which appear among the top ten contributing countries in the RECON model but are absent in Utrack's top 10. Instead, Utrack includes Austria and Canada, which do not feature in RECON's list.

Finally, both models include Switzerland and Croatia among the top ten contributors, although Utrack assigns greater importance to Croatia compared to RECON.

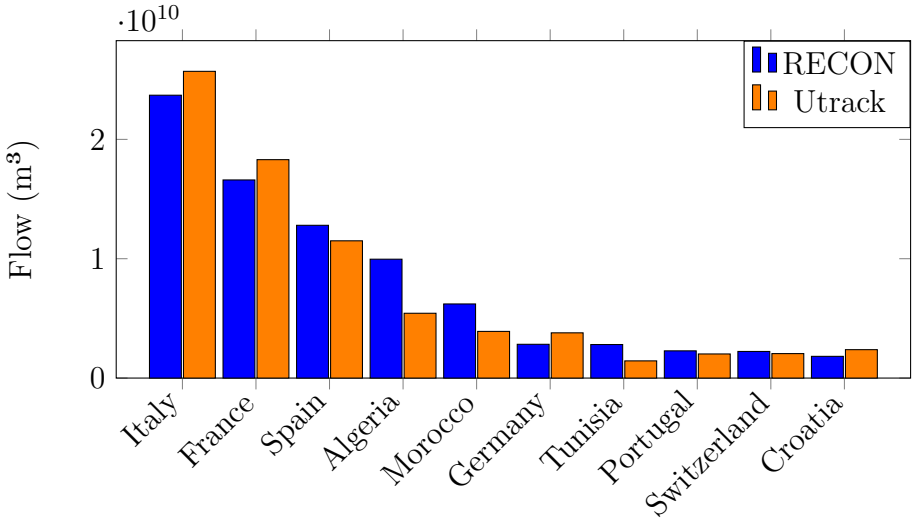

Figure 3.31: Top 10 contributing countries to precipitation in Italy according to the RECON model, compared with the respective results obtained using the Utrack model.

Main contributing seas comparison

The top ten contributing seas to Italian precipitation according to RECON is presented in Fig.3.32. As for the previous case, the values of each sea is compared to the corresponding Utrack's value, while for the top ten for Utrack refer to Fig.3.13. In this case as well, the top six contributors appear in the same order across both models, with a slight overestimation of the volumes according to RECON compare to Utrack (as shown in Table 3.21, the 'Volume from the sea' in RECON is 17% higher than in Utrack).

The RECON model identifies the North Atlantic Ocean as the largest and unquestioned contributor, with an evaporation volume of 1.08E+11 cubic meters, slightly higher than Utrack's estimate of 9.24E+10 cubic meters. Both models agree that

the Western Basin (WB) of the Mediterranean sea is the second largest contributor, with RECON estimating 4.12E+10 cubic meters, which is 20% higher than Utrack's estimate.

For the Tyrrhenian Sea, RECON estimates a volume of 2.11E+10 cubic meters, while Utrack provides a similar estimate of 1.85E+10 cubic meters. A more significant difference is observed in the contribution from the eastern Mediterranean basin, where RECON calculates a volume of 1.81E+10 cubic meters, higher than Utrack's estimate of approximately 1.05E+10 cubic meters.

The Adriatic Sea is another basin where both models show similar estimates: RECON reports 8.37E+9 cubic meters, while Utrack provides a slightly higher value of 8.61E+9 cubic meters.

For the minor contributors, the order in the hierarchy between the two models starts to marginally change, though a good alignment is still visible.

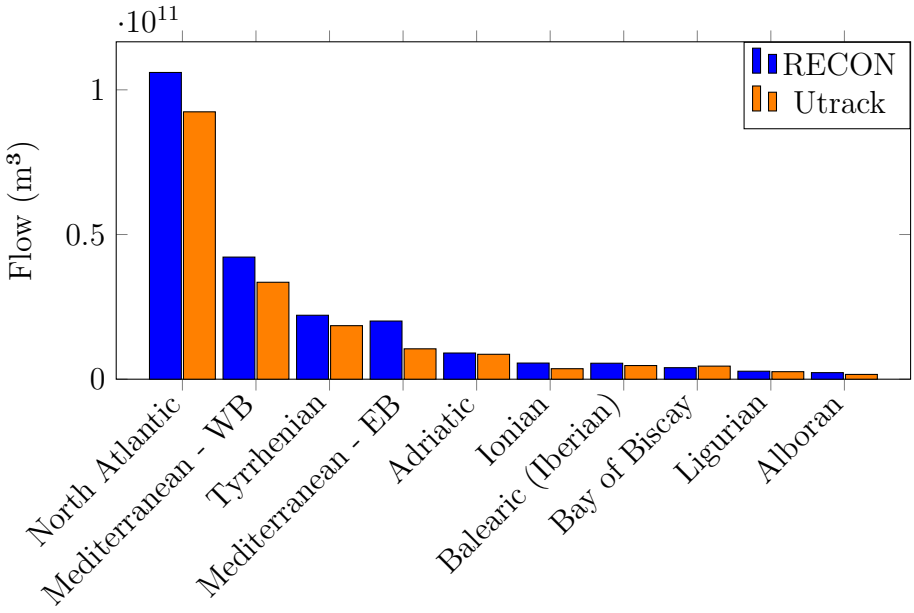

Figure 3.32: Confronto dei volumi ricevuti (in miliardi) per vari mari italiani tra i modelli RECON e Utrack BACKWARD

3.3.4 Regional backward footprint

In Figure 3.33, the annual-scale precipitationsheds estimated by the RECON model are shown for the three reference regions: Piemonte (a), Lazio (b), and Sicilia (c).

A comparison with the precipitationsheds estimated by Utrack can be made by examining Fig.3.14 (e), 3.15 (e), and 3.16 (e).

For each region, the maps from both models appear quite similar in terms of the extent and intensity of the precipitationsheds. However, a more detailed quantitative analysis, as shown in Table 3.24, highlights the differences between the two models more clearly.

Regarding the precipitated volume, the RECON model estimates higher quantities for all regions. Piemonte shows the largest difference, with a volume of 3.91E+10 cubic meters, nearly 40% higher than Utrack's estimate. This is followed by Lazio, with 1.79E+10 cubic meters, differing by +8.4%, and Sicilia, with 1.63E+10 cubic meters, showing a +5.8% difference. Furthermore, while for Piemonte the difference between the models in the estimation of the total volume keeps the same discrepancy between the contributions from the seas and from the landmasses (almost +40% recorded for RECON in both 'Volume from the Sea' and 'Volume from the Land'), for Lazio the trend is different. Indeed, here, RECON estimates a greater contribute (almost 17%) of the volume coming from the land compared to the respective Utrack's estimation. On the contrary, Utrack estimates a greater contribution of the volume coming from the sea, compared to the RECON's estimation. This pattern, seen for Lazio, is even more pronounced when looking at Sicilia.

Passing then to the area containing 90% of the precipitationsheds, as observed for Italy, Utrack estimates larger areas (ranging from 5% in Piemonte to 11% in Lazio) compared to RECON. This suggests a slightly higher concentration of precipitationsheds in the RECON model. Nevertheless, these areas remain fairly extensive, as indicated by the high percentage of overlap between the two models across the three regions.

Another characteristic, already noted for Italy, lies in the centroid position. For each region, the two models agree on the centroid's longitude, with a maximum longitudinal difference of 0.6° observed in Sicilia. However, in terms of latitude, RECON consistently positions the centroid further south, with a minimum difference of 2 degrees for Piemonte and a maximum of 3.1 degrees for Sicilia. RECON places the centroid near the northern borders of Morocco and Algeria, whereas Utrack positions it near the Balearic Islands.

As seen in the italian analysis, this trend can also be observed in the graphs shown in Figure 3.36, which depict the zonal distribution of precipitationsheds (During the span of a year) for the three regions.

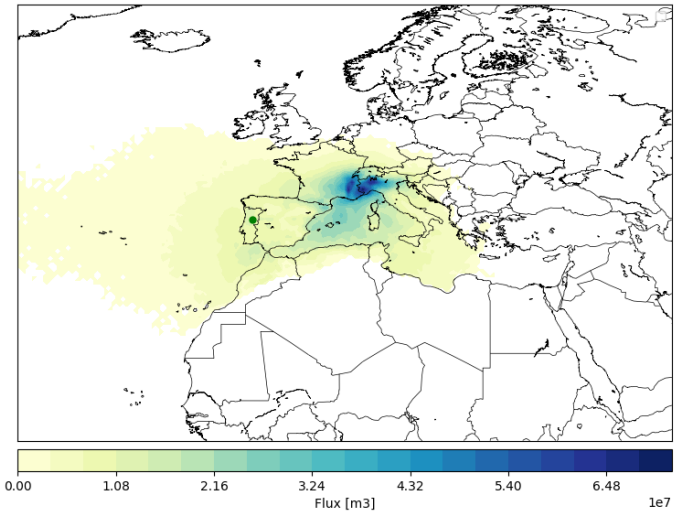

(a)

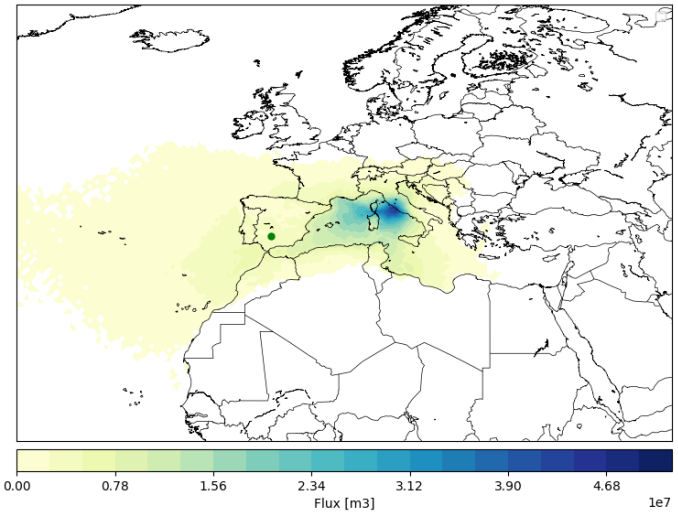

(b)

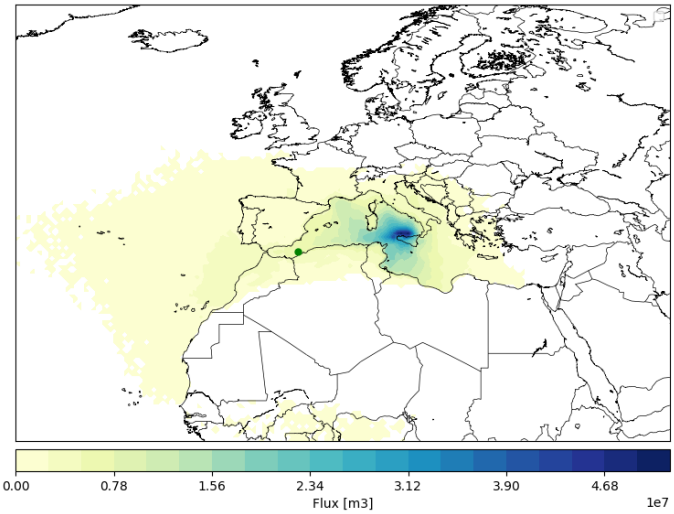

(c)

Figure 3.33: Annual backward footprint according to RECON. Piemonte (a), Lazio (b), Sicilia (c).

All three regions exhibit a peak followed by a sharp decline. For Piemonte, with a peak between 40-45°N, the curve appears more smoothed, and a significant gap is

evident between RECON (blue curve) and Utrack (orange curve), with Utrack showing a more contained distribution. This aligns with the results in Table 3.24, where the difference in estimated precipitated volume for Piemonte is the largest.

For Lazio (peak at 40°N) and Sicilia (peak at 35°N), the distributions are narrower, and the RECON and Utrack curves overlap more closely.

Similar to the case for Italy, the Utrack curve exceeds the RECON curve at higher latitudes, while it falls below RECON at lower latitudes. This is in contrast to the results obtained from the forward analysis (Figure 3.26). Additionally, unlike the forward analysis, in this case, the curves exhibit only a primary peak, without a secondary peak around 10°N, except for a minor peak observed for Sicilia.

Despite these differences, the correlation coefficient between the two models is very high for each region. Interestingly, the highest correlation coefficient, 0.983, is observed for Piemonte, the region with the largest difference in estimated precipitated volume between the models. Although this may seem counterintuitive, the models can still exhibit a similar spatial distribution of precipitation. The correlation coefficient measures how well the models follow the same pattern or trend (e.g., areas with higher or lower precipitation), even if the absolute quantities differ. Thus, the models can be highly correlated in terms of relative variations while differing in absolute values.

In fact, when examining the curves for Piemonte, it is noteworthy that they show a particularly close alignment in the latitudinal band between 45°N and 55°N, highlighting substantial agreement between the two models in this range. For Lazio, and even more distinctly for Sicilia, a clearer inversion of dominance between the RECON and Utrack curves is observed. While the point of inversion for Lazio occurs at 45°N, it shifts to 40°N for Sicilia, indicating a lower degree of alignment at higher latitudes compared to Piemonte.

Table 3.24: Comparison of RECON and Utrack parameters in the backward footprint processing for Piemonte, Lazio, and Sicilia.

Parameter	**RECON**	**Utrack**	**Difference**
Piemonte			
Total Volume (m^3)	3.91E+10	2.82E+10	38.72%
Volume from the Sea (m^3)	2.54E+10	1.83E+10	39.10%
Volume from the Land (m^3)	1.37E+10	9.85E+09	38.36%
Latitude (°)	40.2	42.1	-2.0
Longitude (°)	-7.4	-7.6	0.2
Distance from Torino (km)	1341	1285	221
Area (km^2)	2.10E+7	2.26E+7	-7.08%
Area Overlap (%)	94.4	87.3	-
Lazio			
Total Volume (m^3)	1.79E+10	1.65E+10	8.42%
Volume from the Sea (m^3)	1.33E+10	1.14E+10	16.70%
Volume from the Land (m^3)	4.51E+09	5.05E+09	-10.70%
Latitude (°)	37.9	40.5	-2.6
Longitude (°)	-4.8	-4.5	0.3
Distance from Rome (km)	1554	1461	284
Area (km^2)	1.93E+7	2.10E+7	-5.13%
Area Overlap (%)	90.4	83.0	-
Sicilia			
Total Volume (m^3)	1.63E+10	1.54E+10	5.81%
Volume from the Sea (m^3)	1.24E+10	1.04E+10	19.23%
Volume from the Land (m^3)	3.90E+09	4.99E+09	-21.84%
Latitude (°)	35.8	38.9	-3.1
Longitude (°)	-0.9	-0.3	-0.6
Distance from Palermo (km)	1285	1227	352
Area (km^2)	2.13E+7	2.41E+7	-11.62%
Area Overlap (%)	87.3	77.4	-

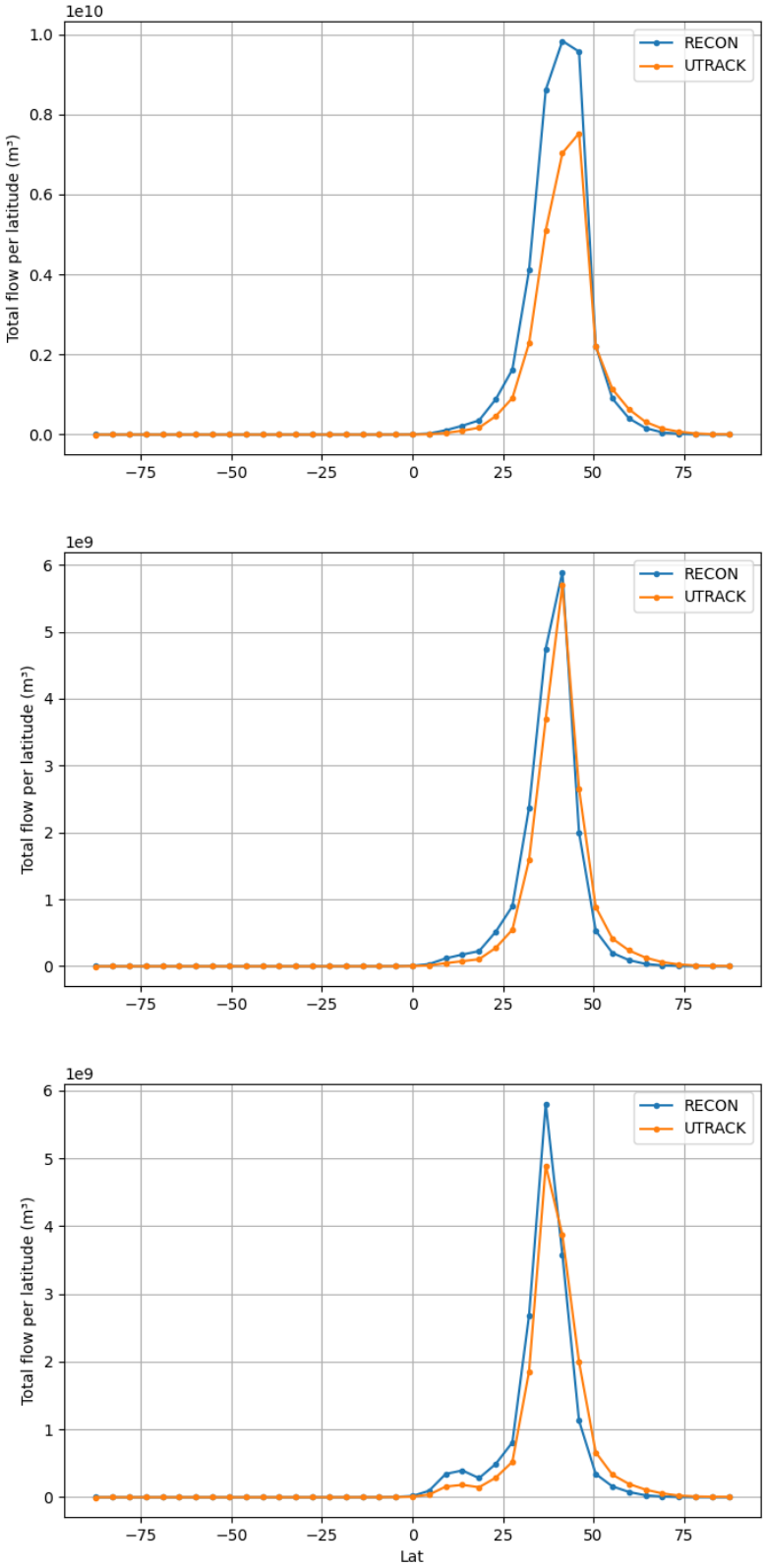

a) Corr: 0.983

b) Corr: 0.977

c) Corr: 0.941

Figure 3.36: Precipitationsheds zonal distribution comparison between RECON (blue line) and Utrack (Orange line) for Piemonte (a), Lazio (b) and Sicilia (c).

Main contributing countries comparison

Fig.3.37 shows the top ten countries that, according to RECON, contribute the most to precipitation in the three regions. For each identified country, the corresponding value computed according to Utrack is complemented (the top ten of the contributing countries according to Utrack is shown in Tab. 3.15, 3.16, 3.17).

For Piemonte, both models identify the same hierarchy among the top six contributing states. France emerges as the main contributor in both models, with RECON estimating a volume of 3.72×10^9 cubic meters compared to Utrack's 2.63×10^9 cubic meters, showing a difference of 29.3%. Similarly, Italy and Spain occupy the second and third positions respectively, with RECON estimating volumes approximately 37% higher for both states compared to Utrack. This trend of higher estimates by RECON repeats for almost all states, indicating a systematic overestimation relative to Utrack. However, the order of the states remains quite similar, suggesting that despite the quantitative differences, the models agree on the hierarchy of the main contributors, as highlighted by the high correlation coefficient.

For Lazio as well, the top six receiving states are identical in both models, with Italy in the first position followed by France, Spain, Algeria, Morocco, and Tunisia. In this case, however, except for Italy, where the values are nearly identical (1×10^9 cubic meters), Utrack tends to overestimate the volumes of contributors compared to RECON. The most noticeable differences are seen for France and Germany, with RECON's estimates being 20% and 40% lower, respectively, compared to Utrack's estimates.

Contrary to Piemonte and similar to Lazio, Sicilia shows a tendency for higher volume estimates by Utrack for almost all states. This result aligns with the data in Table 3.24, which highlights a lower contribution from land for RECON by just under 22%.

Additionally, more significant inversions in the hierarchy occur, even among the top states, which explains the lower correlation coefficient observed for this region. Specifically, RECON and Utrack agree on Italy and Algeria as the two main contributors. For Italy, RECON shows a volume 36% lower (9.23E+8 cubic meters compared to 6.77E+8) than Utrack, while for Algeria, both models estimate a similar volume of around 6E+8 cubic meters. However, France, which holds the third position in Utrack, drops to the fifth in RECON, showing a nearly 50% lower value. Only the African states of Nigeria, Mali, and Niger show higher values in RECON, consistent with the previously discussed result that RECON positions the precipitationsheds further south compared to Utrack.

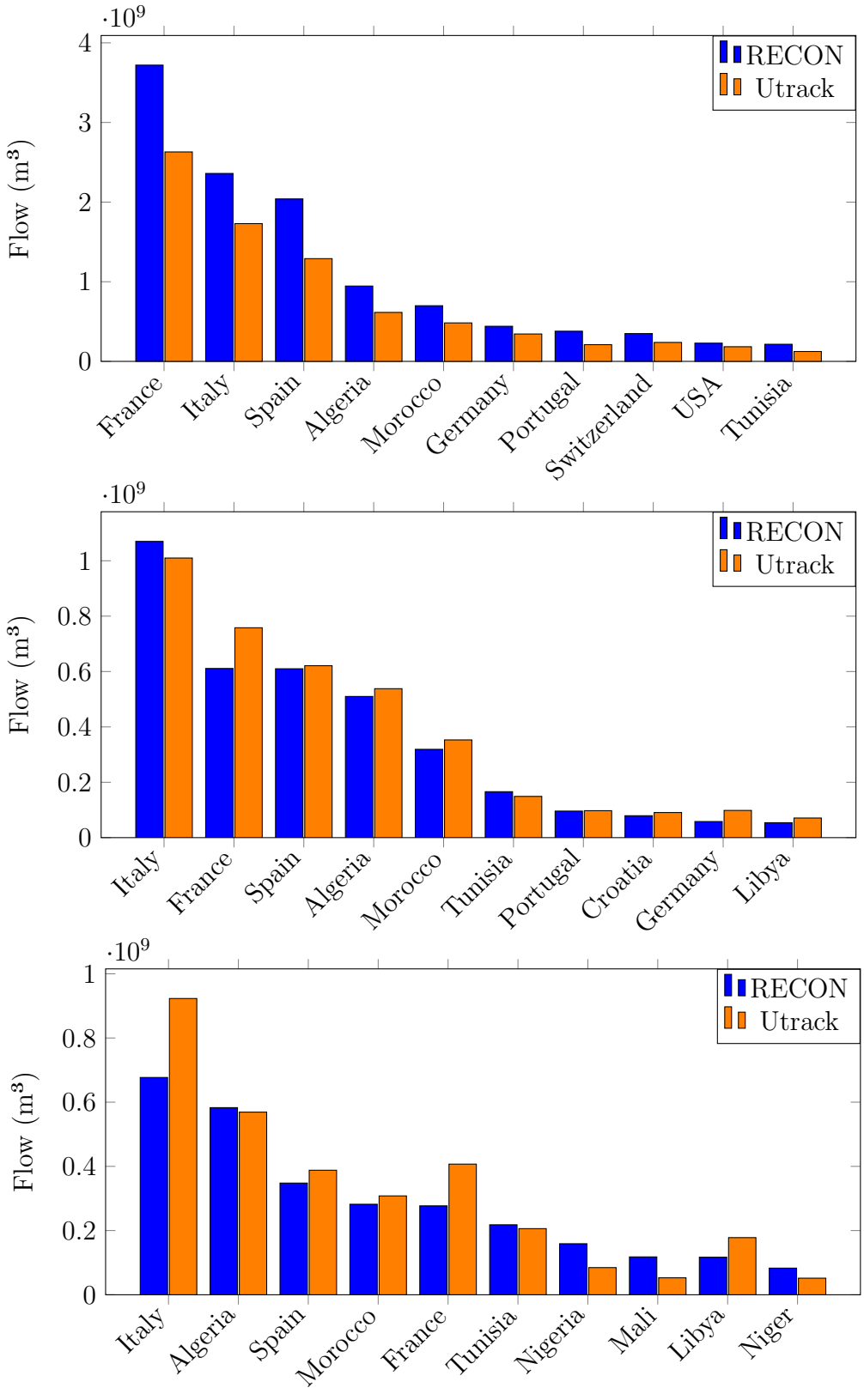

Figure 3.37: Top 10 contributing countries to precipitation in Piemonte, Lazio ans Sicilia according to the RECON model, compared with the respective results obtained using the Utrack model.

Main contributing seas comparison

Regarding the main contributing seas, the results are shown in Fig. 3.38. Here the top ten contributing seas to the precipitation in the three regions according to RECON is analysed. As for the previous cases, the RECON results are compared with the respective results recorded through the Utrack elaboration (Tab3.18, 3.19, 3.20 shows the top ten contributing seas according to Utrack for the three regions).

For nearly all the seas (at least for the most influential ones), RECON estimates higher volumes across the three regions. This aligns with the results in Table 3.24, which systematically shows higher sea-derived volume values for all three regions in RECON. Nevertheless, both models consistently identify the Atlantic Ocean, the Western and Eastern Mediterranean basins, and the Tyrrhenian Sea as the four most influential seas, although their order varies depending on the region and the considered model.

Starting with Piemonte, a significantly higher contribution from the Atlantic Ocean is observed, exceeding the Utrack estimate by 40%. With nearly 1.5E+10 cubic meters, the Atlantic Ocean emerges as the undisputed leader in providing water that precipitates in Piemonte, accounting for almost 40% of the region's rainfall according to RECON. Following this is the Western Mediterranean basin, which ranks second in both models. However, RECON, with 4.15E+10 cubic meters (10% of Piemonte's rainfall), overestimates the corresponding Utrack value by 20%.

The next two seas, although contributing significantly less (about 1/9 of the Atlantic Ocean's contribution), are the Eastern Mediterranean basin and the Tyrrhenian Sea for RECON, each contributing around 1.5E+10 cubic meters. For Utrack, the positions of these two seas are reversed.

For Lazio and Sicilia, similar patterns are observed, with the Atlantic Ocean remaining the leader in both models, although with a less marked difference compared to the subsequent contributing seas, as seen in Piemonte. In RECON, the Atlantic Ocean contributes to about 35% of the precipitation for Lazio and 28% for Sicilia. For both regions, both models maintain the same hierarchy of the top four seas, and it can be observed that from the fifth sea onwards, the contribution is significantly lower compared to the main contributors.

A consistent pattern in this case is that RECON tends to estimate overall higher volumes than Utrack for the southern seas, such as the Mediterranean Sea (both the Western and Eastern Basins), the Tyrrhenian Sea, and other neighboring seas in the Mediterranean. Conversely, Utrack assigns greater significance to northern seas like the North Sea and the Norwegian Sea, which do not appear in the top 10 for RECON in any of the regions.

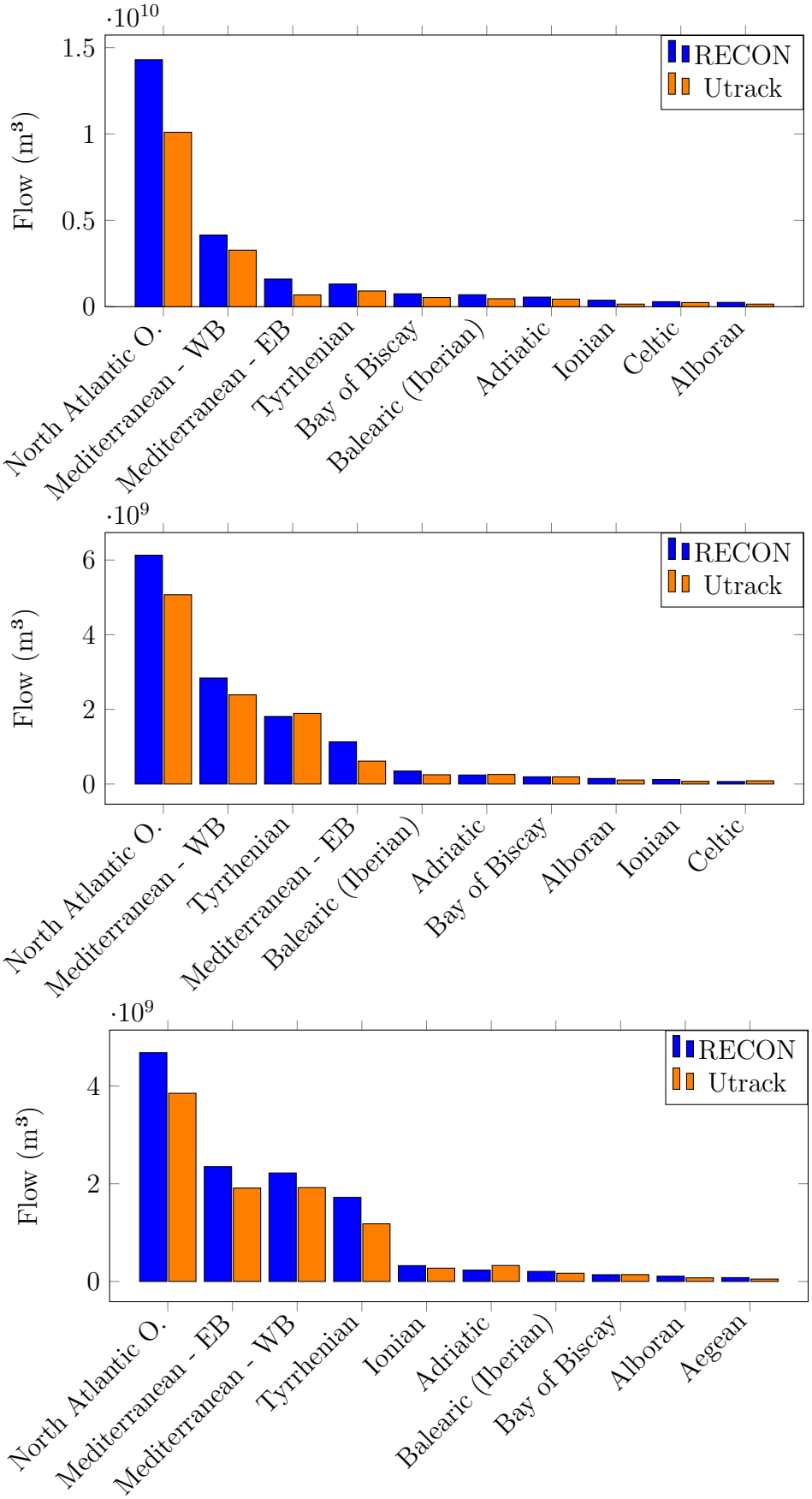

Figure 3.38: Top 10 contributing seas to precipitation in Piemonte, Lazio ans Sicilia according to the RECON model, compared with the respective results obtained using the Utrack model.

3.3.5 Comparative analysis between RECON and Utrack

As highlighted in this chapter, the two models under examination provide some similar results in terms of precipitationsheds and evaporationsheds but, generally, could provide even remarkable differences when analyzing when considering some specific parameters.

To begin, it might be observed that a high correlation coefficient is recorded for all the study areas, indicating, for each region, a strong spatial similarity in all the distributions. When considering this parameter, it has been noted that the backward footprint returns higher values than the forward footprint for all the considered areas.

Passing then to other parameters, greater mismatching starts to appear. Specifically, for the national territory, the differences in total evaporated and precipitated volumes between the RECON and Utrack models are about 10%: RECON shows a 10% lower estimate compared to Utrack for the forward analysis, while for the backward analysis, the difference is 10% higher, with RECON overestimating the volume compared to Utrack. However, these discrepancies tend to increase for smaller areas, such as the regions, with some differences even exceeding this percentage.

Regarding the individual regions, in the forward case, Lazio is where the maximum difference in evaporated volume between the two models is observed, with RECON estimating a value 23% lower than Utrack. In the backward case, the largest difference in precipitated volume is found in Piemonte, where RECON records a value almost 40% higher than Utrack.

Continuing, the analysis where the greatest differentiation between the two models has been observed regards the identification of the principal countries and seas receiving the Italian and regional evaporation. Here, a large diversification on the estimated volume and, in part, on the hierarchy stands out, highlighting some differences in the global extension of the evaporationsheds. In parallel, the counterpart analysis in the precipitationsheds, thus the main contributing countries and seas, displays a greater fit between the results of the two models.

Based on this brief resume on the comparison between the RECON and Utrack elaborations and on the different outcomes that stem from them, it become necessary to evaluate which model gives the most reliable results.

To assess which of them fulfills this goal, it is useful to start with a qualitative analysis that considers the extent of the precipitationsheds and evaporationsheds in relation to the characteristics of the westerlies. As widely discussed, these winds, which blow from southwest to northeast, play a fundamental role in determining the distribution of precipitation and evaporation in Italy. In fact, the westerlies are responsible for positioning the precipitationsheds mainly on the western side of the

peninsula, while the evaporationsheds are more concentrated in the east.

An interesting aspect that emerged from the analysis of the results is the difference in the positioning of the precipitationsheds and evaporationsheds between the two models. In particular, RECON tends to place the precipitationsheds further south compared to Utrack, while it positions the evaporationsheds further north.

Consistent with these observations, this difference becomes more evident when examining the annual centroid of the evaporationsheds and precipitationsheds for each model. In fact, for almost all the regions considered, the annual centroid of the evaporationsheds for Utrack is slightly south of the region's barycenter, while that of the precipitationsheds is located further north relative to the region barycenter. Conversely the opposite arrangement is observed for RECON: the centroid of the evaporationsheds is positioned further north compared to the region's centroid, while that of the precipitationsheds is located further south.

This behavior of RECON appears to be more consistent with the direction of the westerlies, suggesting that this model might better reflect the actual atmospheric dynamics, indicating a closer correspondence with the real geographical and climatic characteristics (see Appendix A for the comparison between evaporationsheds and precipitationshed in the two models).

Proceeding with a more quantitative comparison, it is possible to analyze the total annual volume of water precipitated and evaporated, obtained through the backward and forward analyses of the two models, and compare them with the ERA5 data presented in Fig. 2.2.

Starting with the forward analysis, for Italy, the total annual volume of water evaporated is estimated at 200 billion cubic meters according to RECON and 220 billion cubic meters according to Utrack (these quantities will be called Total Evaporation Volume or TEV). Converting these volumes in terms of average annual evaporation over the Italian surface (Average Evaporation Height or AEH), the outputs are 661 mm for RECON and 728 mm for Utrack, respectively.

Similarly, the backward analysis reveals that the total annual volume of water precipitated (Total Precipitation Volume or TPV) is 332 billion cubic meters for RECON and 298 billion cubic meters for Utrack. These values correspond to an average annual precipitation (Average Evaporation Height or APH) of 1098 mm for RECON and 986 mm for Utrack.

Table 3.25: Comparison of AEH and APH for ERA5, RECON, and Utrack.

Parameter	**ERA5**	**RECON**	**RECON vs ERA5**	**Utrack**	**Utrack vs ERA5**
AEH	675 mm	661 mm	-2.0%	728 mm	7.9%
APH	1078 mm	1098 mm	1.9%	986 mm	-8.5%

Regarding the ERA 5 dataset, in the same reference period as Utrack and RECON, an APH of 1078 mm and an AEH of 675 mm are observed for Italy. These values show significant concordance with RECON's estimates, which deviate by just 2% for both precipitation and evaporation. On the contrary, Utrack's results show a more pronounced discrepancy, with an underestimation of 8.5% for precipitation and an overestimation of 7.9% for evaporation.

These differences highlight a greater accuracy of RECON in representing the annual dynamics of precipitation and evaporation, in line with the ERA5 data, compared to Utrack. There results are summarized in Tab3.25

The last critical factor in evaluating the reliability of the models is the consistency between Evaporation Recycling (ER) and Precipitation Recycling (PR). Both ER and PR measure the recycling of water within the hydrological cycle, but from opposite perspectives: ER focuses on the fraction of local evaporation that contributes to local precipitation, while PR looks at the fraction of local precipitation that originates from local evaporation.

Considering the TEV and the TPV, the volume of water recycled within the region (denoted V) can be expressed as:

$$V_{ER} = ER \times TEV$$

$$V_{PR} = PR \times TPV$$

Table 3.26: Comparison of Utrack and RECON for evaporation and precipitation recycling.

Model	**TEV ($\mathbf{m^3}$)**	**ER (%)**	**$\mathbf{V_{ER}}$ ($\mathrm{m^3}$)**	**TPV ($\mathbf{m^3}$)**	**PR (%)**	**$\mathbf{V_{PR}}$ ($\mathrm{m^3}$)**
Utrack	2.2×10^{11}	13.46%	2.96×10^{10}	2.98×10^{11}	8.62%	2.57×10^{10}
RECON	2.0×10^{11}	12.28%	2.46×10^{10}	3.32×10^{11}	7.48%	2.46×10^{10}

From the perspective of evaporation (ER), the total evaporation is used to determine the proportion of volume that returns as precipitation within the region. Conversely, from the perspective of precipitation (PR), the total precipitation is used to estimate the proportion of volume that originates from local evaporation within the region.

For a physically consistent hydrological model, the volumes of water (V) calculated using the evaporation recycling ratio (ER) and the precipitation recycling ratio (PR) should be approximately equal, as they represent the same process of water recycling within the region. Both calculations describe the same hydrological process but from different perspectives.

The concept of mass conservation applies here. This means that the volume of water evaporated should roughly equal the volume of precipitation sourced from that same evaporation

In line with this principle, according to RECON the volumes of water that evaporate and then precipitate back into the region (calculated from ER) and the volumes of precipitation that come from local evaporation (calculated from PR) are the same quantities, that is 2.46×10^{10} (See Tab.3.26 for these results).

On the contrary, Utrack suggests that more water is evaporated and precipitates back into the region ($2.96 \times 10^{10}\,\mathrm{m}^3$) than what is locally sourced from precipitation ($2.57 \times 10^{10}\,\mathrm{m}^3$). This indicates a violation of mass conservation in the model: more water is being recycled than can be accounted for by local evaporation, which is not physically realistic.

The fact that ER is higher than PR in Utrack suggests the model might be overestimating how much of the local evaporation is falling back as precipitation.

Chapter 4

Final considerations

The study conducted in Chapter 3 revealed a better consistency of the results through the RECON analysis, which it will be used in this last chapter to elaborate the final considerations.

The outputs of this model shew that Italy has a positive water balance, which agrees with the ERA5 data as presented in Chapter 1. The country receives approximately 3.32×10^{11} m^3 of water annually through precipitation, while losing 2.00×10^{11} m^3 through evaporation. The difference gives rise to a yearly surplus of about 1.32×10^{11} m^3 of water. The surplus, amounting to about 438 mm of water a year over a spatial area of 301,340 km^2, represents that volume of water available for the maintenance of both the terrestrial and aquatic ecosystems, besides supporting human activities.

A portion of this excess water soaks through the ground, recharging aquifers. This process is therefore essential in maintaining groundwater supplies, feeding springs, and supporting the base flow of streams and rivers in the dry time.

The rest of the surplus nourishes the superficial hydrographic network, thereby sustaining the hydrological dynamics of rivers and maintaining the water level of natural and artificial lakes, wetlands, and aquatic ecosystems, besides supplying water for civil, agricultural, and industrial activities.

It should be noted that this annual average surplus of 438 mm conceals considerable spatial and temporal variability. The precipitation in Italy is very uneven, ranging from about 500 mm in the dry southern areas to more than 2000 mm in some Alpine regions. Such spatial heterogeneity causes unequal surplus of water available across the country. One proof of this inequality is seen in the data collected for the selected regions, which shows that Sicily has an annual water deficit, opposite to the national average and the cases of the regions of Piedmont and Lazio.

4.0.1 Italian recycling waters

Regional-scale hydrological cycling contains detailed dynamics that could be illustrated by two major parameters: Evaporation Recycling (ER) and Precipitation Recycling (PR). These quantities provide primary information on the completion of the local hydrological cycle and the interlinkages between evaporation and precipitation processes over a given geographical space.

Evaporation recycling denotes the proportion of water that has evaporated and subsequently falls as precipitation within the same geographic area.

In Italy, the data show that 12.28% of the water that evaporates from its national territory—about 2.46×10^{10} m^3/y—falls back as precipitation within its own country borders. The value here provides a quantitative index of the degree of autonomy in the regional hydrological cycle and offers an insight into the ability of the territory to support closed hydrological cycles, which points out the importance of local atmospheric processes in the region's water budget.

Precipitation Recycling, complementary to ER, represents the percent of total precipitation that is sourced from local evaporation. Over Italy, it amounts to 7.41%, which corresponds to about 2.46×10^{10} m^3 per year. This parameter can measure the contribution of local evaporation to the amount of precipitation, which gives an indication of the reliance on outside moisture sources, allowing for the evaluation of the relative importance of local processes versus the processes on a larger scale.

The equality between the absolute values of ER and PR is not coincidental but rather reflects a fundamental principle of mass conservation in the local hydrological cycle. This correspondence confirms consistency in the data and robustness in the measurements, thus proving the closure of the hydrological cycle at a regional scale and cross-validation for the two parameters.

Quantitative analysis of atmospheric moisture flux is revealing one very important fact concerning Italy: it is strongly connected with neighboring meteorological systems and shows structural dependence on outside sources of moisture. The data shows that 92.59% of its precipitation originates from outside the country, while 87.72% percent of the water that evaporates crosses national boundaries, highlights a clear condition of hydrological interdependence.

4.0.2 The limits of water sovereignty

Italy's location in the middle of the Mediterranean basin makes it a critical hub for moisture transportation. Italy is an "atmospheric bridge," with most of its moisture coming from the western Mediterranean Sea and the Atlantic, which then redistributed through evaporation and atmospheric circulation eastward to the eastern

Mediterranean, the Balkans, and even Russia. And this "bridge" function is not just a simple meteorological phenomenon but one with very important geopolitical consequences.

The data collected shows the impossibility of any statements on self-sufficiency in Italy. The concept of "water autarky" is scientifically unsustainable; Italy is, by its geographical features and location, essentially dependent on moisture arrivals from the Mediterranean and Atlantic areas. The fact that the percentage of 7.41% of precipitation falling as a consequence of local evaporation is relatively low emphasizes that Italy can't secure its water supply relying just on national resources.

In the frame of atmospheric moisture dynamics, it gives rise to an interesting paradox that challenges common perceptions toward national sovereignty and the idea of state self-sufficiency. Italy has a double role as one of the largest recipients and one of the prominent donors of atmospheric water resources: 92.59% of its precipitation originates from outside its borders, while 87.72% of its evaporated water is transported to other regions. This constant, unconscious reciprocity constitutes a sort of "natural forced solidarity" that overrides political separations and national aspirations.

The phenomenon of involuntary hydrological exchange serves as a powerful metaphor for the fundamental interconnectivity inherent to our planet. Unlike other natural resources, which can be policed, harvested, and commercially traded according to specific political and economic goals, the flow of atmospheric water is conducted primary according to the laws of nature— disregarding political frontiers and claims of national sovereignty.

This is not true for Italy alone. As stated by Rockström et al. (2023), there is no country in the world that receives more than fifty percent of its moisture from within its own borders, meaning even the largest countries rely on evaporation from other areas to support their precipitation. Even Russia, which retains the largest share of its local moisture, still heavily relies on evaporation from neighboring countries (20%) and from oceanic sources (35%).

continental destinations of annual Italian evaporation contributing to landmass precipitation

This phenomenon requires a certain level of humility on the part of nations: no nation, however powerful, can successfully directly control or regulate these movements. The natural flow of atmospheric water puts into light the limits of human power and highlights the need to recognize a type of interdependence that cannot be negotiated or altered through treaties or international agreements. However, if it is true that a strict domination of these fluxes is not possible, it is also true that changes on them are more and more frequent, affecting the water cycle in each inch

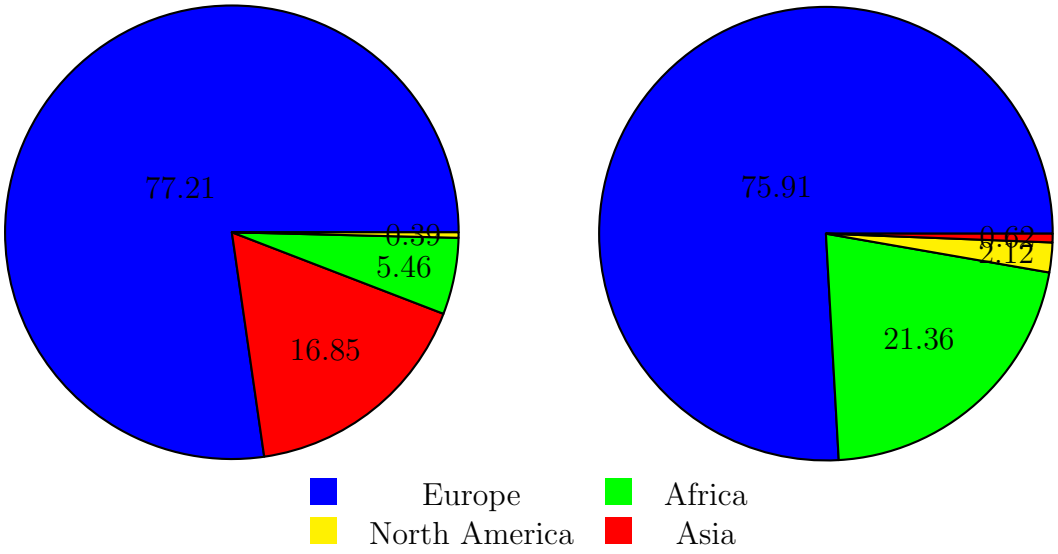

Figure 4.1: On the left, continental destinations of annual Italian evaporation contributing to landmass precipitation (forward footprint analysis). On the right, continental origin of terrestrial evaporation contributing to Italy's annual precipitation (backward footprint analysis). Results are obtained from RECON elaboration.

of the globe.

The aforementioned interconnection indeed means that environmental actions in one part of the world can have climatic repercussions thousands of kilometers away, highlighting the need for a global approach to natural resource management. It sheds light on the necessity of shared responsibility. For instance, through the elaboration of the RECON backward footprint results,it has been discovered that in Italy, 20% of terrestrial-origin precipitation over its territory comes from the African continent (Fig.4.1). When deforestation projects, often financed by Western countries, are implemented in Africa, the consequences extend far beyond local borders. The reduction in forest cover in Africa not only harms local ecosystems and populations but also significantly alters hydrological cycles: it decreases forest evapotranspiration, disrupts atmospheric moisture pathways, and could subsequently impact precipitation patterns in the states that finance the projects, including Italy.

In addition, it has been displayed that 17% of Italian evaporation that precipitates on land ends up in Asia. This means that land-use changes or other environmental alterations within Italy could not only impact precipitation patterns domestically,

but also disrupt atmospheric moisture flows and precipitation in distant regions like Russia.

4.0.3 The water ripple effect

These reflections face multiple issues and topics that span beyond just meteorology and engineering, delving into questions related to ethics, philosophy, geopolitics, and economics. The interconnected features of Earth's climates and their ecological effects touch on complex perplexities that surpass disciplinary boundaries.

Italy, like all countries in the world, depends on oceanic systems and foreign countries for supporting its meteorological system, which in turn affects both natural ecosystems and human activities within its territory. As a result of that, environmental changes—even in geographically distant areas can alter moisture flows and climate patterns in other regions through a cascading effect.

The study of atmospheric moisture dynamics is a double-edged complexity. On one hand, there is the need to contend with a series of inherently intricate and interconnected natural mechanisms: atmospheric moisture movement is governed by wind systems, circulation cells, and the influence of terrain, including mountains, valleys, and seas. Added to this already complex natural dynamic is the input of anthropogenic activity that disturbs these processes with elements like urbanization, changing natural landscapes, industrial emissions that impact air quality, and land-use changes that alter patterns of evaporation. A complete understanding of the dynamics of moisture in the atmosphere demands taking into account the complex network of natural processes, together with the large modifications caused by anthropogenic activity, making this field of study particularly complex and challenging.

It should be noted, in the context of anthropogenic changes, that the effects of land use change are different from those of global warming. The former are more localized and direct, with changes that are more easily measurable because the affected areas are well defined and surface properties—albedo, roughness, water retention capacity—vary in more predictable ways. This enables more direct "before/after" comparisons in the same area and better ties changes in evaporation to shifts in land use. In contrast, global warming produces more global, interconnected effects with much less predictable evaporation patterns due to multiple feedbacks involving temperature, atmospheric circulation, and cloud cover. These effects are spatially and temporally more variable and depend also on large-scale atmospheric teleconnections interacting with a great variety of climate processes.

The IPCC says that, on a global scale, climate projections indicate the frequency of heavy precipitation events is likely to increase, while the overall frequency of

all precipitation events is likely to decrease. This seemingly paradoxical projection suggests an increase in both drought and flooding and an intensification of extreme events.

Indeed, every 1 °C of global warming increases global mean precipitation by 1–3%, and it may increase by as much as 12% by the end of the century compared with the period 1995–2014. The AR6 Atlas concludes that regions where the annual mean rainfall likely will increase include the Ethiopian Highlands, East, South and North Asia, south-eastern South America, northern Europe, northern and eastern North America, and the Polar Regions. On the other hand, regions where annual mean rainfall is likely to decrease include southern Africa, coastal West Africa, Amazonia, south-western Australia, Central America, south-western South America, and the Mediterranean region. CMIP5 models also project an increase in evapotranspiration over most land areas (medium confidence) (Laîné et al., 2014). Changes in regional evapotranspiration could also depend on changes in soil moisture and vegetation, which modulate the moisture flux from land to atmosphere. Evapotranspiration is increased in most land regions, except where areas are projected to become moisture-limited (owing to reduced precipitation and increased evaporative demand), such as the Mediterranean, South Africa, and Amazonian basin (medium confidence).

On the other hands, geographic modelling reveals that land-cover change decreases annual Terrestrial evapotranspiration by pproximately 3,500 km3 yr-1 (5%) and that the largest variations in evapotranspiration are related to the wetlands and reservoirs.

Results of Sterling et al. (2012) indicate that human LUC (from potential land cover to actual land use) has led to decline in evaporation and precipitation, and to rises in surface runoff, for most of the world. Evaporation has decreased primarily over Southwest China, Europe, West Africa, south of Congo, and southeast South America resulting from substantial pasture and agricultural expansion (Ramankutty et al., 2008). Along major wind trajectories, successive Precipitation has declined in all tropical realms, in South Central China, east coast US, and Europe

Given the complexity of the described systems and the risks associated with disturbances in water cycles, a structured, multidisciplinary scientific approach is necessary. To effectively inform environmental policies, it is essential to assess stocks and flows of green and blue water (both locally and globally), utilizing satellites, big data, and Earth system models (Rockstrom et al. 2020). Identifying where and through which processes global change is altering freshwater cycles and availability is particularly crucial.

In this respect, an intensive study of precipitationsheds and evaporationsheds becomes of relevant importance. Such concepts allow to perceive and understand the connectivity between different areas through the study of moisture flows in the atmosphere and give us hints on how these flows may change in the future. Coupling of such models with climate change forecast can enable to predict future changes in rainfalls and evaporation more effectively around the globe, thereby helping to prepare better adaptation plans and mitigation strategies.

Furthermore, this deeper understanding of water interdependencies between countries could reveal potential future geopolitical tensions, underscoring the importance of viewing water as a global common good and the need for strengthened international cooperation. As highlighted by Gleeson et al. 2023, it is especially important to identify regions experiencing the most rapid changes in water flows and to assess their impact on the various functions of the Earth system.

Conclusions

This thesis has investigated the detailed hydrological relations and dynamics of atmospheric moisture that involve Italy and its regions—Piedmont, Lazio, and Sicily—by using the theoretical constructs of precipitationshed and evaporationshed. More specifically, through the application of two distinct modeling approaches—Utrack and RECON— it has been possible to elucidate both similarities and differences in the assessment of atmospheric water transfers, hence serving an overall perspective of the hydrological cycle in Italy.

Both models agree that the majority of evaporationsheds are located east of Italy and spread over vast regions of Asia, including Russia. On the other hand, the majority of precipitationsheds are located to the west of Italy, where the Atlantic Ocean appears as the main source of moisture for national precipitations. The reason of this phenomenon has been identified in the role of prevailing westerlies, which blow from southwest toward northeast, hitting these areas and hence affecting their atmospheric moisture dynamics.

However, some discrepancies in the estimated amounts of evaporation and precipitation through the different areas highlight a rather mismatch between the two dataset. More specifically, the RECON analysis estimates an annual evaporation amount for Italy of about 200 billion cubic meters, which is about 10% less than the corresponding estimate by Utrack. This reduction is consistently found for all the regions analyzed in the forward analysis. The largest discrepancy occurs in Lazio, where RECON predicts a volume of $1.22 \times 10^{10}\,\mathrm{m}^3$, 23% less than Utrack. On the other hand, in the backward analysis, RECON systematically estimates larger precipitation volumes than Utrack. At the national scale, RECON predicts an annual precipitation volume of $2.26 \times 10^{11}\,\mathrm{m}^3$, 17% larger than Utrack's estimate. At the regional scale, Piedmont shows the largest deviation, with RECON's estimate of $3.91 \times 10^{10}\,\mathrm{m}^3$ being about 40% larger. Next, Lazio has an estimate 8.4% larger ($1.79 \times 10^{10}\,\mathrm{m}^3$), and Sicily has a 5.8% larger estimate ($1.63 \times 10^{10}\,\mathrm{m}^3$).

Additionally, the misalignment in the results is not limited to differences in volume estimations but is also evident in the spatial distribution. This is particularly

noticeable in the forward footprint analysis, where the main contributing country to national precipitation is Russia according to Recon, while for Utrack it is Italy itself. Generally, it has been observed that RECON model tends to position the evaporationsheds further north compared to Utrack, while, on the contrary, it places the precipitationsheds further south.

Differences of this magnitude reflect the complexity involved in modeling atmospheric moisture and the challenges in correctly quantifying water fluxes.

After these considerations, a detailed comparison shown that, although both models could exhibit some similar patterns, RECON generally presents a more consistent and detailed picture. It especially excels at depicting the evaporationshed and precipitationshed extension with respect to the prevailing wind directions, showing better agreement with the ERA5 dataset but also providing better consistency in enforcing mass conservation for local moisture recycling. Due to these reasons, RECON has been considered an enhancement of Utrack and has been selected as the reference model for the final evaluations.

The closing analysis has revealed the low level of self-sufficiency in the water cycle of Italy, which demonstrates the country's dependence on moisture originating from abroad. The RECON's results show that 92.59% of the precipitation falling over Italy originates from outside its national borders, while 87.72% of the water that evaporates is transported to other regions. This demonstrates Italy's connectivity with different areas, even scattered, in the global water cycle, highlighting the reliance on external sources for most of its national precipitation, combined with its substantial contribution to global moisture flows,

These outcomes highlight Italy's role as an "atmospheric bridge". It receives most of its precipitation from the moisture of the Mediterranean Sea and the Atlantic Ocean, which stands out as the main contributor to Italian precipitation. Thereafter, the majority of this water, once evaporated again in the national territory, is transferred to eastern and northern Europe, with Russia being the main recipient of Italian evaporation.

This study represents the first comprehensive investigation of moisture dynamics in these regions, making direct comparisons with similar analysis impossible. Nonetheless, it represents an essential step toward a deeper understanding of atmospheric moisture patterns which, although often overlooked in the hydrological cycle, are central to ecosystem services and, by extension, human activities.

The insights obtained from this study become very relevant when considering global changes and alterations in land use that strongly impact atmospheric moisture fluxes and, consequently, the global freshwater cycles and its availability. It

underlines the long paths of the moisture particles from source to destination, showing the connectivity of distant areas around the globe and pointing out the need to treat water as a shared resource. This knowledge will gradually develop into fundamental building blocks for designing practical mitigation and adaptation policies in response to a warming climate futures.

Bibliography

[1] Istituto nazionale di statistica (Istat). "Le superfici dei comuni, delle province e delle regioni italiane". In: *Statistiche - report* (2005).

[2] Istituto nazionale di statistica (Istat). "Territorio". In: *Annuario statistico italiano* (2020).

[3] Benjamin W Abbott et al. "A water cycle for the Anthropocene". In: *Hydrological Processes* 33 (23 2019), pp. 3046–3052. ISSN: 10991085. DOI: 10.1002/hyp.13544.

[4] Benjamin W. Abbott et al. "Human domination of the global water cycle absent from depictions and perceptions". In: *Nature Geoscience* 12 (7 2019). ISSN: 17520908. DOI: 10.1038/s41561-019-0374-y.

[5] Richard P. Allan et al. *Advances in understanding large-scale responses of the water cycle to climate change*. 2020. DOI: 10.1111/nyas.14337.

[6] Peter G. Baines. "The zonal structure of the Hadley circulation". In: *Advances in Atmospheric Sciences*. Vol. 23. 2006. DOI: 10.1007/s00376-006-0869-5.

[7] Mara Baudena et al. "Effects of land-use change in the Amazon on precipitation are likely underestimated". In: *Global Change Biology* 27 (21 2021). ISSN: 13652486. DOI: 10.1111/gcb.15810.

[8] B. Bisselink and A. J. Dolman. "Recycling of moisture in Europe: Contribution of evaporation to variability in very wet and dry years". In: *Hydrology and Earth System Sciences* 13 (9 2009). ISSN: 16077938. DOI: 10.5194/hess-13-1685-2009.

[9] Intergovernmental Panel on Climate Change (IPCC). "Water Cycle Changes". In: Cambridge University Press, 2023. DOI: 10.1017/9781009157896.010.

[10] H. Douville et al. "Water Cycle Changes". In: *Climate Change 2021: The Physical Science Basis. Contribution of Working Group I to the Sixth Assessment Report of the Intergovernmental Panel on Climate Change*. Ed. by V. Masson-Delmotte et al. Cambridge, United Kingdom and New York, NY, USA: Cambridge University Press, 2021, pp. 1055–1210. DOI: 10.1017/9781009157896.010.

[11] Paul J. Durack. "Ocean Salinity and the Global Water Cycle". In: *Oceanography* (2015). Program for Climate Model Diagnosis and Intercomparison, Lawrence Livermore National Laboratory, Livermore, CA, USA. DOI: 10.5670/oceanog.2015.03.

[12] Rudi J. Van Der Ent and Hubert H.G. Savenije. "Oceanic sources of continental precipitation and the correlation with sea surface temperature". In: *Water Resources Research* 49 (7 2013). ISSN: 19447973. DOI: 10.1002/wrcr.20296.

[13] Rudi J. Van Der Ent et al. "Origin and fate of atmospheric moisture over continents". In: *Water Resources Research* 46 (9 2010). ISSN: 00431397. DOI: 10.1029/2010WR009127.

[14] Malin Falkenmark, Lan Wang-Erlandsson, and Johan Rockström. "Understanding of water resilience in the Anthropocene". In: *Journal of Hydrology X* 2 (2019). ISSN: 25899155. DOI: 10.1016/j.hydroa.2018.100009.

[15] Luis Gimeno et al. "On the origin of continental precipitation". In: *Geophysical Research Letters* 37 (13 2010). ISSN: 00948276. DOI: 10.1029/2010GL043712.

[16] Tom Gleeson et al. "Illuminating water cycle modifications and Earth system resilience in the Anthropocene". In: *Water Resources Research* 56 (4 2020). ISSN: 19447973. DOI: 10.1029/2019WR024957.

[17] Tom Gleeson et al. *The Water Planetary Boundary: Interrogation and Revision*. 2020. DOI: 10.1016/j.oneear.2020.02.009.

[18] Kevin M. Grise and Sean M. Davis. "Hadley cell expansion in CMIP6 models". In: *Atmospheric Chemistry and Physics* 20 (9 2020). ISSN: 16807324. DOI: 10.5194/acp-20-5249-2020.

[19] Yansong Guan et al. "Human-induced intensification of terrestrial water cycle in dry regions of the globe". In: *npj Climate and Atmospheric Science* 7 (1 2024). ISSN: 23973722. DOI: 10.1038/s41612-024-00590-9.

[20] Hans Hersbach. "The ERA5 atmospheric reanalysis." In: *AGU fall meeting abstracts*. Vol. 2016. 2016, NG33D–01.

[21] Steven J. De Hertog et al. “Effects of idealized land cover and land management changes on the atmospheric water cycle”. In: *Earth System Dynamics* 15 (2 2024). ISSN: 21904987. DOI: 10.5194/esd-15-265-2024.

[22] Kristopher B. Karnauskas and Caroline C. Ummenhofer. “On the dynamics of the Hadley circulation and subtropical drying”. In: *Climate Dynamics* 42 (9-10 2014). ISSN: 14320894. DOI: 10.1007/s00382-014-2129-1.

[23] P. W. Keys et al. “Analyzing precipitationsheds to understand the vulnerability of rainfall dependent regions”. In: *Biogeosciences* 9 (2 2012). ISSN: 17264170. DOI: 10.5194/bg-9-733-2012.

[24] Patrick W Keys. “The precipitationshed: Concepts, methods, and applications”. PhD thesis. Stockholm Resilience Centre, Stockholm University, 2016.

[25] Patrick W Keys et al. “The dry sky: future scenarios for humanity’s modification of the atmospheric water cycle”. In: *Global Sustainability* 7 (2024), e11.

[26] Patrick W. Keys et al. *Invisible water security: Moisture recycling and water resilience*. 2019. DOI: 10.1016/j.wasec.2019.100046.

[27] Jonathan Krönke et al. “Dynamics of tipping cascades on complex networks”. In: *Physical Review E* 101 (4 2020). ISSN: 24700053. DOI: 10.1103/PhysRevE.101.042311.

[28] Z. W. S Kundzewicz et al. “Climate change and water: technical paper VI”. In: *Eos, Transactions American Geophysical Union* 71 (12 2008). ISSN: 23249250.

[29] Andreas Link et al. “The fate of land evaporation - A global dataset”. In: *Earth System Science Data* 12 (3 2020). ISSN: 18663516. DOI: 10.5194/essd-12-1897-2020.

[30] Chunlei Liu et al. “Observed variability of intertropical convergence zone over 1998-2018”. In: *Environmental Research Letters* 15 (10 2020). ISSN: 17489326. DOI: 10.1088/1748-9326/aba033.

[31] Jian Lu, Gabriel A. Vecchi, and Thomas Reichler. “Expansion of the Hadley cell under global warming”. In: *Geophysical Research Letters* 34 (6 2007). ISSN: 00948276. DOI: 10.1029/2006GL028443.

[32] David McGee et al. “Hemispherically asymmetric trade wind changes as signatures of past ITCZ shifts”. In: *Quaternary Science Reviews* 180 (2018). ISSN: 02773791. DOI: 10.1016/j.quascirev.2017.11.020.

[33] Joaquín Muñoz-Sabater et al. "ERA5-Land: A state-of-the-art global reanalysis dataset for land applications". In: *Earth System Science Data* 13 (9 2021). ISSN: 18663516. DOI: 10.5194/essd-13-4349-2021.

[34] John C. O'Connor et al. "Atmospheric moisture contribution to the growing season in the Amazon arc of deforestation". In: *Environmental Research Letters* 16 (8 2021). ISSN: 17489326. DOI: 10.1088/1748-9326/ac12f0.

[35] Taikan Oki and Shinjiro Kanae. *Global hydrological cycles and world water resources*. 2006. DOI: 10.1126/science.1128845.

[36] Giampietro Paci. "Italia fisica". In: *Guardare il mondo, Zanichelli Editore* (2005).

[37] Ma Cristina Paule-Mercado et al. "Climate and land use shape the water balance and water quality in selected European lakes". In: *Scientific Reports* 14.1 (2024), p. 8049.

[38] Elena De Petrillo et al. *Reconciling tracked atmospheric water flows to close the global freshwater cycle*. Under review. 2024. DOI: 10.21203/rs.3.rs-4177311/v1.

[39] Johan Rockström et al. *Malin Falkenmark: Water pioneer who coined the notion of water crowding and coloured the water cycle*. 2024. DOI: 10.1007/s13280-024-01989-7.

[40] Johan Rockström et al. *Why we need a new economics of water as a common good*. 2023. DOI: 10.1038/d41586-023-00800-z.

[41] Pedro José Roldán-Gómez et al. "The role of internal variability in ITCZ changes over the Last Millennium". In: *Geophysical Research Letters* 49.4 (2022), e2021GL096487.

[42] Jacob Schewe et al. "Multimodel assessment of water scarcity under climate change". In: *Proceedings of the National Academy of Sciences of the United States of America* 111 (9 2014). ISSN: 00278424. DOI: 10.1073/pnas.1222460110.

[43] Tapio Schneider, Tobias Bischoff, and Gerald H. Haug. *Migrations and dynamics of the intertropical convergence zone.* 2014. DOI: 10.1038/nature13636.

[44] Douglas Sheil. *Forests, atmospheric water and an uncertain future: the new biology of the global water cycle*. 2018. DOI: 10.1186/s40663-018-0138-y.

[45] Rogert Sorí et al. "A Lagrangian perspective of the hydrological cycle in the Congo River basin". In: *Earth System Dynamics* 8 (3 2017). ISSN: 21904987. DOI: 10.5194/esd-8-653-2017.

[46] Arie Staal et al. “Feedback between drought and deforestation in the Amazon”. In: *Environmental Research Letters* 15 (4 2020). ISSN: 17489326. DOI: 10.1088/1748-9326/ab738e.

[47] Arie Staal et al. “Forest-rainfall cascades buffer against drought across the Amazon”. In: *Nature Climate Change* 8 (6 2018). ISSN: 17586798. DOI: 10.1038/s41558-018-0177-y.

[48] Shannon M. Sterling, Agnès Ducharne, and Jan Polcher. “The impact of global land-cover change on the terrestrial water cycle”. In: *Nature Climate Change* 3 (4 2013). ISSN: 1758678X. DOI: 10.1038/nclimate1690.

[49] Jolanda JE Theeuwen et al. “Local moisture recycling across the globe”. In: *Hydrology and Earth System Sciences* 27.7 (2023), pp. 1457–1476.

[50] J. R. Toggweiler. “Climate change: Shifting Westerlies”. In: *Science* 323 (5920 2009). ISSN: 0036-8075.

[51] Kevin E. Trenberth. “Atmospheric moisture recycling: Role of advection and local evaporation”. In: *Journal of Climate* 12 (5 II 1999). ISSN: 08948755. DOI: 10.1175/1520-0442(1999)012<1368:amrroa>2.0.co;2.

[52] Kevin E. Trenberth, John T. Fasullo, and Jessica Mackaro. “Atmospheric moisture transports from ocean to land and global energy flows in reanalyses”. In: *Journal of Climate* 24 (18 2011). ISSN: 08948755. DOI: 10.1175/2011JCLI4171.1.

[53] Obbe A. Tuinenburg and Arie Staal. “Tracking the global flows of atmospheric moisture and associated uncertainties”. In: *Hydrology and Earth System Sciences* 24 (5 2020). ISSN: 16077938. DOI: 10.5194/hess-24-2419-2020.

[54] Obbe A. Tuinenburg, Jolanda J.E. Theeuwen, and Arie Staal. “High-resolution global atmospheric moisture connections from evaporation to precipitation”. In: *Earth System Science Data* 12 (4 2020). ISSN: 18663516. DOI: 10.5194/essd-12-3177-2020.

[55] L. Wang-Erlandsson et al. “The role of freshwater in climate mitigation: biophysical interdependencies”. In: *The Essential Drop to Reach Net-Zero: Unpacking Freshwater’s Role in Climate Change Mitigation*. Stockholm International Water Institute, 2022.

[56] Lan Wang-Erlandsson et al. “Remote land use impacts on river flows through atmospheric teleconnections”. In: *Hydrology and Earth System Sciences* 22 (8 2018). ISSN: 16077938. DOI: 10.5194/hess-22-4311-2018.

[57] Nico Wunderling et al. “How motifs condition critical thresholds for tipping cascades in complex networks: Linking micro- To macro-scales”. In: *Chaos* 30 (4 2020). ISSN: 10897682. DOI: 10.1063/1.5142827.

[58] Dawen Yang, Yuting Yang, and Jun Xia. *Hydrological cycle and water resources in a changing world: A review*. 2021. DOI: 10.1016/j.geosus.2021.05.003.

[59] D. C. Zemp et al. “On the importance of cascading moisture recycling in South America”. In: *Atmospheric Chemistry and Physics* 14 (23 2014). ISSN: 16807324. DOI: 10.5194/acp-14-13337-2014.

Appendix A

Fig. A compares the zonal distribution of evaporationsheds and precipitationsheds for both Utrack and RECON over the Italian territory. Both models highlight a higher peak in the precipitationsheds, which also display a more diffuse distribution. This trend is more pronounced in the RECON model.

Through the analysis of the distributions, it is possible to notice the tendency of the precipitationsheds to be located more southward compared to the evaporationsheds as a consequence of the westerlies direction. Furthermore, observing Utrack, there is an almost perfect fit of the two curves when latitudes are higher than 45°N. Regarding RECON, above 50°N, the curve of the evaporationsheds surpasses the curve of the precipitationsheds, indicating an inversion of the dominance between the two quantities. These results align with the comparisons performed in Tab.3.21 and 3.23.

The correlation coefficient between evaporationsheds and precipitationsheds is similar for both models, with a value of 0.58 for Utrack and 0.52 for RECON.

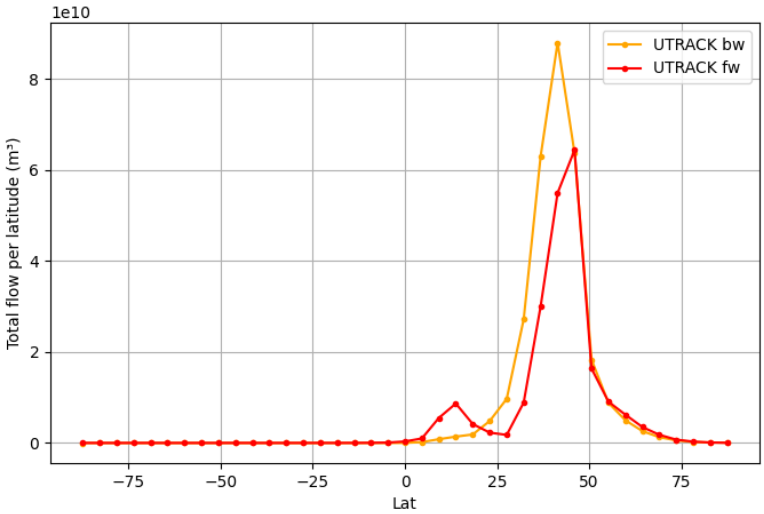

a) corr.= 0.58

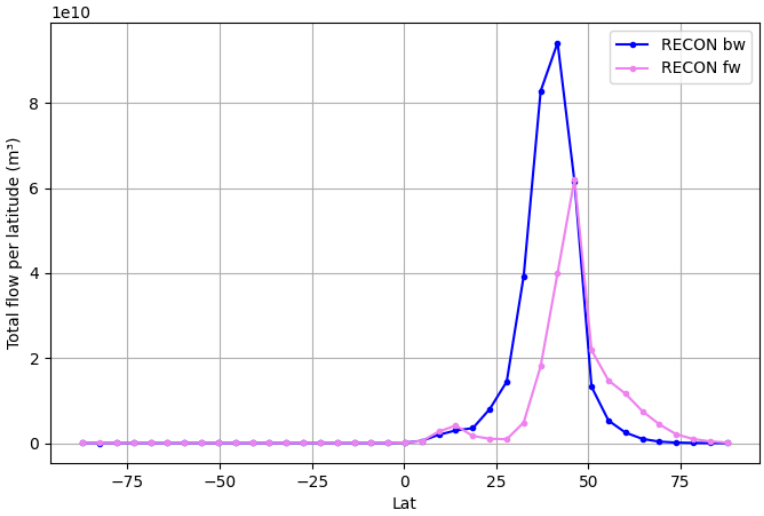

b) corr.= 0.52

Figure A: a) Zonal distribution comparison between Utrack's Italian precipitationsheds (orange line) - backward (bw) footprint - and Utrack's Italian evaporationsheds (red line) - forward footprint. b) Zonal distribution comparison between RECON's Italian precipitationsheds (blue line) - backward (bw) footprint - and RECON's Italian evaporationsheds (violet line) - forward footprint.